ADDIS ABABA UNIVERSITY

ADDIS ABABA INSTITUTE OF TECHNOLOGY

SCHOOL OF CIVIL AND ENVIRONMENTAL ENGINEERING

NUMERICAL ANALYSIS OF EMBANKMENT DAMS WITH AND WITHOUT GEOSYNTHETIC REINFORCEMENTS

(Case Study On Kalid-Dijo Zoned Embankment Dam)

A Thesis in Geotechnical Engineering

By

Gemechis Ayana Birasa

Advisor

Dr.-Ing. Tensay Gebremedhin

June, 2024

Addis Ababa, Ethiopia

A Thesis

Submitted in Partial Fulfillment of the Requirements for the Degree of Master of Science

ADDIS ABABA UNIVERSITY

ADDIS ABABA INSTITUTE OF TECHNOLOGY

SCHOOL OF CIVIL AND ENVIRONMENTAL ENGINEERING

NUMERICAL ANALYSIS OF EMBANKMENT DAMS WITH AND WITHOUT GEOSYNTHETIC REINFORCEMENTS

(CASE STUDY OF KALID DIJO ZONED EMBANKMENT DAM)

By Gemechis Ayana Birasa

The undersigned have examined the thesis entitled '**Numerical Analysis of Embankment Dams With and Without Geosynthetic Reinforcements (Case Study of Kalid-Dijo Zoned Embankment Dam)**' presented by **Gemechis Ayana**, a candidate for the degree of **Master of Science** and hereby certify that it is worthy of acceptance.

Board of Examiners

Dr.-Ing. Tensay Gebremedhin		25/06/24
Advisor	Signature	Date
Dr. Tezera Firew		24/06/24
Internal Examiner	Signature	Date
Henok Fikre (Dr. Ing.)		24/06/24
External Examiner	Signature	Date
	Abrham Gebre (Dr.) Dean, School of Civil & Environmental Engineering	
Chair Person	Signature	Date

UNDERTAKING

I certify that research work titled "**Numerical Analysis of Embankment Dams with and without Geosynthetic Reinforcements (Case Study on Kalid-Dijo Zoned Embankment Dam))**" is my own work. The work has not been presented elsewhere for assessment. Where material has been used from other sources, it has been properly acknowledged / referred.

Signature of Student

Gemechis Ayana

ABSTRACT

Soil reinforcement technology is now well-established technique for geotechnical applications in most parts of the world. This thesis was intended to numerically investigate the benefits of soil reinforcement techniques, in static and dynamic stability of zoned embankment dams in Ethiopia. The dam section designed by ECDSWCo has been considered for the case study. The detail static and dynamic analyses were conducted for the dam without geosynthetic reinforcements initially and then the slopes of this dam was considered to be reinforced with horizontal layers of geosynthetic reinforcements (geotextiles) by replacing the rock fill zone with granular shell fill for cost minimization. The analysis was carried out by using state of the art software Geo-Slope International Ltd, finite element and limit equilibrium based packages, based on analysis type. Different analysis alternatives were conducted for the reinforced dam by varying the spacing of the reinforcement layers to optimize safety and economy.

Hence, this study demonstrated that reinforcing embankment dam slopes with horizontal layers of geosynthetic reinforcements improves the embankment dam's safety and economy. By using only six layers of geosynthetic reinforcements, arranged in 4m c/c spacing for both upstream and downstream slopes, the static stability factor of safety was improved by an average value of 34.5%, the amplification value at the dam crest was reduced by about 59%, vertical crest displacement was reduced by about 24% and approximately 25% of the embankment fill construction cost was saved from the dam without geosynthetic reinforcements.

KEY WORDS: Embankment Dam, Numerical Analysis, Geo-Slope, Geosynthetic

ACKNOWLEDGEMENTS

Above all, Great praise to Almighty God, who helped and guided me from the beginning to the end. Without his presence, it was impossible to come with the end.

I would like to express my most sincere gratitude to Dr.-Ing. Tensay Gebremedhin for his guidance, comments, precious and excellent advice throughout the course of this research. I am also grateful to the firm 'Ethiopian Construction Design & Supervision Works Corporation' for providing me the chance and financial support for my study and for providing me the necessary data, I need for my research. My thanks also go to my staff members of ECDSWCo; Teshale F and Yared M; for their direct and indirect contributions.

I am grateful to my classmates (class of 2014 E.C regular Geotechnical Engineering students, for their cooperation and harmony, especially Biniam Y.

I would also like to thank my beloved family, particularly my wife Ayelu Adugna, for her encouragement and support. I want to say thanks a lot for all your invaluable contributions for the success of this study.

At last, but not least, I extend my thanks to all AAiT professors, staffs, librarians and others who directly or indirectly have contributed to the accomplishment of this thesis.

TABLE OF CONTENTS

LIST OF TABLES

LIST OF FIGURES

LIST OF ABBREVIATIONS

ATH Acceleration Time History

ASTM American Associations of Testing Materials

BC Boundary Condition

C/c Center to center

D/s Downstream

ECDSWCo. Ethiopian Construction Design and Supervision Works Corporation

EERC Earthquake Engineering Research Center

Eqn. Equation

EQL Equivalent Linear

FEMA Federal Emergency Management Agency

FHWA Federal Highway Administration

IJGGE International Journal of Geosynthetics and Ground Engineering

FS Factor of Safety

GIGEUDSWS Geotechnical Investigation, Geotechnical Engineering and Underground Works Design & Supervision Works Sector

G_{max} Maximum dynamic shear modulus

GSR Geosynthetic Reinforcement

IFAI Industrial Fabrics Association International

K Seismic coefficient

Ka Shear Stress Correction Function

K_s Overburden Pressure Correction factor

K_h Horizontal seismic coefficient

kPa Kilopascal

K_v Vertical seismic coefficient

LL Liquid Limit

MCE Maximum Credible Earthquake

M_s Surface-wave magnitude

M_w Moment magnitude

N Number of cycles of an earthquake

NL Number of cycles required to cause liquefaction

OBE Operation Basis Earthquake

PI Plasticity Index

PWP Pore Water Pressure

PGA Peak Ground Acceleration

SEE Safety Evaluation Earthquake

Sec Second

Tm Mean period

USGS United States Geological Survey

U/s Upstream

USNRC United States National Research Center

WEDSWS Water and Energy Design and Supervision Works Sector

CHAPTER 1 INTRODUCTION

1.1 Background

Dam construction is one of the most fundamental civil engineering activities. The majority of dams built throughout history have been embankment (earth/rock fill) dams. Nowadays, given the constraints imposed by local circumstances and economic factors, embankment dams are a more appealing alternative to concrete dams. Embankment dams have two main advantages over concrete dams: they can be built with locally available materials and do not require relatively a stable foundation.

In most of the world today, soil reinforcement is a widely recognized method for geotechnical applications. During the soil reinforcement process, tensile elements are introduced into the soil to enhance stability and manage deformation. The reinforcement needs to pass over the soil mass's possible failure surface in order to be in effect. Because of the strains in the soil mass, which in turn cause strains in the reinforcement itself, tensile stresses are generated in the reinforcement. By preventing soil movement, these tensile stresses boost shear strength. Because of this, the shear strength of the composite soil reinforcement system is much higher than that of the soil mass alone. Reinforced soil is more economical than other construction techniques.

One common type of soil strengthening material is geosynthetics. Planar polymeric materials known as geosynthetics are integrated with soil, rock, or other materials related to geotechnical engineering to form a crucial part of a constructed project, structure, or system. Today, geosynthetics are widely used in construction all over the world for geotechnical and other purposes. These products' reputation in the construction industry has exploded because of how straightforward they are in relation to the solutions they offer. Although they can absorb and transfer less dynamic forces to engineered structures, geosynthetics are typically used for static loads.

1.2. Statement of the problem

Nearly, entire earth fill dams in our Country were designed and built using traditional techniques. However, the majority of these dams were built in earthquake-prone areas, which jeopardized the dams' safety and performance. Furthermore, experience has shown that the availability of appropriate and sufficient quantities of construction materials for embankment fill (particularly rock fill material) is a major issue for some embankment dams in Ethiopia.

To address the aforementioned and other issues, geosynthetic reinforcement was widely used in the dam projects around the world. It was found to be beneficial in improving the dam's safety and economy. These benefits were especially gained by incorporating geosynthetic reinforcements into embankment slopes, which saves construction material volume by allowing for the construction of steeper slopes and, in turn, saves construction time by allowing for the use of relatively locally available earthen materials (rather than rock fill materials) with geosynthetic reinforcement.

Hence, this study is intended to consider the numerical investigations, to check the advantages/benefits of geosynthetic reinforcements in improving the safety and economy of the embankment dams in Ethiopia (Case study on Kalid- Dijo zoned embankment dam) by comparing the dams with and without geosynthetic reinforcements.

1.3. Objective of the study

1.3.1. General Objective

- The study's overall goal is to evaluate the benefits of geosynthetic reinforcement on embankment dam design in terms of stability and cost.

1.3.2. Specific Objectives

- To perform static and dynamic stability analysis of the dam with and without geosynthetic reinforcement for different loading conditions,

- To compare the dynamic response of the reinforced dam and the dam without geosynthetic reinforcement using selected performance indicators such as deformations, vertical crest displacements and input ground motion amplifications at the top of the dam.

- To assess the suitability of geosynthetic reinforcement for improving embankment dam safety and economy.

1.4. Scope of the study

Safety and economy analyses of embankment dams is a vast area of research in geotechnical engineering. Besides, the reinforced soil technology has also very wide applications. However, this thesis is intended to address some benefits of geosynthetic reinforcements in improving the safety and economy of embankment dams (earth fill dams) in Ethiopia, performing an investigation on Kalid-Dijo embankment dam, which is on erection in the southern portion of the country.

Besides, in the current research, the reinforcements will be introduced into embankment dam slopes and the safety factor and economy of the dam will be optimized by changing geosynthetic reinforcement spacing, without changing the embankment slopes.

1.5. Significance of the study

In Ethiopia, almost all embankment dams under construction are developed based on conventional methods. However, this conventional way of design and construction require high quality and bulk volume of fill materials such as rock fill materials and long construction time. However, geosynthetic reinforcement has demonstrated advantages in improving the safety and economics of embankment dams in other parts of the world, including earthquake-prone areas as stated in section **(**2.5.1).

Since there is no such practices of using geosynthetic reinforcement in design and construction of embankment dams in Ethiopia So far, the current study will urge Ethiopian engineers and designers to consider the possibility of developing safer and cost-effective geosynthetic reinforced embankment dams.

1.6. Research Questions

- Can geosynthetic reinforcement improve the stability and economy of embankment dams (earth fill dams) in Ethiopia?
- How much the static factor of safety and seismic response of geosynthetic reinforced embankment dam will be improved under static and dynamic loading conditions, than the dam without geosynthetic reinforcements?

1.7. Hypothesis

The use of geosynthetic reinforcements in earth fill dam slopes will significantly increase the dam's static stability factor of safety, improve dynamic response and economy.

1.8. Materials and Methods (Methodology)

The approach used in this investigation was as follows:

- A thorough study of the literature was undertaken on embankment dam reinforcing techniques, seismic response of geosynthetic reinforced dams, and embankment dam stability and economic evaluations.
- The designed portion of the Kalid-Dijo earth-rock fill dam by ECDSWCo, which is now under construction in southern Ethiopia, was evaluated for the case studies.
- Geotechnical parameters, geometry and other relevant data for the dam analysis are collected from geotechnical investigation and final design reports prepared by the design organization, ECDSWCo.
- The dam was modelled using state of art Geo-Slope International Ltd software, version 2018 R2. This program included tools such as SEEP/W, SLOPE/W, SIGMA/W, and QUAKE/W, which were used for various types of analysis.

- The dam under study was modeled three times by changing the dam zones and reinforcement conditions. These are:

1) The dam without geosynthetic reinforcement, but with rock fill zone (Zoned, Earth-rock fill dam)

2) The dam without geosynthetic reinforcement and without rock fill zone (Zoned, earth-fill dam) and

3) The dam without rock fill zone, but with geosynthetic reinforcement (Reinforced, zoned earth fill dam).

- Detail analyses were conducted for each case. At the beginning, the detail analysis was carried out for the dam without geosynthetic reinforcements (originally designed dam section by ECDSWCo) Zoned, earth-rock fill dam and then the rock fill zone was removed from the dam and replaced with granular shell fill and then detail static stability analysis was undertaken. Finally, the horizontal layers of geosynthetic (geotextile) reinforcements were introduced in to zoned, earth fill dam slopes by varying the reinforcement spacing and modeling and detail analyses have been carried out for each case, for optimization purposes.

- The analyses results for the reinforced and unreinforced dam were compared and the economic analysis were conducted for the dam with and without geosynthetic reinforcements.

- Finally, conclusions and recommendations were presented based on the analysis results.

1.9. Organization of the thesis

This thesis is divided into five chapters and appendices, each with condensed content entitled. The sections are summarized below;

Chapter 1: This chapter introduces the thesis, beginning with how the research idea was generated. It then describes the thesis's goal, all of the methods used to conduct the research, its scope, and constraints.

Chapter 2: This chapter examines a diverse body of literature on the subject, including works by previous scholars. It provides an overview of recent works on soil reinforcing techniques. The fundamentals of limit equilibrium and the finite element approaches of slope stability analysis applied by various experts were discussed.

Chapter 3: Depicts the materials and approaches employed in the current research and provides an overview of the project location and its various formations. It explains how data is collected and briefly outlines the background of the software packages used. This chapter describes the overall approach and process of doing an analysis systematically for each methodology specified in Chapter 1.

Chapter 4:- The findings of an examination of Kalid-Dijo zoned embankment dam were presented. The section includes analysis and discussions on stability analyses results of the dam with and without geosynthetic reinforcements. The Comparison between analyses results is also made in this chapter.

Chapter 5: Presents the study's findings and conclusions. It also includes valuable recommendations for practical works and additional researches. Finally, all important information and software outputs are presented from Appendix A-C.

CHAPTER 2 LITERATURE REVIEW

2.1. Embankment dams

One of the core civil engineering operations is the construction of dams. An embankment has been the type of dam most often constructed throughout history and they can be classified in to two major types; Earth fill and Rock fill dams.

A dam is classified as an earth fill, if more than half of the material poured into it is made up of compacted soils. The majority of this dam is constructed from specially designed soils that have been rigorously and continuously compacted into layers of a given thickness while maintaining controlled moisture levels. Generally speaking, this dam type is composed of an impermeable core composed of clayey soils, granular shell materials composed of variable soils to ensure the stability of the structure and the right weight to withstand the water load, and filters and drains composed of sandy and gravelly soil to prevent the core from washing out (Novak, et al, 2007).

A dam that relies on rock either dumped in lifts or compacted in layers, as a major structural element is categorized as a rock fill dam. A large portion of rocky sand and other larger particles make up rock-fill dams. There's usually no need for a drainage layer because the fill naturally drains well. In order to stop seepage, rock-fill dams have an impermeable zone inside the embankment or on the upstream side of the dam. Masonry, concrete, plastic, steel sheet piling, wood, or clay can all be used to build an impermeable zone (Beadenkopf, 2013).

2.2. Static Stability Analysis

2.2.1. Limit Equilibrium Fundamentals

The earliest numerical analysis method in geotechnical engineering for evaluating the stability of earth slopes is limit equilibrium analysis, which was first used in the 20th century. Complex stratigraphy, irregular pore water pressure, shear strength models, slip surface shapes, concentrated loads, and structural reinforcement are just a few of the increasing analysis complexity issues that recent LE package, like SLOPE/W, can handle. The application of this technique to evaluate sliding stability and structural stability under

high horizontal loading is growing. Solutions, however, only meet conditions of equilibrium (SLOPE/W, 2018).

2.2.2. Stress-based Stability Analysis

Using a finite element analysis, the stress-based stability analysis technique first determines the stress distribution in the ground and then uses these stresses in the analysis. Either a static or dynamic stress-strain analysis can be used to define the stresses in this 2D method. Instead of calculating the shear strength that must be decreased to bring the system into equilibrium, the method now determines the stability factor, which is the same as the factor of safety. (SLOPE/W, 2018).

The stress-based technique is typically useful when a stress-strain analysis is already being utilized to account for deformations and/or pore water pressures, when the problem involves soil-structure interaction, or when the limit equilibrium analysis fails to converge (SLOPE/W, 2018).

2.3. Dynamic Stability Analysis

2.3.1. General

An earthquake is defined as a sudden release of energy that causes the earth to vibrate (Tarbuck, 1996). Evaluating the dynamic analysis of earth dams during earthquakes requires addressing two key issues; stability and deformation.

2.3.2. Liquefaction Analysis

Liquefaction is the process by which granular material transforms from solid to liquid when pore water pressure rises and effective stresses falls (Marcuson, 1978). When granular materials are exposed to cyclic shear deformation, they tend to compress, increasing pore water pressure. The change in condition happened most easily in loose to moderately thick granular soils with poor drainage, such as silty sands and gravel covered by or with impermeable sediment layers (Kramer, 1996).

In the field of geotechnical earthquake engineering, liquefaction is a significant, intriguing, difficult, and controversial topic. Over a three-month period in 1964, geotechnical engineers learned of the catastrophic aftermath of the Good Friday earthquake (Mw = 9.2)

in Alaska and the Niigata earthquake (Ms = 7.5) in Japan. Dramatic examples of liquefaction-induced damages were caused by both earthquakes. (Figure 2-1).

In the thirty years since these earthquakes, liquefaction has been the subject of extensive research by hundreds of researchers worldwide. Although there has been much to learn from this, the path has not been simple. There have been many different terms, strategies, and analysis techniques available, and it has taken a while for a dominating approach to emerge.

Figure 2-1: Bearing capacity failures caused by liquefaction, after the 1964 Niigata earthquake (source: USGS).

The most common places for liquefaction to occur are shallow, loose, saturated deposits of non-cohesive soils that are severely shaken by large-scale earthquakes. Fine, loose sands are usually associated with liquefaction. The field's loose sand was probably formed in a placid river or sedimentation environment without having been loaded and unloaded before. It seems as though the content is typically consolidated in some ways. This process results in two distinct types of liquefaction phenomena. (Kramer, 1996);

- Flow liquefaction and
- Cyclic mobility

Of all liquefaction-related events, flow liquefaction is the most severe, leading to massive instabilities that are referred to as flow failures. Flow liquefaction happens when the shear stress in a soil mass needed for static equilibrium (the static shear stress) is more than the shear strength of the liquefied soil.

Cyclic mobility is extra method that might create undesirable persistent deformations during earthquake shaking. Dissimilar flow liquefaction, cyclic mobility occurs when the static shear stress is less than the shear strength of the liquefied soil. During earthquake shaking, deformations caused by cyclic mobility failure rise progressively. Unlike flow liquefaction, cyclic and static shear stresses can produce cyclic mobility deformations (Kramer, 1996).

2.3.3. Seismic slope stability analysis

For many years, static slope stability analysis techniques have been employed and validated against an extensive variety of real-world slope failure situations. Seismic slope stability analyses employ a much smaller database for calibration (Kramer, 1996). When analyzing the seismic stability of slopes, the two scenarios listed below must be considered:-

- Dynamic stresses brought on by shaking during earthquakes, and
- The effects of those stresses on the strength and stress-strain behavior of the slope materials.

Depending on which of these effects predominates on a particular slope, seismic slope instabilities can be divided into two categories. These are the following:

a) **Inertial Instabilities**: When dynamic earthquake stresses momentarily surpass the soil's strength, slope deformations transpire, despite the soil's shear strength lasting constant.
b) **Weakening Instabilities:** are those where the ground is so weakened by an earthquake that it is unable to withstand stress brought on by the earthquake. Typically, weakening stability is caused by cyclic mobility and flow liquefaction.

2.3.3.1. Analysis of Inertial Instability

Earthquake movements can generate large horizontal and vertical dynamic stress in slopes. These pressures provide dynamic normal and shear stress on the slope's possible failure surfaces. When dynamic shear pressures combine with previously established static shear stresses, they might surpass the soil's available shear strength, resulting in slope inertial instability. A number of techniques for assessing inertial instability have been developed. The primary distinction between these methods is the accuracy with which seismic motion

and slope dynamic reactivity are depicted. The pseudostatic and sliding block by Newmark analysis are two significant instances, which will be addressed more below.

2.3.3.1.1. Pseudo-static Analysis

Similar to static limit equilibrium analyses, pseudo-static analysis produces a factor of safety against seismic slope failure. With the horizontal force being represented by the product of the weight of the potential sliding mass, W, and a seismic coefficient, K, the analysis is regarded as a static problem. There is an assumption that the dam acts like a rigid body, with accelerations constant throughout the section and always equal to the accelerations on the ground.

Despite the fact that this analysis approach is comparatively easy to understand, it has the drawback of representing the intricate, fleeting, dynamic effects of seismic shaking by a single, obviously very basic, constant unidirectional pseudostatic acceleration. According to Terzaghi (Terzaghi, 1950), "the concept it conveys of earthquake effects on slopes is very inaccurate, to say the least," and even in cases where the computed pseudostatic factor of safety is greater than 1, a slope may still be unstable. Furthermore, this approach's primary drawback is that the maximum acceleration will be developed in a dam for only a short period, so that the deformation resulting from it may be small.

Pseudostatic analyses describe earthquake shaking caused by pseudostatic accelerations, which result in inertial forces F_H and F_V acting through the failure mass's centroid as shown in (Figure 2-2). The magnitudes of the Pseudostatic forces are given by:

$$F_{H=}\frac{a_{h*W}}{g} = K_h * W \quad \text{2-1}$$

$$F_{V=}\frac{a_{V*W}}{g} = K_V * W \quad \text{2-2}$$

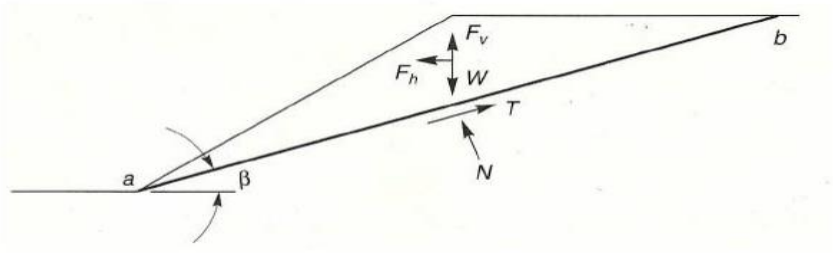

Figure 2-2: Forces acting on triangular wedge of soil above planar failure surface in Pseudostatic slope stability analysis (Kramer, 1996).

$$FS = \frac{Resisting\ force}{Driving\ force} = \frac{C * l_{ab} + [(W - F_v)Cos\beta - F_{h}Sin\beta]tan\emptyset}{(W - F_{v)}Sin\beta + F_{h}Cos\beta} \quad \text{2-3}$$

Where;

F_H and F_V = Horizontal and vertical Pseudostatic forces, respectively

a_h and a_v = Pseudostatic accelerations in x and y directions, respectively,

K_h and K_v = Dimensionless pseudostatic coefficients in x and y directions, respectively,

W = the failure mass weighs

C and ϕ = Are the Mohr-Coulomb strength parameters that describes the shear strength on the failure plane,

l_{ab} = The extent/length of the collapse plane

β = Angle between the vertical and the line passing through the C.G. of the slice

2.3.3.1.2. Newmark's Sliding Block Analysis

(Newmark, 1965) predicted earthquake-induced displacements in embankments by assuming that movements occur when pressures on a stiff block of soil above a designated potential failure surface exceed its sliding resistance. He argued that the slope bent only during the earthquake, when out-of-slope seismic pressures reduced the pseudo-static factor of safety to less than one. He has developed an approach for rigid-plastic materials that includes determining the yield acceleration, kyg, at which sliding will commence and computing the displacements that occur when this acceleration is surpassed. Figure 2-3 illustrates the procedure. If the acceleration pattern applied to a hypothetical sliding mass is the same as shown in the figure, no displacement will occur until time t1, when the generated acceleration surpasses the yield acceleration for the first cycle, ky1. The velocity will continue to rise until time t2, when the acceleration falls below the yield value again, and the velocity will eventually fall to zero at time t3, since the sliding body's direction

can be established by integrating the velocity versus time relationship. Figure 2-5 shows the final outcome.

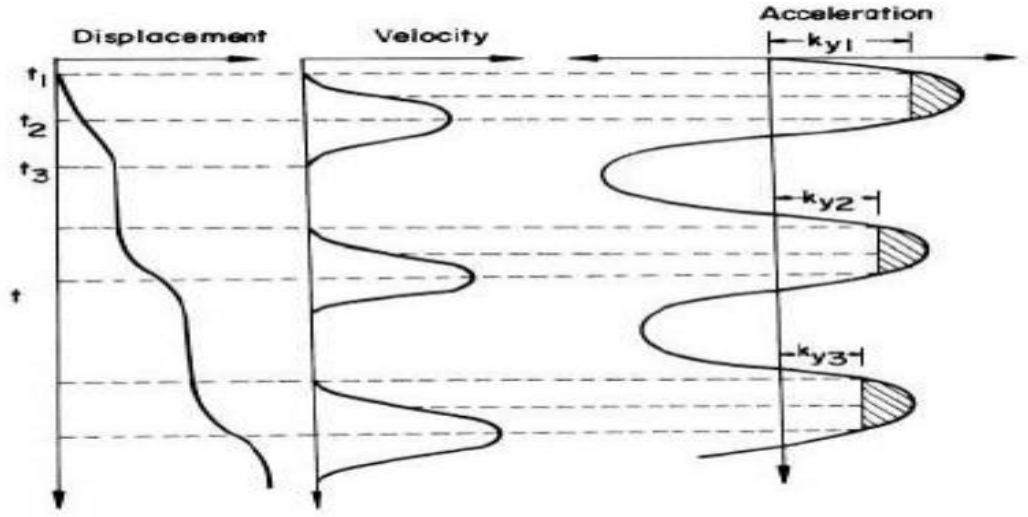

Figure 2-3: Integrating accelerograms to calculate downslope displacement

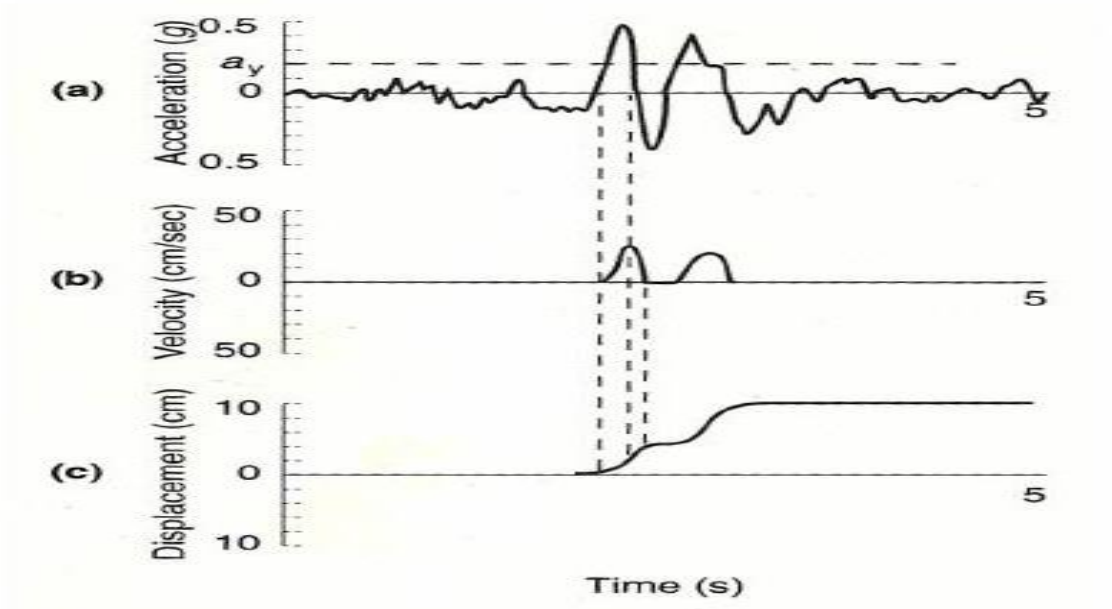

Figure 2-4: Create permanent slope displacements for actual earthquake ground motion. (Following Wilson and Keefer, 1985).

2.4. Reinforced Soil Technique

The traditional approach of building embankment dams to a stab slope for a specific height may result in high expenses for construction material, construction equipment, construction time, and base area increment. These difficulties, however, can be addressed by using proper solutions. One solution to this challenge is to make the dam slopes somewhat steeper than they would be with traditional design processes. The embankment dam slopes can be steepened by strengthening them with appropriate reinforcing material. (Duncan, 2005) Categorized reinforcement applications into four types:

Reinforced slopes: Several sheets of reinforcements at varying altitudes inside fill slopes have been used to advance the factor of safety for slip planes that pass through the reinforcement, allowing for steeper slopes than ever be possible deprived of reinforcement.

Reinforced dams on unstable bases: Reinforcement at the bottommost of an earth fill/rock fill dams on a poor strata can rise the safety factor for slip surfaces going via the embankment, allowing the embankment to be built higher than it would otherwise be.

Reinforced soil walls or mechanically stabilized earth barriers: Numerous patented technologies have been developed for reinforced soil walls, which are utilized as an alternative to old-fashioned retaining walls.

Anchored walls: To provide vertical support for excavations and fills, standing soldier pile walls and slurry trench concrete walls can be "tied back" or anchored at one or many levels. Anchored walls have served both momentary and lasting functions.

2.4.1. Types of Soil Reinforcement

Geosynthetics are commonly employed in soil reinforcement procedures. Geosynthetics are planar polymeric products that are used in conjunction with soil, rock, earth, or other geotechnical engineering-related materials as an integral component of a artificial project, construction, or pattern.

Geotextiles, Geogrids, Geonets, Geomembranes, Geosythetic clay liners, Geopipe, Geofoam, and Geocomposites are many forms of geosynthetic products. Figure 2-5 depicts two different forms of geosynthetics: geotextiles and geogrids.

Geotextile product is formed when synthetic fibers are woven into a flexible, porous fabric using normal weaving machines or matted together in woven and nonwoven manner and geogrids are plastic sheets that have been shaped into a very open net-like arrangement.

Both of these materials are often used in soil reinforcing methods because they are corrosion resistant, have a low stiffness, and can sustain large deformation. These qualities distinguish them from steel reinforcing components in soil (Koerner, 2005).

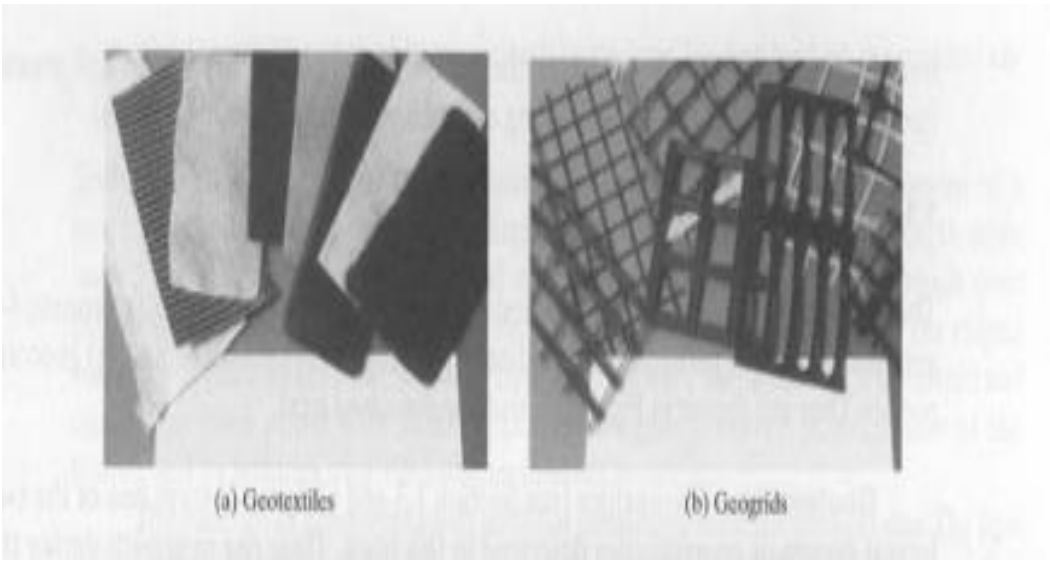

Figure 2-5: Geotextiles and Geogrids (reinforcing materials) (Koerner, 2005).

2.4.2. Applications of Geosynthetics

During the performance life of a geosynthetic, it is anticipated to execute one or more functions. The function(s) to be achieved by the geosynthetic in that particular purpose have a significant effect on its selection for that application region. Geosynthetics have numerous uses in civil engineering. When they come into contact with soil, rock, or any other material utilized in engineering, the primary roles are as follow:

- reinforcement,
- separation,
- filtration,
- drainage,
- fluid barrier, and
- Protection.

When a geosynthetic is added to soil, it strengthens it mechanically. When soil and geosynthetic reinforcement are combined, a composite material known as ‘reinforced soil' is formed, with high compressive and tensile strength. In actuality, the primary role of any geosynthetic reinforcing material is to sustain applied stresses while preventing unwanted deformations in geotechnical constructions. In this approach, the geosynthetic functions as a tensioned element that is linked to the soil/fill material by friction, adhesion, interlocking, or confinement to ensure soil mass stability.

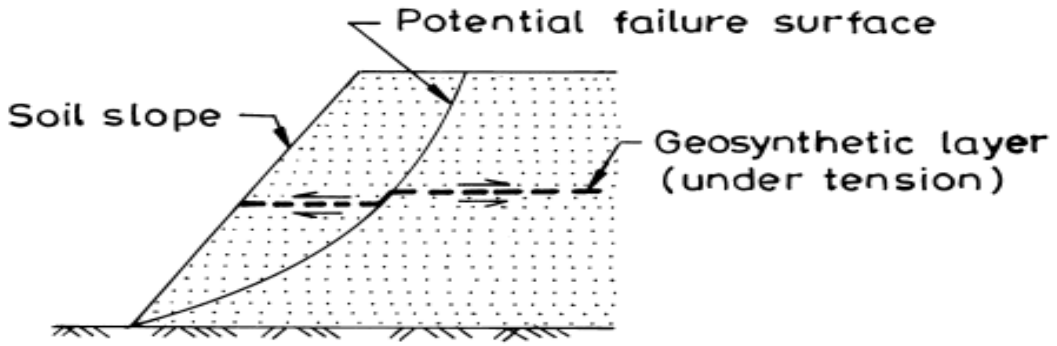

Figure 2-6: The fundamental mechanism involved in the reinforcing function.

The most common reinforcing materials used for slopes and embankments are geotextile fabrics, geogrids, steel strips, steel grids, and high strength steel tendons.

2.4.3. Geotextile and Geogrids as reinforcement

Geosynthetic (fabric) treatment appears to be particularly effective for slope and subgrade reinforcement problems. Currently, it appears that the great majority of geosynthetics are utilized in this application. The concept is technically sound, as the geosynthetic reduces soil stress levels caused by horizontal shear stresses created by vertical loads. This puts the fabric under tension (similar to a pre-stressing tendon in reinforced concrete), spreading the load across a wide region and reducing its severity. That is, the unit vertical stress decreases. Reduced stress indicates a lower probability of failure and/or settlement. Typical occurrences include the following.

- Enhance the stability of embankment dams,
- Reinforced wall construction and reinforcing material

- Minimizing the obligation to eliminate current soil (with generally weak properties) in marginal situations,

2.4.3.1. Geotextile Materials

Geotextiles are manufactured by weaving polymeric fibers into a fabric or by matting the fibers together to form a continuous nonwoven fabric. Specifically, geotextiles are made from polypropylene, polyester, polyethylene, polyamide (nylon), polyvinylidene chloride, and fiberglass (Koerner, 2005). Polypropylene and polyester are the most used material for the geotextiles. Geotextiles are available in a variety of structures and polymer compositions designed to meet a wide range of applications. It is important all geotextiles be composed of strong, durable, chemical inert polymeric materials that are resistant to the effects of site specific ground conditions, whether, and aging (Koerner, 2005).

2.4.3.1.1. Woven Geotextiles

In woven constructions, the warp yarns, which run parallel with the length of the geotextiles panel (machine direction), are interlaced with yarns called till or filling yarns, which run perpendicular to the length of the panel (cross direction). Woven construction produces geotextiles with high strengths and moduli in the warp and fill directions and low elongations at rupture. The modulus varies depending on the rate and direction in which the geotextile is loaded. When woven geotextiles are pulled on a bias, the modulus decreases, although the ultimate breaking strength may increase. The construction can be varied so that the finished geotextile has equal or different strengths in the warp and fill directions. Woven construction produces geotextiles with a simple pore structure and narrow range of pore sizes or openings between fibers. Woven geotextiles are commonly plain woven. Woven geotextiles can be composed of monofilaments or multifilament yarns. Generally, woven fabrics exhibit high tensile strength, high modulus and low elongation.

Multifilament woven construction produces the highest strength and modulus of all the constructions but also highest cost. A monofilament variant is the slit-film or ribbon filament woven geotextile. The fibers are thin and flat and made by cutting sheets of plastic into narrow strips. This type of woven geotextile is relatively inexpensive and is used for separation, i.e. the prevention of intermixing of two materials such as aggregate and fine-

grained soil. Woven geotextiles are stiffer, stronger than nonwoven geotextiles, and more useful for reinforced slope applications (FEMA, 2008).

Figure 2-7: Photograph showing examples of Woven Geotextiles (FEMA, 2008).

2.4.3.1.2. Non-Woven Geotextiles

A process other than weaving or knitting forms non-woven geotextiles, and they are generally thicker than woven products. These geotextiles may be made either from continuous filaments or from staple fibers. The fibers are generally oriented randomly within the plane of the geotextile but can be given preferential orientation. In the spun bonding process, filaments are extruded, and laid directly on moving belt to process described below:

Needle punching: - Bonding: Bonding by needle punching involves pushing many barbed needles through one or several layers of a fiber mat normal to the plane of the geotextile. The process causes the fibers to be mechanically entangled. The resulting geotextile has the appearance of a felt mat.

Heat bonding: - This is done by incorporating fibers of the same polymer type but having different melting points in the mat, or by using hetro filaments, that is, fiber composed of one type of polymer on the inside and covered or sheathed with a polymer having a low melting point.

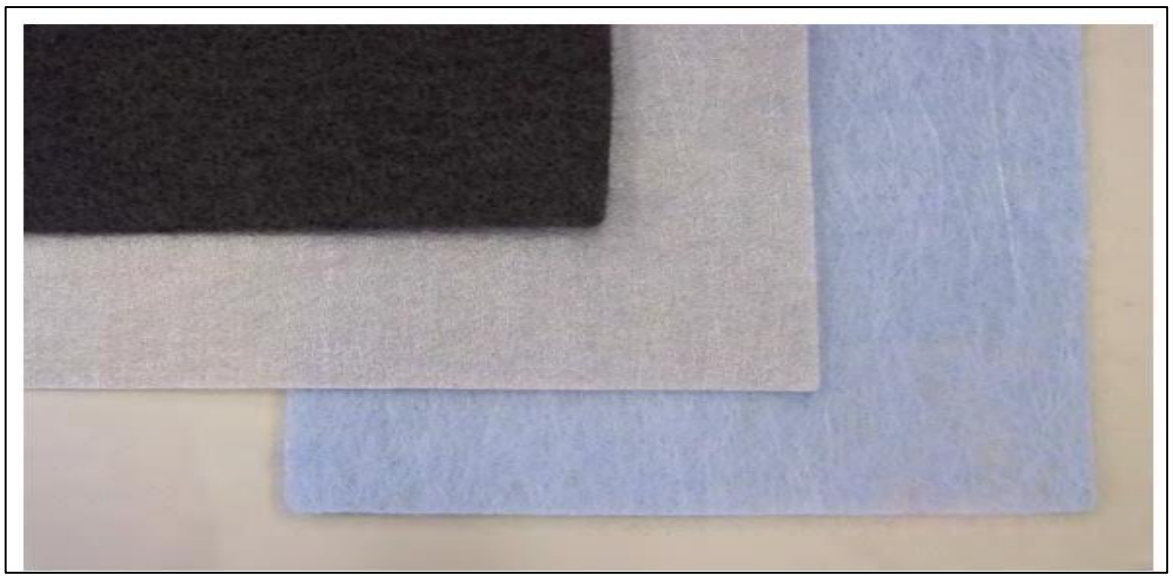

Figure 2-8: Photograph showing examples of Non-woven Geotextiles (FEMA, 2008)

2.4.4. Soil-geotextile interaction properties and mechanisms

Soil-geotextile interaction properties are critical in a wide range of geosynthetic applications, especially when employed for soil reinforcement. Soil reinforcement is the process of incorporating appropriately aligned materials into soil to improve the qualities of the new material (reinforced soil) in contrast to unreinforced soils. The primary goal of reinforcing is to prevent the formation of tensile stresses in the soil and, as a result, to sustain tensile stresses that the soil cannot hold. Tensile stress produced by reinforcing improves soil mechanical properties by lowering the shear stress that the soil must bear while increasing the available shearing resistance as the normal tension acting on potential shear surfaces grows.

Several factors influence the property of reinforced soil, including:

- Mechanical properties of the soil and reinforcement
- Mechanism and features of the interaction between soil and reinforcing
- Reinforced System Geometry
- Reinforcements: shape, quantity, position, and alignment
- Method of construction, etc.

Even though all of the contributing factors stated above have an influence on soil-reinforced activities, soil-reinforcement interaction mechanisms and the factors that can influence them require special attention; because the effectiveness of transferring tensile stresses from soil to reinforcements, as well as the behavior of the reinforced soil system, is dependent on them. This problem will be examined in the following sections, with a primary focus on geosynthetic materials as reinforcement, supplemented by an examination of methodologies for assessing soil-reinforcement interactions. Reinforced systems can be classified according to three interaction mechanisms:

- Skin friction across the reinforcement
- Friction between soils and
- Passive thrust on the bearing parts of the reinforcement.

Shear strength mobilization between granular soils and geotextiles is a two-dimensional process that allows for soil dilatancy and is highly influenced by geotextile extensibility. In geogrids, the phenomena may be thought of as three-dimensional, with skin friction mobilizing for small displacements and passive push on the grid's bearing components mobilizing gradually as displacement grows. Skin friction is the sole way geotextiles and strips provide soil-geosynthetic interface resistance.

2.4.5. Reinforcement fundamentals in a limit equilibrium analysis

In a limit equilibrium analysis, each reinforcement is represented as a concentrated point load. Concentrated point loads act on the free body, which is the probable sliding mass, and hence must be considered in moment and force equilibrium calculations. Even if there are various simple approaches to specify the reinforcement's characteristics, the specified parameters are finally used to create a concentrated point load in factor of safety estimations (SLOPE/W, 2018).

2.4.6. Factors of Safety for Reinforcing Forces and Soil Strengths

2.4.6.1. Reinforcement forces

T_{lim}, or long-term reinforcement capacity, is determined by the following parameters (Duncan, 2005):

- Tensile strength: Tensile strength in geosynthetics is determined using short-term wide-width tensile testing.

- Creep characteristics: Geosynthetic materials creep significantly. Tensile loads used in the design of geotextile- and geogrid reinforced walls must be reduced to values lower than those observed in short-term tensile testing, resulting in stresses low enough to induce little or no creep deformation during the structure's design life.

- Installation damage: Geotextiles and geogrids are prone to damage during installation, resulting in holes and tears.

- Durability: Chemical and biological degradation degrades the mechanical properties of geosynthetic materials over time. Steel is prone to corrosion.

- Pullout resistance: Capacity is limited around the extremities of the reinforcement due to resistance to pullout or slip between the reinforcement and the soil in which it is embedded.

- Reinforcement stiffness and tolerable strain within the slope: The reinforcing material must be stiff and robust in order for slope reinforcement to be successful. An extremely strong but easily extensible rubber band would not be an efficient reinforcement because it would have to extend so far to mobilize its tensile capacity that it would be unable to restrict the slope's deformation.

Pullout Resistance

To increase tensile strength, reinforcement must be constrained by ground friction. The peak pullout resistance (Tpo) is proportional to effective overburden pressure. When the embedded length is zero, Top starts at 0 at the end of the reinforcement and gradually increases with distance. The gradient of the curve representing Tpo's fluctuation with distance must be supplied as follows:

$$\frac{dT_{po}}{dL} = 2\gamma z\alpha F^{*} \text{---------- (2-4)}$$

Where;

T_{po} - is the pullout resistance (F/L);

L - The embedment's length or distance from the end of the reinforcing (L); - the unit weight of fill above the reinforcement (F/L3);

z - The depth of fill over the reinforcing (L);

α- the correction factor for extensible reinforcement (dimensionless); and

F* - the pullout resistance factor (dimensionless)

The FHWA (2000) recommends α and F* values, as shown in Table 2-1. These figures are estimates. Larger values may be applicable and useful if proven by testing of the specific soil and reinforcing materials. Equation (2.5) computes the slope of the pullout resistance curve at any position. The withdrawal resistance may be expressed as follows:

$$T_{po} = \quad 2\gamma z\alpha F^{*}Le \text{----------} \quad (2\text{-}5)$$

Where Le is the distance from the end of the reinforcement or length of embedment (L).

Table 2-1: Pullout Resistance Factors and F* for use in Eq. 2.5

Pullout resistance	Type of reinforcement	Resistance factor value
α	Geotextiles	0.6
	Geogrids	0.8
	Steel strips & steel grids	1.0
F*	Geotextiles	0.67tanϕ
	Geogrids	0.8tanϕ
	Steel strips & steel grids	1.0tanϕ

Reinforcement Stiffness

Reinforcing materials must be strong enough to evenly distribute reinforcing forces without causing undue strain. T_{lim} should not exceed the product of the reinforcement's long-term secant modulus and the slope's permissible strain.

$$T_{\text{lim}} \leq E_{Secant} \in_{tolerable} \text{----------} (2\text{-}6)$$

Where; E_{secant} is the secant modulus of reinforcing at axial strain $\epsilon_{tolerable}$ (F/L) and $\epsilon_{tolerable}$ is the strain inside the slope at the place of the reinforcing that can be tolerated without extreme slope distortion or failure (dimensionless).

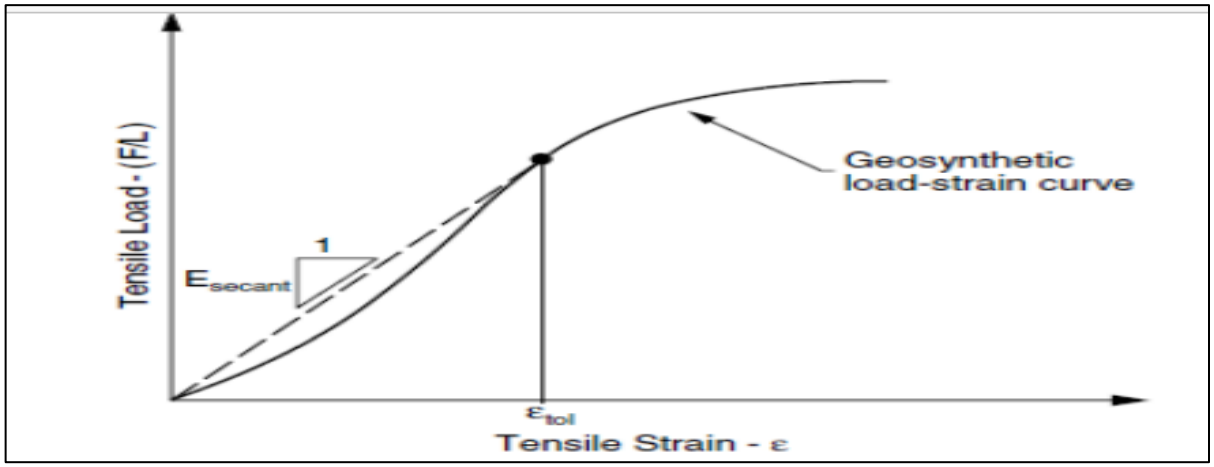

Figure 2-9: Koerner (2005) defines Esecant for geosynthetic reinforcement

Geosynthetic materials' stiffness may be low sufficient to lessen the value of T_{lim} for applications with a modest tolerable strain. Figure 2-9 illustrates that E_{secant} is the slope of a line from the origin to the point on the T-e curve when the strain equals ´ acceptable. It should be noted that, like T_{lim}, Esecant units represent force per unit length. Tolerable strain levels are based on the findings of finite element calculations (Rowe and Soderman, 1985), as well as experience (Fowler, 1982; Christopher and Holtz, 1985; Haliburton et al., 1982; Bonaparte et al., 1987), and a summary of published recommendations is given in Table 2 2 (Duncan, 2005).

Table 2-2: Tolerable Strains for Reinforced Slopes and Embankments

Application	ε tolerable (%)
Reinforced Soil walls	10
Reinforced slopes of embankments on firm foundations	10
Reinforced embankments on non-sensitive clay, moderate crest deformations non tolerable	10
Reinforced embankments on non-sensitive clay, moderate crest deformations tolerable	5-6

Reinforced embankments on highly sensitive clay	2-3

Source: Compiled from (Fowler, 1982), (Christopher, et al., 1985), (Haliburton, et al., 1982), (Rowe, et al., 1985) and (Bonaparte, et al., 1987).

2.4.6.2. Mobilization of reinforcement forces

Reinforcement can have both an immediate and delayed impact. A pre-stressed anchor, for example, acts fast and generates force due to the pre-stressing. Dissimilarity, the force in a geosynthetic can progress through time in the course of construction and after completion due to stress re-distribution. In other words, when the soil strains, the reinforcing forces mobilize in the same manner as soil strength does.

Reinforcement can also be viewed as minimizing activating or destabilizing forces. The reinforcement reduces gravity's pushing force. Alternatively, the strengthening improves shearing resistance, thereby raising the safety factor.

The SLOPE/W equilibrium equations rely on mobilized shear at each slice's base, which is calculated by dividing the shear strength by the safety factor. The mobilized shear Sm can be analytically represented as (SLOPE/W, 2018):

$$\text{Mobilized Shear } (S_m) = \frac{\text{Shear Stregth of the soil } (S_{soil})}{\text{Factor of Safety}} \quad \text{---------- (2-7)}$$

If reinforcement is employed to improve shear resistance, it need to be divided by the safety factor. According to SLOPE/W (2018), S_m is:

$$\text{Mobilized Shear } (S_m) = \frac{\text{Shear Stregth of the soil } (S_{soil})}{\text{Factor of Safety}} + \frac{S_{Reinfocement}}{\text{Factor of Safety}} \text{---------- (2-8).}$$

It is important to note that soil strength and shear resistance due to reinforcement are both divided by the same overall global factor of safety. The implication is that soil and reinforcing shear resistance are produced and deployed concurrently.

When reinforcement is thought to contribute to the lowering of the destabilizing force, it is expected that it is fully mobilized immediately, so that the reinforcement forces are not divided by the overall global factor of safety. Reduction factors can be utilized to reduce the allowed loads in the reinforcement, although they are not directly employed in the SLOPE/W factor of safety calculations. The indicated or permitted reinforcing forces are immediately applied in the SLOPE/W calculation.

SLOPE/W allows both of these methods to include reinforcement in stability calculations. The option is selected by labeling the reinforcement as "F of S dependent", either Yes or No. The "Yes" option increases shear resistance, and the reinforcement forces are divided by the global factor of safety to calculate the deployed reinforcement forces. The "No option" immediately evaluates the provided permitted reinforcement forces.

The so-called "F of S Dependent" The Yes option is deemed acceptable for ductile reinforcement, such as certain polymeric geosynthetics. The No option is recommended for pre-stressed anchors or nails that are rigid in relation to soil stiffness (SLOPE/W, 2018).

2.5. Related researches/Case Histories

Geosynthetic reinforcements have been widely employed worldwide in the design and construction of embankment dams. Some case histories regarding this subject have listed below; considering both international and local practices:

2.5.1. International Case Histories

1) Title: “Slope Stability and Soil Liquefaction Analysis of Earth dams with a proposed method of Geotextile Reinforcement” (Case Study on Al-Adhaim Dam, Iraq).

   - ✓ ***(****By Nabeel S. Mahmood and Nadhir Al-Ansari)*

     - The Slope stability and soil liquefaction analysis was performed for this dam with and without geotextile reinforcement.

     - Geotextile reinforcement was suggested to reduce the effect of the soil liquefaction that was observed in the front shell of the dam.

2) Title: “Seismic Response of Geosynthetic Reinforced Earth dams”

   - ✓ ***(****By A. Edincliler and Y.S. Toksoy)*

     - In this study, the effects of reinforcing the slopes with geosynthetics on seismic response of the earth dams were evaluated.

     - Unreinforced and reinforced earth dam models were subjected to different destructive ground motions by using the two-dimensional

finite element code and numerical results were evaluated and represented with respect to the selected performance indicators of the study.

- Results reveal that geosynthetic reinforcement technique using sequential geogrid layers has a noticeable effect on the seismic response.
- Total displacements and displacement concentrations at the embankment slope are successfully reduced.

3) Maraval Dam, France

- This dam was constructed in 1976 GC and stands as the first dam in which geosynthetics had been introduced for reinforcement purpose.
- Because of the multi-layered geotextile soil mass with high strength PET woven geotextile reinforcement (strength equal to 210kN/m), downstream face of the dam could be made vertical thereby allowing for the construction of a short spillway.

4) Taylor Draw Dam, USA

- This dam was built in 1983 on the White River in Colorado to alleviate the major issue of flooding due to ice jams.
- The dam created Kennedy reservoir and Reinforced Earth was used to increase the height of the dam and reservoir capacity.
- The reinforcement facilitated for the vertical downstream slope and construction of spillway.

2.5.2. Case Histories in Ethiopia

Despite the benefits described above, few case studies have been published in Ethiopia. Some of the relevant research undertaken regarding reinforced embankment dams in Ethiopia include:

1) Ashenafi Y. (2015) studied Gidabo earth fill dam, which is located in the Southern part of the country within Oromia and SNNPR States. The primary goal of this study is to examine the stability of the dam under static loading conditions by incorporating geotextile reinforcements into the dam slopes. The study has proven the possibility of steepening the dam slopes and saving the volume of the dam fill materials because of reinforcements.

2) Hiwot Y. (2019) analyzed Ajima embankment dam, which is found in Northern part of the country, in the Amhara region, by incorporating horizontal layers of geotextile reinforcements. This study focused only on static factor of safety improvement and construction cost minimizations by steepening the dam slopes similar to the first study.

Both researches mentioned above (in Ethiopia) does not include the investigation on the benefits of geosynthetic reinforcements in improving seismic response or dynamic stability of the dams and both studies used SLOPE/W, Limit equilibrium based package of Geo-Slope International Ltd only, for stability analysis. Finite Element method of stability analysis was not tried or checked in these studies.

CHAPTER 3 MATERIALS AND METHODS (METHODOLOGY)

3.1. Study area description

3.1.1. Location of the project

Kalid Dijo Embankment dam, which is under construction in Ethiopia's southern region, has been used for the case study. Kalid Dijo Dam and Irrigation project is located in Sothern Nations Nationality People Regional State of Silte zone, around Dalucha town, at about 200 km from Addis Ababa. The proposed dam is located on Dijo Seasonal River and it will be used to supply water for the proposed potential land just downstream of the dam. Basin wise, the project is located in Rift Valley River Basin with geographic coordinates of 868194 UTM Northing and 413216 UTM Easting. The main dam body is designed with Rock and Shell fill (Earth-rock fill) with central clay core. Downstream and upstream filter, drainage zone is provided to protect migration of soil and to drain seepage water and smooth transition from fine to coarse textured dam fill materials. The embankment crest length is about 1731m and the maximum height above riverbed level is 25.5m.

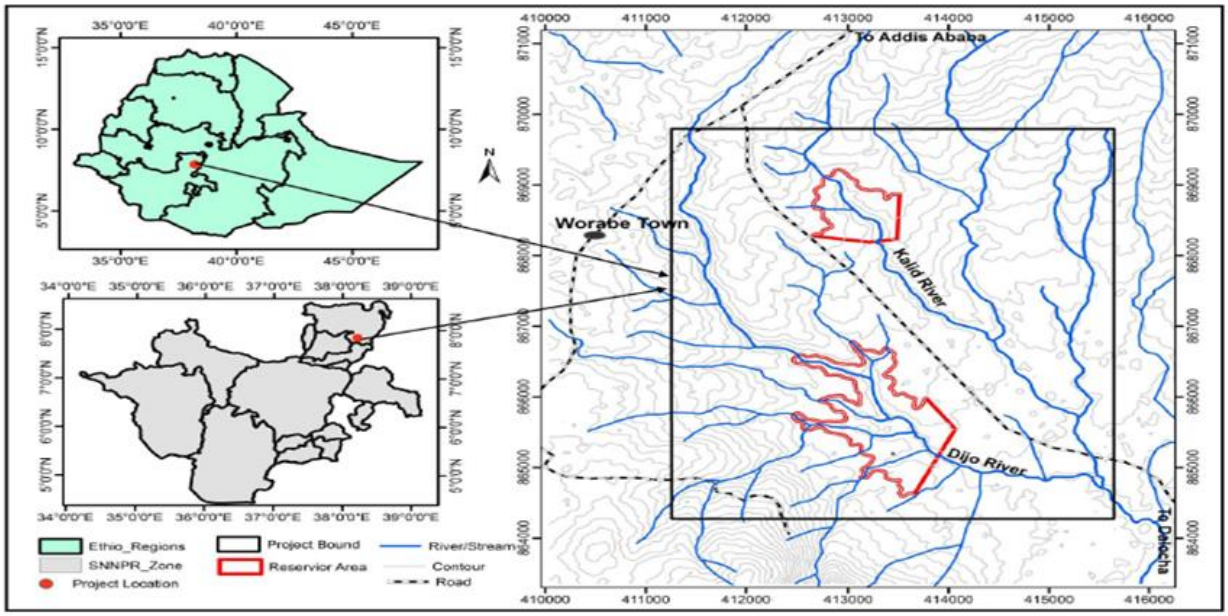

Figure 3-1: Location map of the project area

3.1.2. The Dam Foundation Situations

As per the geotechnical study findings stated in the Geology and Geotechnical Investigation Report, Volume (II), (ECDSWC, 2019), the dam and spillway foundations are constituted of three geotechnical units (i.e. GTL-GTL-II, GTL-III, and I).-

A) GTL-I: - (ML SOIL, SILT of low plasticity): -

This soil cover the foundation site both\ at the right and left bank of dam axis, except in the valley part. Top Soil overlies this soil up to 2m depth. On average, it is 11m thick volcanic ash and residual deposit of tuff layers with brownish to dark greyish color fragments of pulverized fine to medium-grained rock and volcanic glasses. From drilling log observation, on natural sections, thickness (the depth of the expected underlying rock unit) of this unit varies from place to place and it is 11.00m in average on both left to the right abutments, and extending to 16.00m depth in DDBH-07 in left abutment and 14.40m in DDBH-06 in right abutment. It occupies the foundation from right end to left end of the abutment, except the riverbanks and channels. According to field and laboratory studies, the soil is loose, soft, and unconsolidated, with an active, slightly flexible, firm to stiff consistency. It has low degree of swelling potential and compressibility. It is characterized by low to medium permeability and is generally semi-pervious. It is susceptible to erosion and found to be highly to intermediately dispersive, implying that it could be source of foundation piping.

B) GTL-II: - (ROCK CLASS IV, Poor Quality Rock Mass, RMR value=24): -

This is layer is found in the middle of the identified layers (geological units). It is mainly consisted of loose, soft, unconsolidated, friable and extremely weathered, very closely jointed to fragmented, weak, pervious, and un-welded to welded tuff with very high deformability. It is relatively pervious but generally semi-permeable layer.

C) GTL-III (ROCK CLASS II, Good Quality Rock Mass, RMR value= 74)

This bottom situated rock mass is found in the whole part of the foundation constituting the lower position in the investigated depths. It is relatively more consolidated and widely spaced jointed pyroclastic deposit (welded tuff). This rock mass has fresh to faintly weathered, soft, friable intact rocks which formed weak, semi-pervious to impervious, moderately deformable rock mass as a result of jointing.

3.1.3. Topography

The project area is situated at the western flank of Central Main Ethiopian Rift (CMER) that belongs to the central highlands, plateaus and associated lowlands and rift valleys of central Ethiopia represented by rugged topography because of uplift and subsequent development of the Main Ethiopian Rift (MER). The investigation area and its surroundings are characterized by elevated landscape at southwest, north & northwest parts and relatively gently flat-leveled dissected landscape at the dam site area and its reservoir extent. Both dam option sites and their reservoir areas form gently sloping topography towards southeast. Gradually flat-laying parts of this area is covered by thick silt to clay fraction black to brownish soil in which observation of bedrock only possible following the deeply dissected gorges, streams and rivers that are outcropped bay un-welded-welded tuffaceous pyroclastic deposits, ash and minor ignimbrites. Locally, low-lying flats of volcanic pyroclastic deposits and soil, incised rivers/streams and dissected erosional gulleys characterize the Dalocha dam and reservoir area. Elevation ranges from 1940 to 2100 meters where the maximum elevation is at southwestern hilly part of the area and the minimum is at southeastern part within Dijo River Bed.

3.2. Seismicity of the Project Area

3.2.1. General

The project location is on the western margin of the Gurage border fault, which is a frequent seismic activity zone on the Central Main Ethiopian Rift System. As per the recent developments in earthquake engineering, large dams and safety relevant structures shall be designed to withstand safety evaluation earthquake (SEE) without creating uncontrolled release of water and threat for life. As the project is situated in major settlement vicinity, the project component shall be addressed for safety issues against possible seismic induced instabilities. Thus, site-specific seismic hazard assessment for different level of return period is necessary for seismic design of dam and other projects structures. Site-specific Probabilistic Seismic Hazard Assessment (PSHA) study of the project site been conducted as part of this project. In the assessment, it is found out that the Kalid Dijo dam site is a point of concern, as it is located at the western margin of the Gurage border fault where seismic activity is frequent. Hence, it has high hazard values. The PGA values for different annual frequency of exceedance have been extracted from uniform hazard spectra. A PGA

value of 0.45g has been cited in the PSHA report for a return period of 2500 years. However, for higher return period, the study does not incorporate the PGA values; hence, estimation has been carried out from uniform hazard spectra (UHS). (ECDSWC, 2019).

As seen in Figure 3-2, Red circles represent earthquakes that occurred for the last 110 years in the region and size of the circles is proportional with magnitude. The yellow rectangle shows the locations of the planned Kalid - Dijo Dam project site.

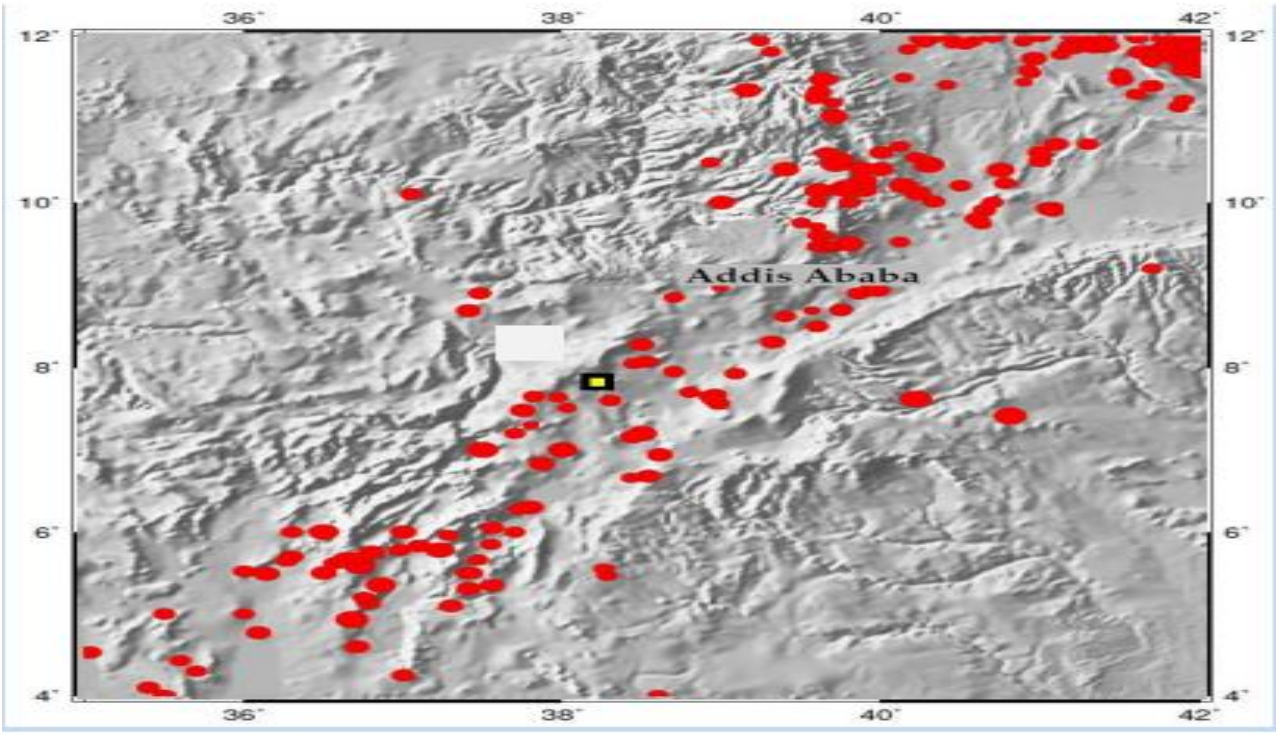

Figure 3-2: Seismic activity data, including the Kalid-Dijo project site (ECDSWC, 2019).

3.2.2. Seismic Study Results

In the Probabilistic Seismic Hazard Assessment (PSHA), Spectral acceleration has been calculated for different annual frequency of exceedance and periods and shown in Table 3-1. It is witnessed that Kalid-Dijo dam site has relatively higher hazard values (ECDSWCo. 2019).

Table 3-1: Spectral acceleration for different annual frequency of exceedance (Source: ECDSWCo, 2019)

Return Period in Years	Ground Motion Amplitude in % of g for Boore-Joyner-Fumal (1993,1997)					
	Period =0.2 sec		Period =1.0 sec		Period =2.0 sec	
	Rock	Soil	Rock	Soil	Rock	Soil
100	15.04	15.99	4.92	5.60	3.23	3.58
500	31.54	33.48	9.13	10.53	5.57	6.31
1,000	41.12	42.76	11.91	13.82	7.05	8.06

2,500	51.16	53.72	16.93	19.81	9.61	11.13
10,000	71.20	75.87	27.64	32.11	15.36	18.14

3.2.3. Fundamental period of Embankment Dam

The first three vibration modes determine the behavior of an embankment dam. An empirical equation may be used to estimate the period in the plane strain problem method. This approach allows for the usage of traditional shear wedge solutions. (Ambraseys, 1967), studies a homogeneous triangular elastic wedge under plane strain circumstances and derives the fundamental period:

$$T_i = 2.61\frac{H}{Vs} \quad \text{(3-1)}$$

$$\mathbf{T_i = 1.13\frac{H}{Vs}} \quad \text{(3-2)}$$

$$\boldsymbol{T_i = 0.72\frac{H}{Vs}} \quad \text{(3-3)}$$

Where, H = Dam height in meters, Vs = Shear wave velocity in m/s.

For the dam under investigation, H is approximately 31 meters from the bottom of the cut-off level, and the embankment material with the lowest average shear wave velocity can be considered for safety concerns among the various dam materials.

Table 3-2: Shear wave velocity for different zones of embankment dam (Source literature)

Zone	Description	Shear wave velocity (Vs) in (m/s)			
		Min	Max	Average Value	Minimum of Average Values (m/s)
Clay Core	High Plasticity Clay (CH)	205	405	305	305
Granular Shell	Sand-Gravel mixture	205	840	522.5	
Rock fill	Sand-Gravel mixture	270	380	325	

Accordingly, the first three fundamental periods are estimated as follows;

Table 3-3: The first three fundamental period of embankment dam

Mode of Vibration	Period	Remark
T1	0.265	Using Eqn. (3.1)
T2	0.115	Using Eqn. (3.2)
T3	0.073	Using Eqn. (3.3)

The Kalid-Dijo Dam site will be investigated for the three vibration modes mentioned above. However, deformation of a dam embankment is often not susceptible to high frequency shaking with periods less than 0.2 second (USBR, Design Standard 13 and Chapter 13). As a result, analysis will be performed for the first period (T1 = 0.265).

3.3. Embankment, Geometry and Zoning

3.3.1. Embankment

The proposed dam is located on Dijo Seasonal River and it will be used to supply water for the proposed potential land just downstream of the dam. Basin wise, the project is located in Rift Valley River Basin with geographic coordinates of 868194 UTM Northing and 413216 UTM Easting.

During the feasibility stage, Ethiopian Construction Design and Supervision Works Corporation suggested two different dam design options based on technical and budgetary considerations. The suggested dam design choices are:

- Alternative 1: Zoned Earth-Rock Fill Dam with Central Clay Core and
- Alternative 2: Composite dam (Zoned Rock fill with gravity spillway overflow section) having central clay core for the embankment section.

However, detail investigation works done at the left and right banks of the central river confirms that the lithology is dominantly composed of soil materials which are relatively susceptible to erosion and hence placing a spillway at the middle of the river will be risky and hence was not for further detailed design. Therefore, during final stage, detailed design

is done for the alternative one i.e. zoned Earth-Rock Fill Dam with Central Clay (ECDSWCo., 2020).

3.3.2. Embankment Geometry

The dam is designed as zoned embankment dam with central clay core. A central core has the advantage of increasing pressure at the contact between the core and the foundation, which reduces the chance of leakage and piping. (USBR, 1973) Points out that the normal freeboard must be sufficient to prevent seepage through a core that has been cracked due to drying out. This suggests that the core crest elevation shall be maintained nearly equal to the normal freeboard. However, the top level of the core is generally fixed at 0.5 to 1 meter above Maximum Water Level (MWL) to prevent seepage by capillary siphoning or equal to PMF level. Based on these considerations, therefore, for Kalid Dijo dam, the MWL being at 1975.1masl, the top level of the core is fixed at EL 1976.5masl adding 1.40m above the MWL which is also corresponding to the PMF level.

The minimum top width of the core as specified by Indian standards is 3m and usually from construction point of view, the minimum width recommended is 3m. Therefore, a top width of 3m is provided.

Fell et al (2005) stated that according to common practice, a core width at the base, or cutoff, should be at least 25% to 50% of the difference between the maximum water level in the reservoir and the minimum tail-water elevation. According to Indian standard, the thickness of a core at any section is specified to be above 30% (preferably not lesser than 50 percent) of the maximum water head acting at that section.

According to Kutzner (1997), typical sloping of the vertical core on both sides is 1V:0.25H to 1V:0.4H. Besides to avoid potential hydraulic fracturing and thus piping hydraulic gradient across the core should be around two but preferably less than ($i<2$). Therefore, based on the above technical considerations and standards consultation and seeing the availability of suitable impervious material, and after evaluating the dam seepage-stability performance a core crest width of 3m and a similar upstream and downstream core face slope of 1V:0.4H is adopted.

3.3.3. Dam Zoning

The dam is designed as zoned embankment dam with central clay core. The shell materials will be composed of inner shell material, which coarser texture earth material whereas the outer shell zone will be rock fill. The proposed zoning is shown in Figure 3-3. The proposed zoning materials are:

Zone 1: Impervious Clay,

Zone 2: Filters i.e. zone 2A fine filter and zone 2B coarse filter

Zone 3**:** Granular shell,

Zone 4: Rock fill and

Zone 5: Riprap.

The shell materials will be composed of inner shell material, which coarser texture earth material whereas the outer shell zone will be rock fill.

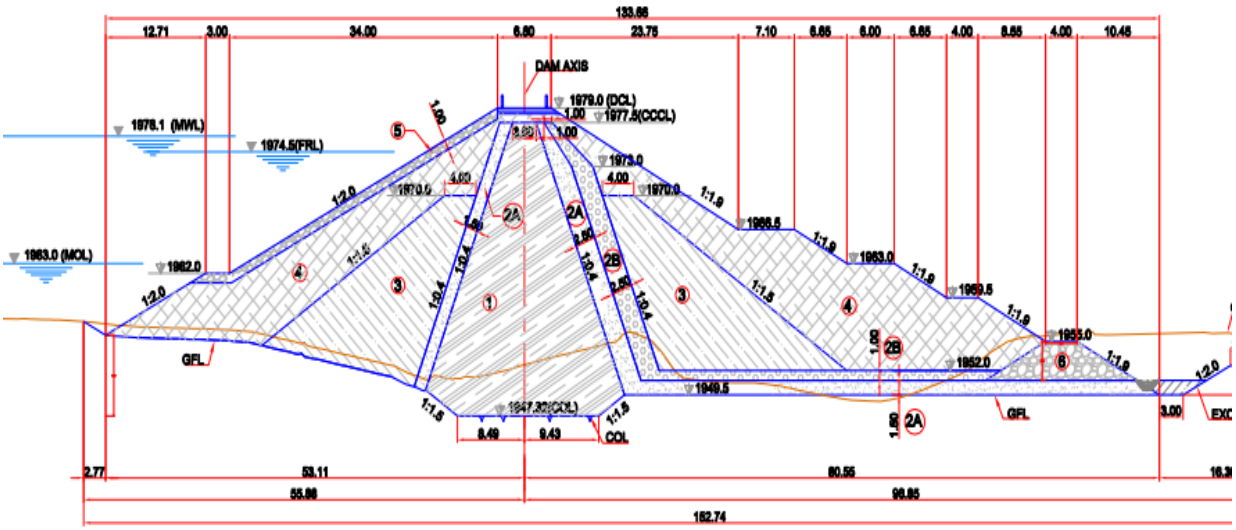

Figure 3-3: Dam Zoning for Zoned Earth-Rock Fill with Central Clay Core at Chainage 1+160 (at deepest cross section).

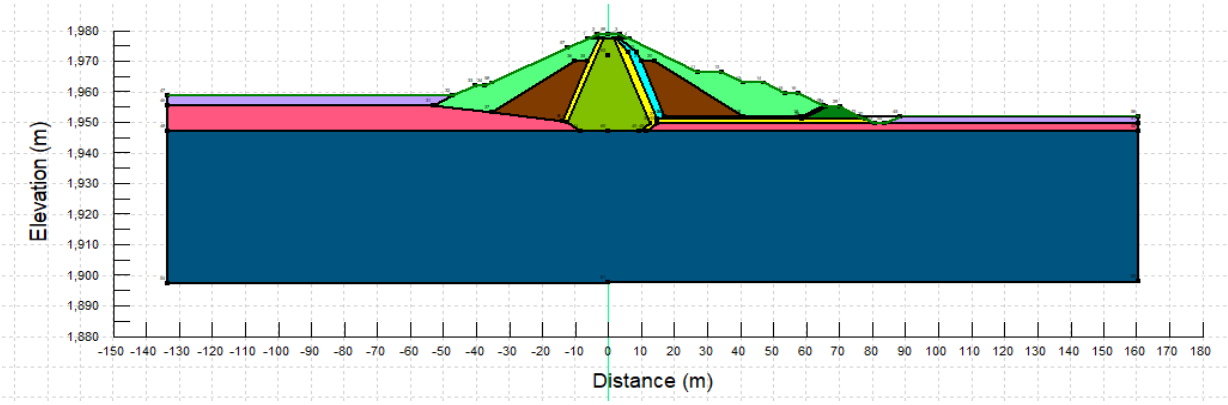

Figure 3-4: Dam Zoning for Zoned Earth-Rock Fill with Central Clay Core including foundation

3.4. Material parameters used in different analyses

The engineering characteristics of soil are key components of any geotechnical investigation. The geotechnical soil parameters utilized in the current study were obtained from the Kalid-Dijo dam project, Geotechnical investigation and Final design reports developed by ECDSWCo, and the others, from Geotechnical Literatures. These are detailed in the sections below.

3.4.1. Hydraulic parameters of embankment and foundation materials

3.4.1.1. Definitions of Some Soil Properties

Coefficient of Compressibility, m_v: - is the slope of the volumetric water content function in the positive pore-pressure region, indicating how much a saturated soil volume will expand or shrink (SLOPE/W, 2018).

Hydraulic Conductivity, K; - The hydraulic conductivity function measures a soil's ability to conduct water under saturated and unsaturated circumstances (SLOPE/W, 2018).

Volumetric Water Content: - Describes the capability of the soil to store water under changes in matric suctions. It describes what portion or volume of the voids remain water filled as the soil drains. Saturated volumetric water content is used as an input to generate the function in SEEP/W (SLOPE/W, 2018). Figure 3-5 shows the volumetric water content verses the matric suction of different materials used in the analysis.

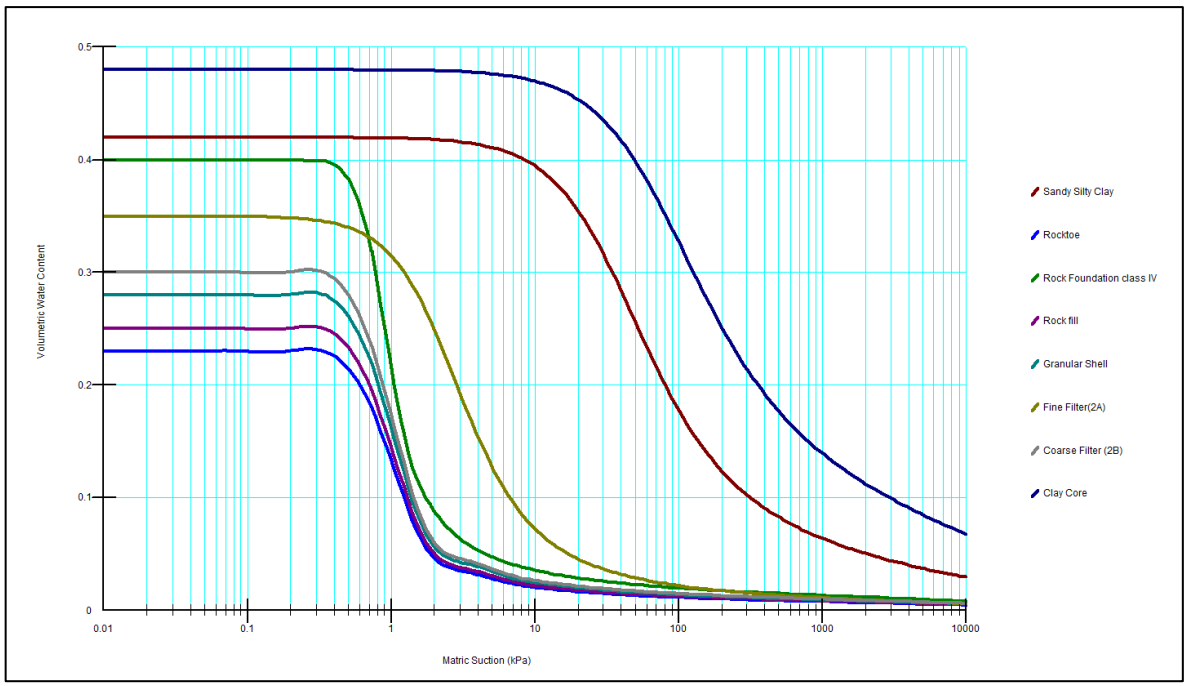

Figure 3-5: Volumetric water content verses Matric suction graph

The hydraulic parameters of dam materials collected from the final design study for the Kalid-Dijo dam project reports and other geotechnical literatures were shown in Table 3-4.

Table 3-4: Seepage analysis parameters (adopted from ECDSWCo. reports, Seep/W modeling Engineering book; Krhan, 2004), P. Novak, 2007) and other Literatures.

No	Description	K(cm/s)(Sat)	SVWC	Coefficient of compressibility, m_v (1/kPa)
1	Clay Core	$6.52x10^{-8}$	0.48	$1.75*10^{-4}$
2	Fine Filter	1x10-4	0.35	$1.5*10^{-4}$
3	Coarse Filter	1x10-3	0.30	$1.0*10^{-4}$
4	Granular Shell	3.2x10-3	0.28	$5.5*10^{-5}$
5	Rock fill	1x10-2	0.23	0
6	Riprap	1x10-2	0.23	0
7	Rock toe	1x10-2	0.23	0
8	Sandy silty clay	1x10-7	0.42	$1.4*10^{-4}$

9	Foundation Rock class IV	2.1x10-6	0.4	$1.0*10^{-4}$
10	Foundation Rock class II	2.62x10-7	0.23	0

3.4.2. Unit weight and Shear Strength Parameters

a) Shear Strength

A soil's shear strength is defined as its maximum resistance to shearing stresses that may be mobilized. Shear strength is often measured using two shear strength parameters:

- Apparent cohesion, c, essentially arising from the complex electrical forces binding clay-size particles together;
- Angle of shearing resistance,ϕ developed by inter-particle frictional resistance and particle interlocking.

Reservoir full/steady state analysis is expressed in terms of effective stress shear strength parameters (c' and ϕ'). The total stress parameters, c and ϕ are only suitable for short-term and approximate analyses, such as stability at an intermediate stage during construction Zoned dam construction requires high compaction effort, resulting in higher c' and ϕ‘values indicating material stiffness (Novak, 2007).

Accordingly, the shear strength parameters for clay core was taken from CU Triaxial test results done at ECDSWCo Geotechnical Laboratory for similar dam projects and also the parameters for gravel shell, rock fill, filters and rock toe materials are taken from Kalid-Dijo dam project design reports; checking it with the values used for other similar projects and literatures.

b) Soil unit weight

The soil is allocated a unit weight so that the sliding mass weight or gravitational force may be applied. The slice weight is determined by multiplying the cross-sectional area by the specified unit weight. The soil's unit weight is calculated by dividing its total weight by its total volume. These material properties are taken from final design report of the Kalid - Dijo dam project and are summarized in the table below.

Table 3-5: Material parameters of embankment fill and foundations employed in seepage and stability study (Kalid-Dijo Geotechnical Investigation Report) (ECDSWCo., 2020).

No	Description	Unit weight (kN/m3)	c'(kPa)	$\phi'^{(0)}$	Remarks
1	Clay Core	17.4	27	21	Adopted from similar dam projects (CU Test Results)
2	Fine Filter	20	0.0	30	Kalid-Dijo Design Reports
3	Coarse Filter	20	0.0	32	" "
4	Granular Shell	18	5	30	" "
5	Rock fill	22	0.0	40	" "
6	Riprap	22	0.0	40	" "
7	Rock toe	22	0.0	40	" "
8	Sandy Clayey Silt	16	30	18	" "
9	Foundation Rock class IV	20	40	20	Typical Values from Literatures
10	Foundation Rock Class II	Bed rock (Impermeable)			Kalid-Dijo Design Reports

3.4.3. Material parameters for Stress Deformation Analysis

The seepage phases of the studies make advantage of the embankment materials' drained stress-strain and strength properties, which is compatible with the idea of employing a long-term steady state seepage as the pre-earthquake stress. The following parameters are used to characterize the soil stress-strain behavior in stress deformation analysis of embankment dams (Jansen, 1988).

- **The modulus number K and the modulus exponent N: -** Calculate the confining pressure based on the initial slope of the stress-strain curve (the initial tangent modulus). The higher the value of K, the larger the soil's initial tangent modulus at a confining pressure of one atmosphere; and the higher the value of n, the faster the modulus rises with increasing confining pressure.

- **The strength parameters C and ϕ: -** Useful in connecting soil strength to confining pressure using the traditional Mohr-Coulomb strength equation.
- **The parameter R_f (Failure ratio):-** The stress-strain curve's shape is determined by the association between actual soil strength, asymptotic deviator stress, and initial tangent modulus value. R_f represents the ratio of actual strength to asymptotic deviator stress.
- **The bulk modulus number $K^{(0)}$ and the bulk modulus exponent m: -** Relate the soil's bulk modulus to the confining pressure. The larger the value of K (0), the greater the bulk modulus at a confining pressure of one atmosphere. The greater the value of m, the faster the bulk modulus rises with increasing confining pressure.

To achieve the expected performance of the zoned embankment dam, the rock fill materials constituting the shells must exhibit sufficient strength, a minimum reduction of strength parameters as strain progresses, manageable settlement, and an adequate degree of permeability in order to effectively control any pore pressure build-up arising with cyclic loading and during embankment construction. The parameters of various dam materials adopted for this analysis are seen in Table 3-6 below.

Table 3-6: Parameters used for static stress deformation calculations (Source: Kalid-Dijo dam report by ECDSWCo and Duncan et al. (1980)).

No	Description	Strength Parameters				Stress-Strain Parameters			
		Unit weight (kN/m3	C'(kPa)	ϕ'(°)	ν	K	N	R_f	$K^{(0)}$
1	Clay Core	17.4	27	21	0.4	150	0.45	0.7	0.826
2	Fine Filter	20	0.0	30	0.33	300	0.4	0.7	0.47
3	Coarse Filter	20	0.0	32	0.33	450	0.4	0.7	0.47
4	Granular Shell	18	5	30	0.2	500	0.4	0.7	0.44

5	Rock fill	22	0.0	40	0.2	800	0.4	0.7	0.33
6	Riprap	22	0.0	40	0.2	800	0.4	0.7	0.33
7	Rock toe	22	0.0	40	0.15	800	0.4	0.7	0.33
8	Sandy Silty Clay	16	30	18	0.4	400	0.5	0.7	0.75
9	Rock Class IV	20	40.0	20	0.22	E = 1000MPa –From KD Design Report			
10	Rock Class II	Bed Rock (Impermeable)			0.2	E = 2000MPa—From KD Design Report			

3.4.4. Dynamic material properties

3.4.4.1. Shear Modulus

In QUAKE/W, the maximum/initial shear modulus (G_{max}) can be defined as a function of soil stress state; as soil stiffness typically rises with confining or overburden stress (QUAKE/W, 2018). G_{max} is regarded as a small-strain shear modulus and thus the maximum value for a specific soil.

QUAKE/W describes soil stiffness as a function of depth using the relationship shown below (QUAKE/W, 2018).

$$G = K_G(\sigma'_m)^n \quad \text{---------- (3-4)}$$

Where G is the shear modulus, K_G is a modulus number, σ'_m is the mean effective stress, and n is a power exponent (generally, n is taken as 0.5).

The broadly employed empirical equation settled by Seed and Idriss (Seed, 1970) was used to compute G_{max} and the analogous modulus number K_G, which are shown below.

$$G_{Max} = 220K_{2max}(\sigma'_m)^{0.5} \text{ (in kPa)} \quad \text{---------- (3-5)}$$

Then, from eqn.3.4 and eqn. 3.5, we obtain:

$$K_G = 220.K_{2max}$$ ---------- (3-6)

Where:

G_{max} = maximum shear modulus, K_{2max} = Stiffness parameter/coefficient which is the function of relative density and soil type and σ'_m = mean effective stress.

The K_2max values for Kalid-Dijo dam materials are collected from the 'Detailed study and design report of Kalid-Dijo dam project', which is established based on Seed and Idriss' curves. The K_2max value for the clay core was also taken from the 'Detailed study and design report of the Kalid-Dijo dam project', which was determined based on the publication by Malla et.al. (2005).

Except for the rock foundations, the maximum shear modulus of entire dam materials in the current study is considered to vary with mean effective stress using the above formulae, as showed in Figure 3-6. Table 3-7, shows the values used for the coefficient K_{2max} in relative to other parameters.

For the rock foundations, the following equation stated in Quake/W, 2007, engineering book, is used to estimate the shear modulus and shown in Table 3-8. The modulus of elasticity was determined for the rock mass (Rock mass class II and IV).

$$G_{max} = \frac{E}{2(1+\nu)}$$ ---------- (3-7)

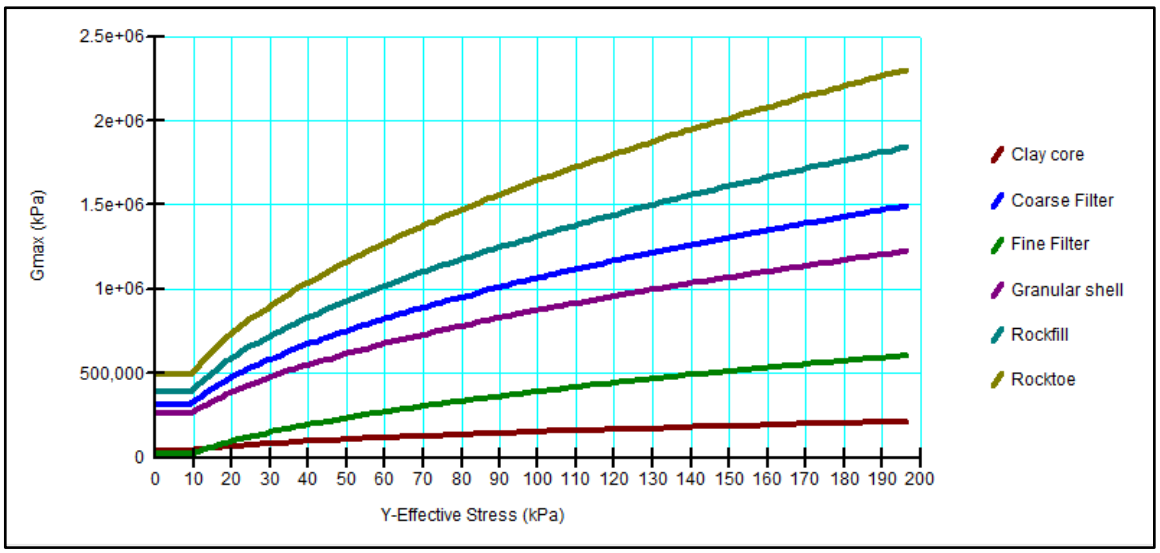

Figure 3-6 : G_{max} functions for dam materials

Table 3-7**:** Coefficient, K_{2max} values (ECDSWCo., 2020).

Material	Zone	K_{2max}	K_G	ν
Clay Core	1	40	8,800	0.4
Filters	2	50	11,000	0.33
Inner Granular Shell	3	90	19,800	0.3
Rock fill	4	80	17,600	0.2
Riprap	5	80	17,600	0.2
Rock Toe		80	17,600	0.15
Sandy Silty Clay		30	6,600	0.4
Foundation rock Class II, E = 2000MPa, ν=0.2 and Foundation rock class IV, E = 1000MPa, ν=0.22.				

Table 3-8: Initial G_{max} values (As per eqn. 3.7).

No.	Foundation type	Initial G_{max} (in MPa)	Remark
1	Highly weathered tuff (Rock class IV)	410	Using Eqn. (3.7)
2	Moderately weathered Pyroclastic rock Welded tuff (Class II)	833	

3.4.4.2. Shear Modulus Reduction Function

Dynamic stresses cause the soil to 'soften' in response to shear strain. Figure 3-7 depicts the Equivalent linear soil model's description of softening, as a ratio to G_{max}. This is called the Modulus Reduction Function (G-Reduction Function). The dynamic shear strain is computed using finite element analysis. The computed shear strain, together with the function and the specified G_{max}, is utilized to create new G values for each iteration (QUAKE/W, 2018).

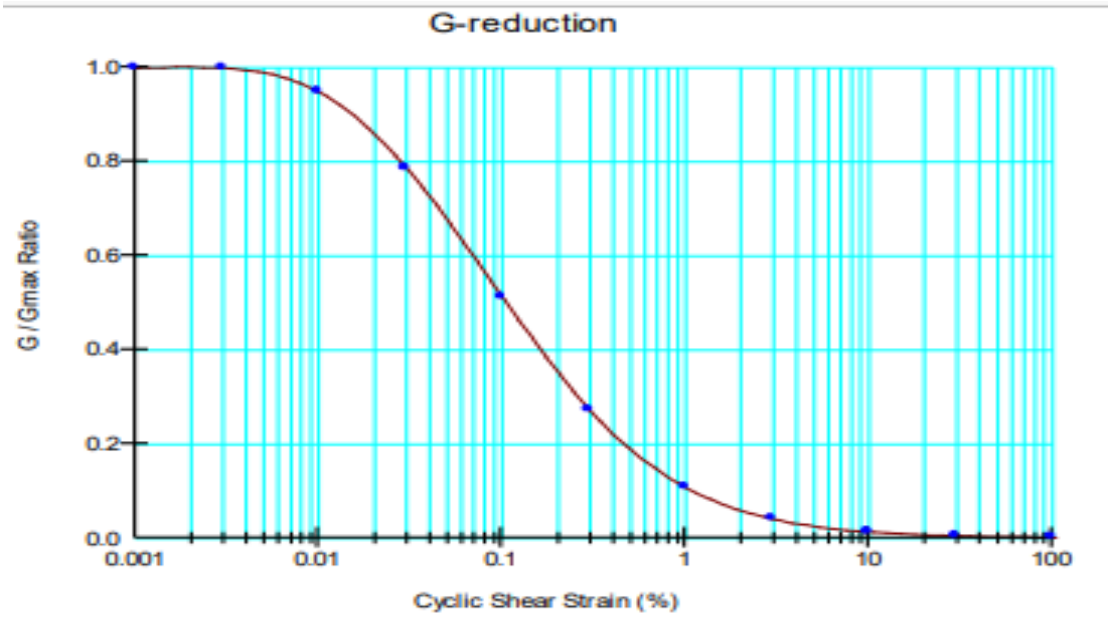

Figure 3-7: A typical G reduction function.

3.4.4.3. Damping ratio/ Damping ratio functions

The damping ratio in QUAKE/W, like G_{max}, can be specified as either a constant or a function. The damping ratio, like the G-reduction function, depends on cyclic shear strain. Figure 3-8, shows a typical damping ratio function. As the dynamic shear strain increases, the effective dynamic shear modulus decreases below the maximum value Gmax. At the same time, the nonlinear response at higher dynamic strains causes a faster rate of energy dissipation, as indicated by an increasing damping ratio (QUAKE/W, 2018).

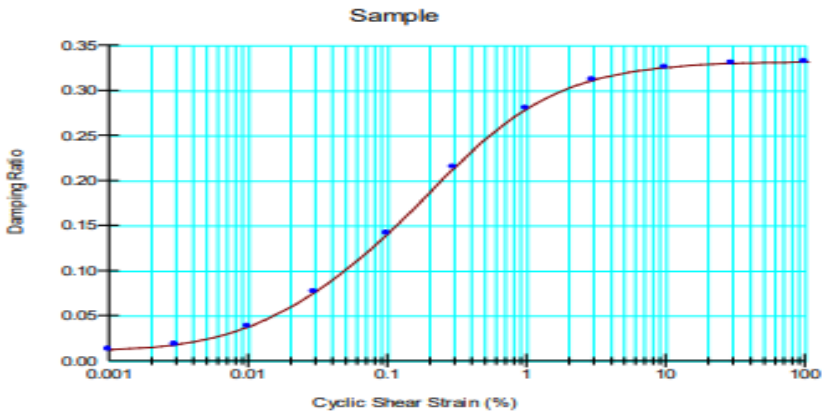

Figure 3-8: Typical damping ratio function

The dam under investigation was dynamically analyzed using strain-dependent dynamic shear modulus and damping ratio functions for various dam and foundation materials.

These functions are summarized in Figure 3-9 and Figure 3-10 represent a summary of these functions.

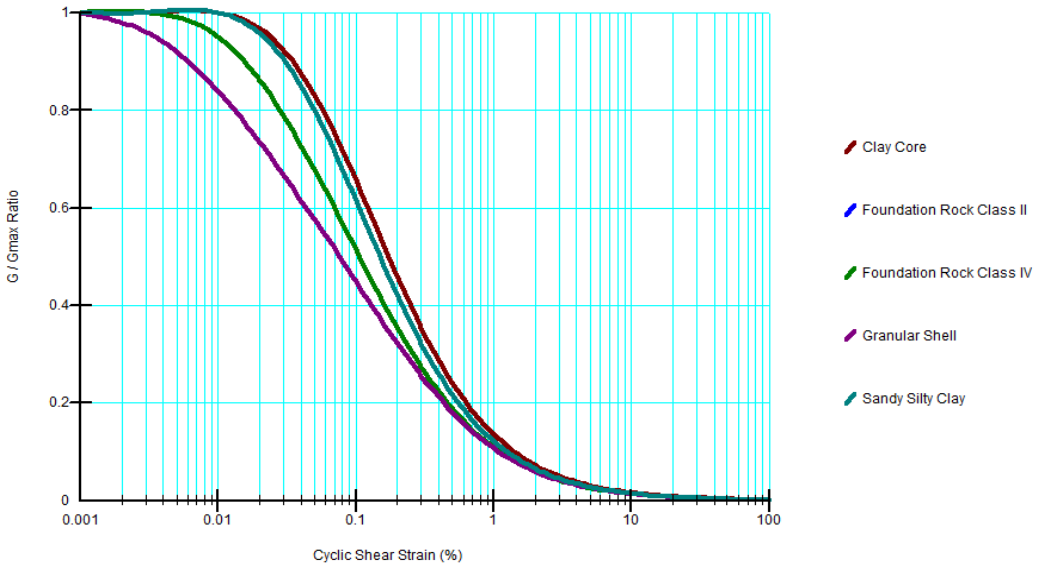

Figure 3-9: G-Reduction functions for dam and foundation materials

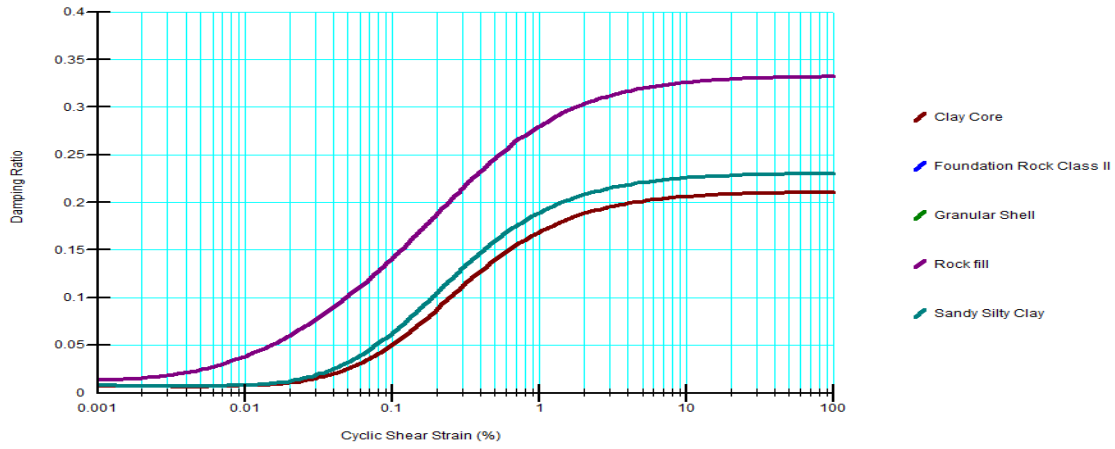

Figure 3-10: Damping ratio functions for dam and foundation materials

3.4.4.4. Excess Pore Pressures resulting from the Cyclic Stress Ratio (CSR)

3.4.4.4.1. General

The Equivalent Linear soil model incorporates a pore-pressure generation model based on Cyclic Stress Ratios (CSR).The idea is that a certain number of shear stress cycles at a specific shear amplitude will generate enough excess pore pressure to cause the soil to liquefy. So, one of the goals of dynamic finite element analysis is to determine the peak CSR values that will occur during the earthquake. Excess pore pressures can be calculated once the CSR of each element is known (QUAKE/W, 2018).

3.4.4.4.2. Pore pressure ratio (R_u) function

The pore pressures formed during earthquake shaking are proportional to the equivalent number of uniform cycles, N for a specific earthquake and the number of cycles N_L required to cause liquefaction in a specific soil under a given set of stress conditions.

3.4.4.4.2.1. Equivalent cyclic stresses

Earthquake shaking is extremely variable and irregular, resulting in highly variable and irregular shear stress in the ground. However, laboratory tests were extensively carried out by scholars; repeatedly applying a uniform stress cycle. As a result, we can understand soil behavior under dynamic loading using uniform stress cycles.

Therefore, to make use of laboratory test data in an earthquake analysis, it is necessary to interpret an irregular shear stress record in terms of an equivalent number of uniform stress cycles (QUAKE/W, 2018).

According to Seed et al. (1975b), the most common approach is to set the uniform cyclic shear amplitude to 65% of the peak shear stress in the irregular shear stress time history. In equation form:

$$\boldsymbol{\tau_{cycle} = 0.65\tau_{peak}} \quad \text{---------- (3-8)}$$

Seed correlated the number of 0.65τ uniform stress cycles with the increase in pore pressures caused by actual ground motions. Figure **3-11** illustrates the result (reproduced from Kramer, 1996).

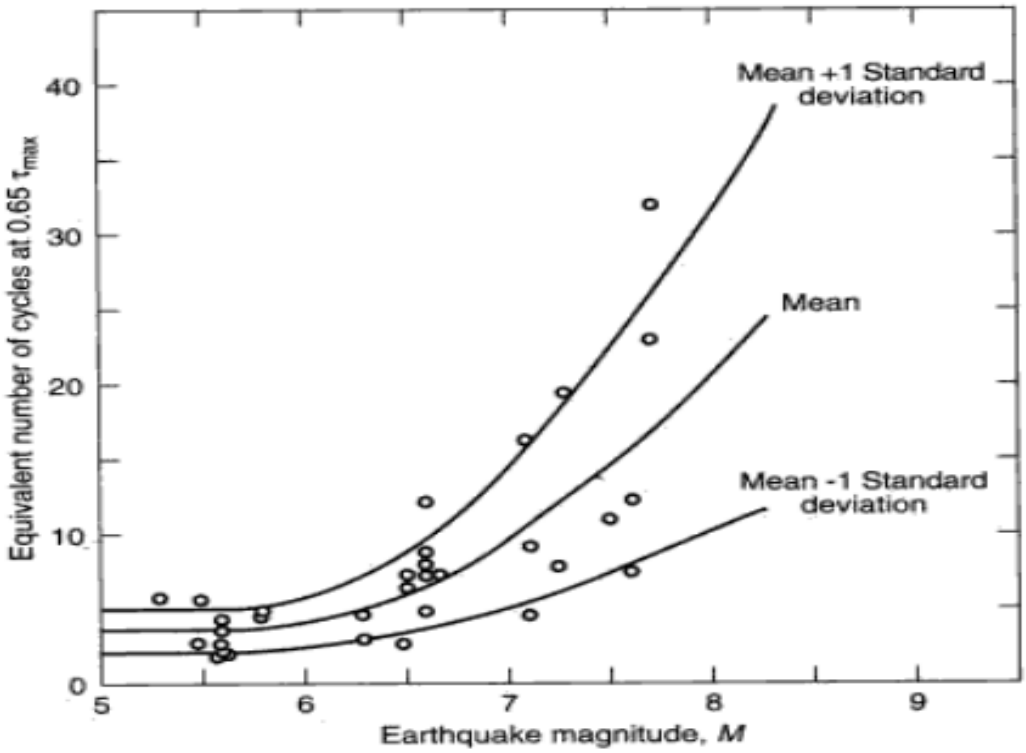

Figure 3-11: Equivalent uniform cycles versus earthquake magnitudes

The uniform cycle amplitude in QUAKE/W is set to $0.65\tau_{peak}$ during the analysis. However, this constant can be adjusted as needed.

Figure 3-11 depicts the relationship between the number of uniform cycles and earthquake magnitude. Each analysis requires a specified number (N) based on site conditions. The pore-pressure calculations utilize N, as explained in the next section.

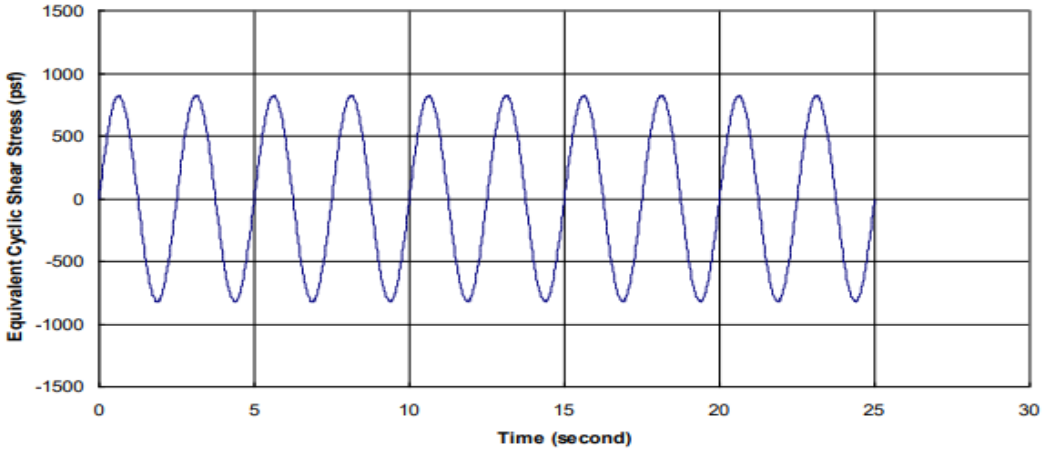

Figure 3-12: Equivalent cyclic shear stress (QUAKE/W, 2018).

3.4.4.4.2.2. Cyclic number functions

A key soil property associated with the concept of CSR's is a relationship between CSR and the number of cycles, N_L required to produce liquefaction. The relationship is described by what is known as a Cyclic Number function. A cyclic number function must be attached to the pore pressure function in order to define N_L. For high shear stress ratios (defined as the ratio of cyclic deviatoric stress to initial static effective vertical stress), only a few cycles may be needed to cause liquefaction, whereas low ratios necessitate a greater number of cycles. The cyclic number function defines this relationship. Figure 3-13 depicts cyclic number function curves obtained from shaking table tests on sand (DeAlba et al., 1976; USNRC, 1985).

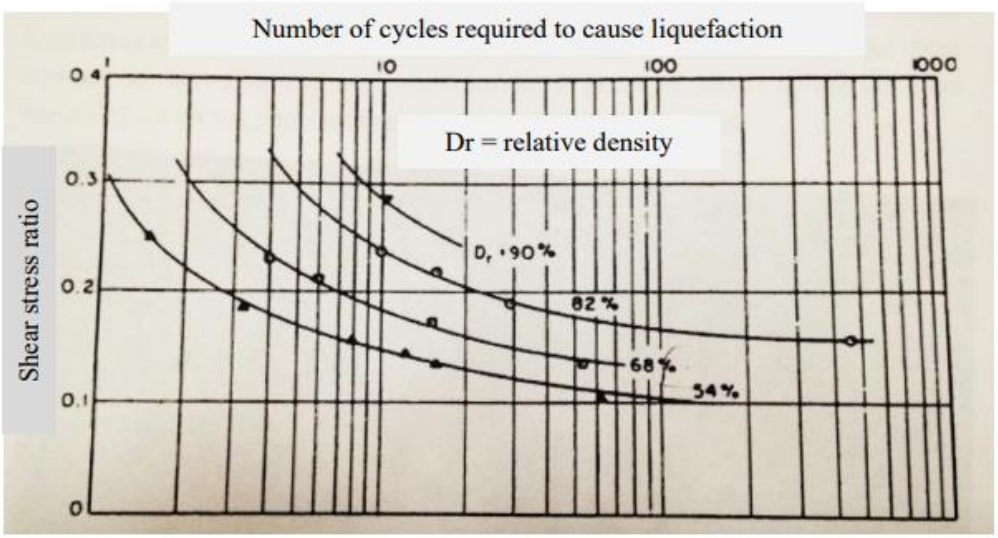

Figure 3-13: Cyclic number function used for analysis ((DeAlba, et al., 1976) (USNRC, 1985).

The cyclic number function for sandy silty clay soil was developed during dynamic modeling in Quake/W and illustrated in Figure 3-14 below.

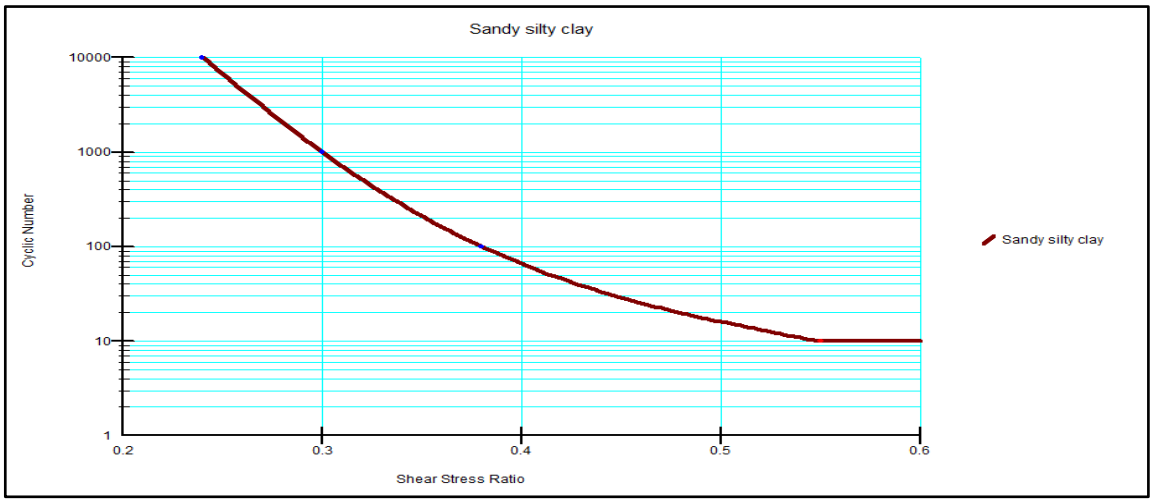

Figure 3-14: Cyclic Number functions for Sandy silty clay foundation soil of Kalid-Dijo dam (taken from Quake/W model)

The N/N_L ratio is then correlated with the pore pressure parameter R_u [(QUAKE/W, 2018), (Kramer, 1996)].

Lee and Albaisa (1974) and DeAlba et al. (1975) discovered the following equation to describe the pore pressure ratio function:

$$R_u = \frac{1}{2} + \frac{1}{\pi}\mathrm{Sin}^{-1}\left[2\left(\frac{N}{N_L}\right)^{1/\alpha} - 1\right]$$ ---------- (3-9).

Where, N = the equivalent number of uniform cycles, N_L = number of cycles required to produce liquefaction, α = is a constant value obtained based on soil properties and test conditions.

In QUAKE/W, the pore pressure function is estimated using the above equation (eqn. 3.8). To estimate different functions, different values of α can be entered based on soil properties and test conditions.

Because the thin layer of sandy silty clay soil foundation found at upstream and downstream of the dam was confirmed to be prone to liquefaction, the pore pressure function developed based on the function stated in equation (3.8) was used only for this foundation soil for confirmation purpose during the dynamic analysis in QUAKE/W. The pore pressure function shown in Figure 3-15 (taken from Quake/W model, which in turn obtained using equation 3.8, for α = 0.7) was assigned for the sandy silty clay foundation soil of the dam under study, for liquefaction analysis.

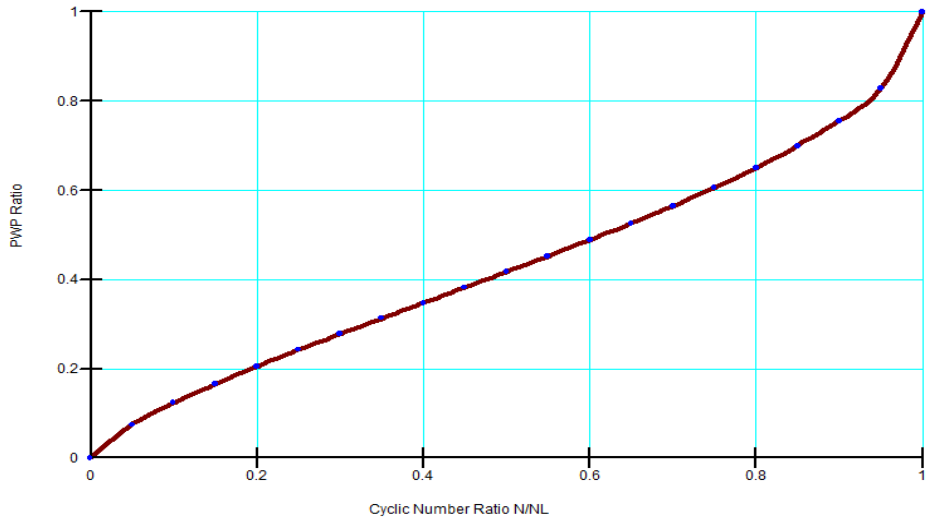

Figure 3-15: Cyclic number ratio N/N_L versus pore pressure ratio, R_u for Sandy silty clay soil and granular shell (taken from Quake/W model).

In most cases, the shell materials are well graded and suitable for good compaction (or densification), reducing the susceptibility to liquefaction. Messele and Hadush's (Messele et al., 2006) dynamic analysis of the Tendaho earth fill dam assumed that sandy gravel

shell as potentially liquefiable soil, and the result has shown that all of that materials have been liquefied. However, the researchers rejected the results, explaining that the pore pressure function similar to shown in Figure 3-15 was designed primarily for potentially liquefiable sands and cannot represent the behavior of these sandy gravel shell materials. Consequently, liquefaction analysis using sandy gravel shell material as a potentially liquefiable material for the Kalid-Dijo zoned earth-rock fill dam yields the same conclusion. Accordingly, the Kalid-Dijo inner shell (zone 3) materials are considered as non-liquefiable soils with only the possibility of pore water pressure build up during earthquake shaking. To account for pore water pressure buildup, a constant R_u value of 0.25 is used for the inner shell (zone 3), and $R_u = 0.40$ is used for the clay core, as shown in Table 3-9 below.

Table 3-9: Pore-water pressure ratio, R_u values for construction conditions (ECDSWCo., 2020)

Material zone	Pore-water pressure ratio, R_u during construction	Pore-water pressure ratio, R_u at the end of construction
Impervious Clay Core(Zone 1)	0.40	0.35
Granular Shell (Zone 3)	0.25	0.20

The number of cycles required to cause liquefaction (N_L) can be adjusted for overburden and initial static shear stresses by incorporating Ka and Ks correction functions into the cyclic number functions, as discussed below.

3.4.4.4.2.3. Overburden Pressure Correction function, K_s

The cyclic shear stress required to cause liquefaction increases in proportion to the confining stress (Kramer, 1996). To account for this, the QUAKE/W specification includes a Ks function. Marcuson et al. (Marcuson, 1978) investigated the relationship between correction factor Ks and effective overburden pressure in various soils. The Ks correction function is defined as part of the cyclic number function data. The overburden correction factor influences N_L and thus affects the calculated pore-water pressure value. Based on this, the K_s function shown in Figure 3-16, (corresponding to the estimated average curve for sand) has been used for the Sandy silty clay soil foundation of the Kalid –Dijo dam.

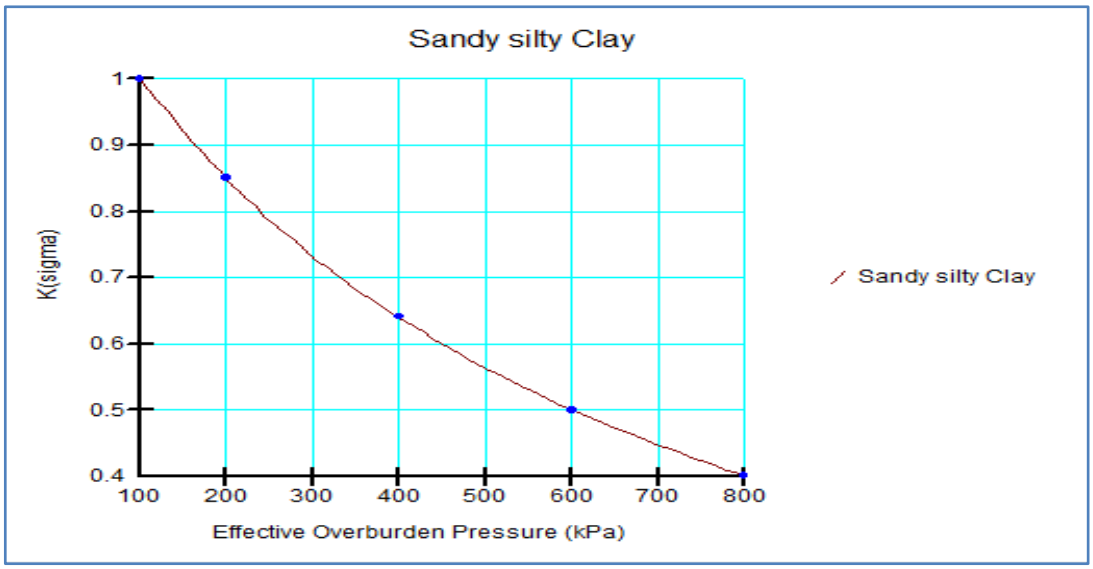

Figure 3-16: K_s Correction function used for the analysis

QUAKE/W includes a sample function for sand and for gravel. These sample function were adapted from data presented by Kramer (1996). These sample functions, like all of the property functions in QUAKE/W, can be modified to meet site-specific requirements if necessary.

The Quake/W computed dynamic stresses could be interpreted as field stresses after corrections ($CSR_{Field\ Corrected}$). Before correction, the Cyclic Number function specified by the user represents the field's cyclic stress ratio (CSR_{Field}). The finite element computed CSR values are divided by Ks to obtain a value that corresponds to the specified values in the Cyclic Number function in Quake/W. In equation form:

$$\mathbf{CSR_{fn}} = \frac{\mathbf{CSR_{FE}}}{\mathbf{K_S}} \quad \text{(3-10)}$$

- Once the finite element computed CSR is divided by Ks, QUAKE/W uses the Cyclic Number function to obtain N_L.

3.4.4.4.2.4. Shear Stress Correction Function, K_a

The initial in situ static shear stresses, like the overburden stress, influence the cyclic stress required to cause liquefaction (Kramer 1996).

This function is determined by soil density. Seed and Harder (Seed et al., 1990) presented the shear stress correction function for various relative densities in Figure 3-17.

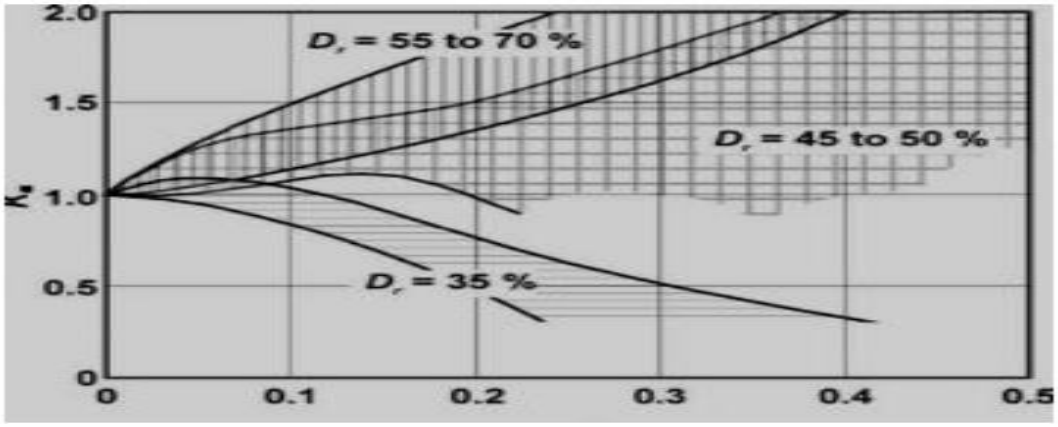

Figure 3-17: Ka Correction factor (Seed, et al.1990)

The Shear Stress Ratio correction value is designated as Ka, where a stands for alpha (α). In QUAKE/W alpha (α) is defined as;

$$\alpha = \frac{q_{Static}}{\sigma'_{vo}} \text{---------- (3-11)}$$

Where, q is the deviatoric stress, in a triaxial tests $\tau_{max} = q/2$.

The QUAKE/W computed dynamic stresses could be thought of as the field stresses after corrections ($CSR_{field\ corrected}$). The user specified Cyclic Number function generally represents the field cyclic stress ratio (CSR_{field}) before correction. Therefore, in QUAKE/W, the finite element computed CSR values are divided by K_a to get a value corresponding to the specified values in the Cyclic Number function. In equation form:

$$CSR_{fn} = \frac{CSR_{FE}}{K_a} \text{ – – – – – – – – – – – – – – (3-12)}$$

- Once the finite element computed CSR is divided by Ka, QUAKE/W goes to the Cyclic Number function to get N_L.

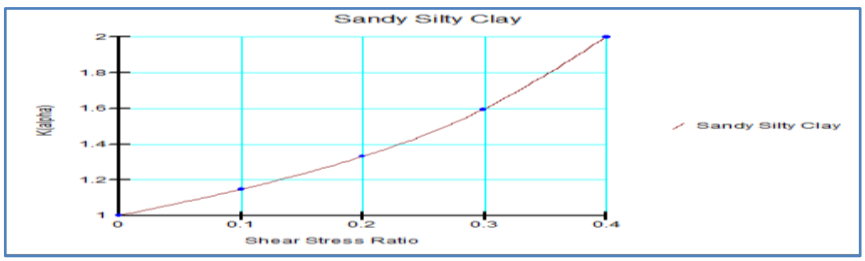

Figure 3-18: Ka Correction function used for analysis

Based on Figure 3-17, the K_a function shown in Figure 3-18 has been used for the sandy silty clay foundation soil of Kalid-Dijo dam.

3.4.5. Geosynthetic (geotextile) reinforcement material parameters

Among the geosynthetic materials in geotechnical applications, the woven geotextile material type was being considered as a reinforcement material for this study. Because, woven geotextiles are an excellent choice for reinforcement and stabilization applications, while nonwoven geotextiles are great for filtration, separation, and drainage applications (FEMA, 2008).

"Geotextiles are a "permeable geosynthetic comprised solely of textiles" (ASTM, 2005). Geotextiles perform a variety of geotechnical engineering functions and are used for a variety of both critical and noncritical applications in all aspects of Civil Engineering design on a large number of dams worldwide (FEMA, 2008). Geotextile structures are comprised of the following two major types:

1) Nonwoven geotextiles

Geotextiles formed with continuous or short fibers arranged in random directions and then bonded together into a planar structure Figure 2-8**,** which can include the following:

- Nonwoven Mechanically Needle punched
  - Continuous Filament Fiber
  - Staple Fiber (short fibers)
- Nonwoven Heat Set
  - Continuous Filament Fiber

2) Woven geotextiles

Geotextiles composed of two sets of parallel yarns or tapes systematically interlaced to form a planar structure Figure 2-7, which can include the following:

- Multifilament woven
- Monofilament woven
- Slit Film woven
- Fibrillated woven

Tensile strength, pullout resistance due to friction or adhesion and the amount of extension exhibited by the element under tensile stress are critical properties of geosynthetic reinforcement needed for this application.

- When the tensile strength of an element is low, it can break or yield and become ineffective.
- If the tensile strength is adequate but its extension under stress is high, then the soil may show large movement (settlement or lateral bulging) because of inadequate stiffness of the soil-reinforcement system
- If the reinforcement element is sufficiently strong and rigid but there is inadequate adherence between the soil and the reinforcement, then relative movement can occur, making the reinforcement ineffective.

Reinforcement in soil interacts with the soil through friction, adhesion or passive/bearing resistance. Among geosynthetic families, geogrids and geotextiles are that mostly can be utilized for soil reinforcement purposes, Geotextile are adopted as reinforcement when the requirement of low extensibility are not very high and when these are also required to perform other functions simultaneously, such as facilitate drainage, separation, or filtration.

Soil-geosynthetic interaction tests are realistic models of soil-geotextile systems that can be used to evaluate specific design properties. In most cases, index tests do not directly relate to the actual design function, especially where the soil properties influence the design. Therefore, for all critical applications or when severe conditions exist, soil-geotextile interaction tests should always be performed. Because this, performance tests using the specific soil conditions, it will be necessary in most cases to preselect the geotextile(s) to be evaluated (USBR-DS-13). However, the interface friction angle and adhesion values used in the analysis of the dam under study were adopted from geotechnical literatures. The following values were taken into consideration by compiling from different literatures that show the values for these parameters, specifically for woven geotextile materials. The pictures of these materials were shown in section 2.4.3 and figures Figure 2-7 and Figure 2-8.

Table 3-10: Interface shear characteristics of various soil-geotextile (IJGGE, 2016).

Interface	Adhesion, α (kPa)	Interface friction angle, δ (^{0})
Red soil-geotextile	13.7	11.7
Geotextile-gravel	0	9.1

- According to Das (2007) and Terzaghi and Peck (1967), the interface friction angle, δ is equal to two third of the angle of internal friction of the granular backfill (ϕ^0). i.e. $\delta = 2/3\ \phi = 0.67\ \phi$.
- According to Bowles (1984), $\delta = 0.6\ \phi - 0.8\ \phi$.
- According to Dr. - Ing. Samuel Lecture Note; on 'Reinforced Soil', 'tan δ' usually varies between '1/2tan ϕ' to 'tan ϕ' i.e. tan δ' = (1/2tan ϕ) to (tan ϕ).

Table 3-11: Frictional properties and stiffness of geotextile (Koerner, 2005).

Geotextile name	**Thickness (mm)**	**Friction (^{o})**	**Stiffness (E) (kPa)**
Comtrac175(W/PET)	4.0	0.86ϕ	1,000,000
Comtrac400(W/PET)	6.0	0.86ϕ	1,250,000

Table 3-12**:** Ultimate tensile strength and long term design strength adopted from geosynthetics magazine (IFAI, 2012)

Name of Fabric	Mass per unit area ASTM D5261 (g/m2)	Reinforcement applications					
		Wide-width Tensile/Elongation ASTM D4595 (kN/m)/ (%)				Creep Limited Strength –MD, ASTM D5262 (kN/m)	LTDS MD kN/m
		Strength @ 5% strain		Ultimate Strength (Tutl) (kPa)			
		Machine Direction	Cross Machine Direction	Machine Direction	Cross Machine Direction		
Comtrac175 (W/PET)	410	90	NA	200(10)	-	122	95
Comtrac400 (W/PET)	700	180	NA	400(10)	50	245	203

As a result, the material parameters of the geotextile reinforcement to be provided for reinforcing the slopes of the dam under study were considered according to Koerner, 2005

that is shown in Table 3-11. The ultimate tensile strength and long-term design strength was adopted from geosynthetics magazine (IFAI, 2012).The allowable strain (elongation) values have also been included as shown in the parenthesis

3.5. Seepage Analysis in SEEP/W

3.5.1. General

A numerical method is a computer-based approach for solving a mathematical problem that does not have an analytical solution. A numerical model is a mathematical representation of a real-world physical process. Numerical modeling is entirely mathematical, which distinguishes it from scaled physical modeling in the laboratory or full-sized field modeling (GEO-SLOPE International Ltd.).

3.5.2. Material Models in Seepage analysis

3.5.2.1. Introduction

Water movement through soil is a significant phenomenon in geotechnical and geo-environmental engineering. Indeed, if water did not exist in the soil, geotechnical engineering would be unnecessary. This is a ridiculous statement: without water in the soil, there would be no way to sustain an ecosystem, no humans on the planet, and no need for geotechnical and geo-environmental engineering. The declaration does, however, stress the importance of water when working with soil and rock (SEEP/W., 2018). Flow quantity is an important factor in determining reservoir seepage losses and locating a potential water source for domestic or industrial use. Pore pressures and groundwater flow are especially important in geotechnical engineering.

3.5.2.2. Material models used in SEEP/W

SEEP/W offers four different material models to choose from. The following is a summary of these models and the required soil properties, as well as a discussion of the individual parameters and functions were presented.

None model: - (used to removed part of a model in an analysis)

Saturated / Unsaturated model:

- Hydraulic conductivity function, ratio and direction

- Water content function

Saturated only model:

- Hydraulic saturated conductivity (Ksat), ratio and direction,
- Saturated water content

Interface model

- Hydraulic normal and tangent conductivity

The Saturated only soil model is extremely useful for quickly defining a soil region that will always remain below the phreatic surface, but it should not be used for soils that will become partially saturated during the analysis. If this occurs, the model will continue to solve, but it is possible to conclude that the unsaturated zone can transmit water at the same rate as saturated soil. This will result in an overestimation of flow quantity, which could lead to an unrealistic water table.

Based on the above stated clues, material models that have been attached to different zones of embankment material have been shown Table 3-13.

Table 3-13: Seepage analysis with Seep/W: material model and properties

Material Zone	Model	Material Properties
Clay Core	Saturated/Unsaturated	Hydraulic Conductivity function Water content function
Fine Filter (2A)	Saturated/Unsaturated	Hydraulic Conductivity function Water content function
Coarse filter (2B)	Saturated/Unsaturated	Hydraulic Conductivity function Water content function
Granular shell	Saturated/Unsaturated	Hydraulic Conductivity function Water content function
Rock fill	Saturated/Unsaturated	Hydraulic Conductivity function Water content function

Riprap	Saturated/Unsaturated	Hydraulic Conductivity function Water content function
Rock Toe	Saturated/Unsaturated	Hydraulic Conductivity function Water content function
Sandy Clayey Silt	Saturated/Unsaturated	Hydraulic Conductivity function Water content function
Foundation	Saturated only	Hydraulic saturated conductivity (Ksat) Saturated water content
Interface element	Both models	Hydraulic saturated conductivity (Ksat) Saturated water content

3.5.2.3. Boundary Conditions in SEEP/W

3.5.2.3.1. Fundamentals

One of the most important aspects of numerical analysis is the ability to control the conditions on a problem's boundaries, which is why these problems are commonly referred to as "boundary-valued" problems. Numerical solutions are direct responses to boundary conditions. A solution cannot be obtained in the absence of boundary conditions. What is the source of the seepage flow? It is the difference in hydraulic total head between two points, or any specific rate of flow into or out of the system. The response within the problem domain to the specified boundary conditions is the answer (SEEP/W, 2012). SEEP/W employs a finite element approach in seepage analysis. For a seepage analysis, the finite element equation is (Seep/W, 2018):

$$[K]\{H\} = \{Q\} \quad ---------- \quad (3\text{-}13)$$

Where: [K] = a matrix of coefficients related to geometry and materials properties,

{H} = a vector of the total hydraulic heads at the nodes, and

{Q} = a vector of the flow quantities at the node

The primary goal of a Finite Element analysis is to solve for the primary unknowns, which in the case of seepage are the total hydraulic head at each node. The unknowns will be computed using the H values specified at some nodes and/or the Q values specified at others. It is impossible to solve the finite element equation without specifying either H or

Q at some nodes. In a steady-state analysis, at least one node in the entire mesh must have the specified H condition. The specified H or Q values serve as boundary conditions. A critical point to remember is that boundary conditions can only be one of two options. At each node, we can only specify one of the H or Q values. These are the only options available, though they can be used in a variety of ways (SEEP/W, 2018).

However, in some cases, we may not know either H or Q. A seepage face is a boundary condition in this case. We know that the pore-water pressure is zero (H equals elevation) at the point where the seepage face forms, but we do not know how big the seepage face will be. In such cases, an iterative procedure is required to test either H or Q boundary conditions until the correct solution is obtained (SEEP/W, 2018).

3.5.2.3.2. Boundary condition locations

Geo-Studio software requires that all boundary conditions be applied directly to geometry components such as region faces, region lines, free lines, and free points. A boundary condition cannot be applied to an element's edge or node. Tying the boundary conditions to the geometry has the advantage of making them independent of the mesh, allowing the mesh to be modified without losing the boundary condition specification (GEO-SLOPE International Ltd).

a) Head boundary condition

The primary unknown or field variable in SEEP/W is total hydraulic head, which is calculated by adding pressure head and elevation. The elevation represents the gravitational component. The total head can be expressed mathematically as follows:

$$H = \frac{u}{\gamma_w} + y \quad (3\text{-}14)$$

Where:

H = the total head (meters)

u = the pore- pressure (kPa) ,

γ_w = the unit weight of water (KN/m3),

y = the elevation (meters).

The term u/γ_w is referred to as the pressure head – represented in units of length

b) Boundary functions

SEEP/W is designed to withstand a wide range of boundary conditions. In a steady state analysis, all boundary conditions are either fixed heads (or pressures) or fixed flux values. However, in a transient analysis, the boundary conditions can also be functions of time or in response to flow amounts leaving or entering the flow regime.

Among the various boundary functions integrated in SEEP/W, the head versus time boundary function is a very useful boundary condition used in the current study, for transient analysis and constant or fixed values boundary conditions, for steady state seepage analysis.

c) Head versus Time boundary function

A boundary function that allows the user to specify the head versus time is extremely useful. The advantage of having a head versus time function on the reservoir side of the dam is that it prevents a "shock" unloading of the dam's water pressure if the reservoir's water level is suddenly reduced to a specific elevation.

3.5.2.4. Analysis Types in SEEP/W

Finite element seepage analysis is divided into two types: steady state and transient. In steady state analysis, the pore pressure is estimated for a long-term steady state situation. As a result, the analytical state remains constant. Transient seepage analysis, on the other hand, takes place in a changing pore water pressure scenario. It is changing because it considers how long it takes the soil to respond to the boundary conditions specified by the user. Both analyses were used in this study.

3.6. Slope Stability Analysis using SLOPE/W

3.6.1. Analysis types

Geo-Slope International Ltd. offers several packages; including SLOPE/W. SLOPE/W has four analysis options in Geo-Studio 2018, which were used in this study. These options are listed below:

- Limit Equilibrium Analysis

- SIGMA/W Stress Analysis
- QUAKE/W Stress Analysis and
- QUAKE/W Newmark Deformation Analysis

I) Limit Equilibrium Method of Stability Analysis in Geo-Studio.

For decades, geotechnical engineers have used limit equilibrium analyses to determine the stability of earth slopes. The idea of dividing a potential sliding mass into vertical slices was first introduced in the early twentieth century, making it the oldest numerical analysis technique in geotechnical engineering.

Modern limit equilibrium softwares, such as SLOPE/W, enables analysts to deal with ever-increasing complexity. Complex stratigraphy, highly irregular pore-water pressure conditions, a variety of linear and nonlinear shear strength models, virtually any slip surface shape, concentrated loads, and structural reinforcement can now all be handled. Limit equilibrium formulations based on the slice method are progressively being used to analyze the stability of structures such as tieback walls, nail or fabric reinforced slopes, and even the sliding stability of structures subjected to high horizontal loading caused, for example, by ice flow. Among limit equilibrium method of analyses available in SLOPE/W, Morgenstern-Price and Spencer approaches are the only ones that contain all interstice forces and satisfy all static equations. As a result, the Morgenstern - Price approach shall be adopted for limit equilibrium analysis purposes of this study.

II) Finite Element Method of Stability Analysis in Geo-Studio

To incorporate a stress-strain relationship into a stability analysis, finite element analysis is used to determine the ground stress distribution, which is then applied to the stability analysis.

In addition to the limit equilibrium methods of analysis, SLOPE/W also provides an alternative method of analysis using the stress state obtained from SIGMA/W, a GEO-SLOPE program for stress and deformation analysis. SIGMA/W Stress, QUAKE/W Stress and QUAKE/W Newmark Deformation Analyses listed above are categorized in finite element method of analysis available in SLOPE/W.

3.6.2. Material Strength and Material models

There are numerous methods for describing the strength of materials (soil or rock) in a stability analysis. In several SLOPE/W soil models, Mohr-Coulomb was used to calculate material strength properties.

a) Saturated shear strength

The most common way to describe the shear strength of geomaterials is by Coulomb's equation, which is expressed in equation form as follows (GEOSLOPE, 2018):

$$\tau = c + \sigma_n \tan\emptyset \quad (3\text{-}15)$$

Where:

τ = shear strength (i.e. shear at failure),

c = effective cohesion,

σ_n = effective normal stress on shear plane, and

$\emptyset$ = angle of internal friction

b) Unsaturated shear strength

Soil suction, also known as negative pore water pressure, increases soil strength. Positive pore-water pressures reduce effective stress and thus strength; conversely, negative pore-water pressures increase effective stress and therefore strength. The unsaturated soil's shear strength is ((GEOSLOPE, 2018):

$$\tau = c' + \sigma_n \tan\emptyset' + (u_a - u_w)_f \tan\emptyset^b \quad (3\text{-}16)$$

Where;

c’ = effective cohesion,

u_a = net normal stress state on the failure plane at failure,

u_w = the pore – water pressure

Φ' = effective angle of internal friction,

Φ^b = angle indicating the rate of increase in shear strength with respect to a change in matric suction, $(u_a - u_w)$

The term $(u_a - u_w)$ is called suction when presented as a positive number. The angle Φ^b is a material property. For practical purposes, Φ^b can be taken to be approximately ½ $\emptyset'$ (SLOPE/W, 2018).

Significant study has been conducted by different scholars, in order to better of a soil's unsaturated shear strength utilizing the soil-water characteristic curve and the effective shear strength parameters (c' and Φ') rather than using Φ^b. The following calculation equation given by Vanapalli et al. (Vanapalli, et al., 1996) is combined in SLOPE/W as a higher alternative to the use of Φ^b to describe the increase in shear strength due to soil suction:

$$\boldsymbol{\tau = c' + (\sigma_n - u_a)\tan\emptyset' + (u_a - u_w)\left[\left(\frac{\theta_w - \theta_r}{\theta_{s-\theta_r}}\right)\right]\tan\emptyset'} \quad ------(3\text{-}17)$$

Where,

θ_w = the volumetric water content, θ_s = the saturated volumetric water content and θ_r = the residual volumetric water content.

During modeling in SLOPE/W, the residual volumetric water content was assumed 10% of the saturated volumetric water content. It is worth noting that Φ^b is not employed in the preceding equation (equation 3.16) and this approach was used for the analysis of the dam under current study.

c) Pore-water Pressure

When effective strength parameters are used in the analysis, the critical slip surface is located in the most realistic position. However, effective strength properties are only useful

when combined with pore-water pressures. As a result, the pore-water pressure in this study was estimated using SEEP/W steady-state seepage and transient analyses.

3.6.3. Mobilization of reinforcement forces in slope stability analysis

In SLOPE/W, equilibrium equations are based on shear mobilized at the base of each slice, which is calculated by dividing shear strength by the safety factor. The mobilized shear S_m is expressed as:

$$S_{m=} \frac{S_{Soil}}{F\,of\ S} \text{----------} \quad (3\text{-}18)$$

If reinforcement is used to increase shear resistance, the reinforcement forces must also be divided by the safety factor. S_m is then given by:

$$S_{m=} \frac{S_{Soil}}{F\,of\ S} + \frac{S_{Reinforcement}}{F\,of\ S} \text{----------} \quad (3\text{-}19)$$

It is worth noting that both soil strength and shear resistance due to reinforcement are divided by the same overall global factor of safety. As a result, soil shear resistance and reinforcement shear resistance both grow and mobilize at the same rate.
If the reinforcement is considered to contribute to the reduction of the destabilizing force, it is assumed that it is fully mobilized immediately, and thus the reinforcement forces are not divided by the overall global factor of safety. Because geo-fabrics (geosynthetics) are used as reinforcing materials, the current analysis takes the approach of viewing reinforcement as an add-on to soil shear resistance.

3.7. Stress-Deformation analysis using SIGMA/W

3.7.1. Introduction

SIGMA/W is a finite element software program for analyzing stress and deformation in earth structures. Its extensive formulation enables it to investigate both simple and complex situations (SIGMA, 2012).

SIGMA/W can calculate stress deformation with or without pore-water pressure changes caused by stress state changes. Soil structure interaction can also be modeled using beam or bar structural elements. The following are some common cases that SIGMA/W can examine (SIGMA, 2012):

Deformation analysis: - The most common application of SIGMA/W is to compute deformations caused by earthworks such as foundations, embankments, excavations and tunnels.

Staged construction: - Soil regions can be activated or deactivated at different stages in a project file, making it possible to simulate the process over time.

Excess pore-water pressures: - The effect of excess pore-water pressures generated during fill placement is often a major consideration in slope stability during construction. SIGMA/W can be used to estimate these types of pore-water pressures.

Soil-structure interaction: - GMA/W can accommodate soil-structure interaction problems by including structural elements in two-dimensional plain strain analyses. These elements can be beam elements, which have flexural stiffness, or bar elements, which have only axial stiffness with no flexural stiffness.

Consolidation analysis: - SIGMA/W can be used together with SEEP/W to perform a fully coupled consolidation analysis. When these two integrated products are run simultaneously, SIGMA/W calculates the deformations resulting from pore-water pressure changes while SEEP/W calculates transient pore-water pressure changes.

3.7.2. Constitutive Models and Material Properties

SIGMA/W is designed to work with a variety of elastic and elastic-plastic soil constitutive models. All models can be applied to two-dimensional plane strain and axisymmetric problems.

3.7.2.1. Linear-elastic model

The linear elastic model, Figure 3-19 is the simplest SIGMA/W soil model, in which stresses are exactly proportional to strains. Young's Modulus, E, and Poisson's Ratio, ν, are the proportionality constants. Table 3-14 includes other crucial parameters.

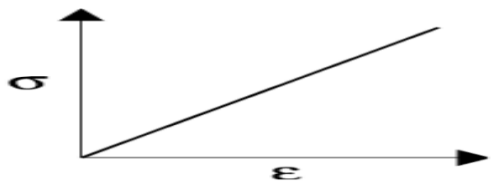

Figure 3-19: Linear- elastic model

Table 3-14: Linear-elastic material properties

Parameter Name	Property/Characteristics
E Modulus	Young's Modulus
Poisson's Ratio	Constant value
Cohesion	Constant value
Friction angle	degrees

3.7.2.2.Elastic-plastic model

The SIGMA/W Elastic-Plastic model describes a relationship that is both elastic and completely plastic. Figure 3-20 depicts the typical stress-strain curve for this model. Stresses and strains are proportional until the yield point is reached. Above the yield point, the stress-strain curve is perfectly horizontal.

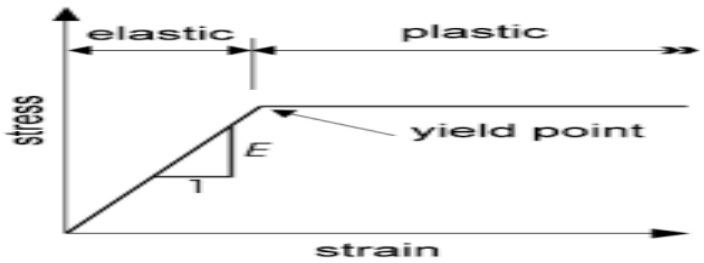

Figure 3-20: Elastic – perfectly plastic constitutive relationship (SIGMA/W, 2018)

The material properties required for this model are given in Table 3-15.

Table 3-15: Elastic –plastic material properties (SIGMA/W, 2018)

Material Name	Property
E Modulus	Initial Linear-elastic stiffness of the soil
Poisson's Ratio	Constant value
Cohesion	Cohesive strength of the soil
Phi	Soil internal friction angle Φ in degrees
Dilation Angle	Soil dilation angle ψ in degrees ($0 \leq \psi \leq \Phi$)

	If a value is not specified, the dilation angle is considered the same as phi (Φ).

As a result, in the current study, an elastic-plastic Mohr-Coulomb constitutive model is used to characterize the geomaterials' behavior because elastoplastic analysis is a useful tool for investigating dam stability under seismic loading.

Functions of the E-modulus

The soil stiffness modulus, E can be expressed either as a constant or as a function of effective overburden stress.

The soil stiffness E is often proportional to the square root of the confining stress. Generally, the relationship is expressed as:

$$E = K\sigma^{n} \quad (3\text{-}20)$$

Where K is a soil property and n is an exponent.

An extensive laboratory testing program was carried out to measure K and n for a wide range of soils at the University of California, Berkley in the 1970's and these values were documented by Duncan et al. (1980) (SIGMA/W, 2018). For SIGMA/W modeling, the values stated in section (3.4.3) or shown in Table 3-6 were used during the analysis of the dam under current study.

To evaluate the functions of E-modulus, we must identify the maximum depth, K-modulus number, exponent n, and K^0 value. SIGMA/W uses these values to estimate data points for a function similar to the one shown in Figure 3-21.

The specified depth value is only used to define a stress range for the function. It is unrelated to any specific point in the problem geometry. The critical issue is to determine the appropriate match between E and the overburden (vertical) stress (SIGMA/W, 2018).

Sample values for K and n are available from a list for Sand/gravel, Silty Sand, Clayey Sand, Low Plasticity Silty-Sandy Clay and High Plasticity Clay in SIGMA/W. Of course, any user-defined values can be utilized as well. Furthermore, individual data points can be inputted to build any unique function deemed appropriate for a specific site (SIGMA/W, 2018).

The E-modulus functions can be defined in terms of total or effective stresses.

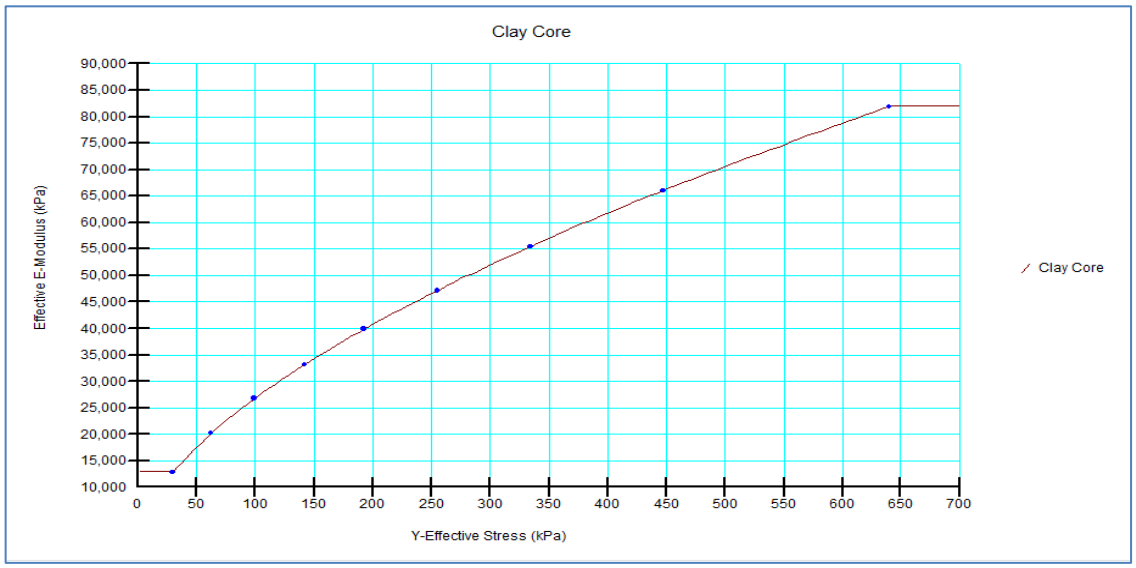

Figure 3-21: Sample E-modulus function for Clay Core (Taken from SIGMA/W Model)

3.7.3. Boundary conditions

To support almost any load-deformation modeling scenario, several boundary condition types are applied. SIGMA/W allows for displacement, force, or spring boundary conditions to be functional to points or nodes along lines, as well as stress and fluid pressure boundary conditions to element edges on lines (SIGMA/W, 2018).

3.7.4. Analysis Types

SIGMA/W is capable of solving different types of analyses. The types of analyses that are defined within a project will depend on the objective(s) of the modelling study. The more common scenario is to define multiple analyses to investigate a single problem. SIGMA/W can accommodate two-dimensional and axisymmetric analyses (SIGMA/W, 2018).

SIGMA/W is one of the packages of Geo-Slope International Ltd and has six (6) analysis alternatives in Geo-Studio, 2018. These are:

- Insitu Stress
- Stress Redistribution
- Load/Deformation

- Coupled Stress/PWP
- Volume Change and
- Dynamic Deformation Analyses.

In this study, insitu stress and dynamic deformation analyses were used. In situ stress analysis was performed to analyze the initial stress state, and dynamic deformation analysis was performed to assess post-earthquake deformation.

3.8. Dynamic analysis with QUAKE/W

3.8.1. Introduction

QUAKE/W is a geotechnical finite element software product used for the dynamic analysis of earth structures subjected to earthquake shaking and other sudden impact loading such as, for example, dynamiting or pile driving (QUAKE/W, 2018).

QUAKE/W is part of Geo-Studio and thus fully integrated with the other components, including SLOPE/W, SEEP/W, and SIGMA/W. The incorporation of QUAKE/W and other products of Geo-Studio significantly broadens the types and range of problems that can be analyzed beyond what is possible with other geotechnical dynamic analysis software. QUAKE/W can be used independently, but one of its main selling points is its integration with other Geo-Studio products.

3.8.2. Dynamic Fundamentals and Equation of Motion

The dynamic finite element equation used in Quake/W software can be expressed as:

$$[\mathbf{M}]\{\ddot{\mathbf{u}}\} + [\mathbf{C}]\{\dot{\mathbf{u}}\} + [\mathbf{K}]\{\mathbf{u}\} = \{\mathbf{P}_{(t)}\} - - - - - - \text{(3-21)}$$

Where;

- [M], [C] and [K] are the mass, damping and stiffness matrices respectively with entries referring to the nodal points,
- $\{\ddot{u}\}$, $\{\dot{u}\}$, $\{u\}$ and {P(t)} are the acceleration, velocity, displacement and external loading vectors respectively,

The stiffness matrix, [K] contains information about the constitutive behavior of the materials. [M], and [K] are obtained by the Finite element procedures and [C] is a viscous damping matric for the FE system (A.K Chopra 1967a). The primary unknown that need to be computed or solved for is displacement, u in the equation and the applied force (P) is the inertial force created by the earthquake. (i.e., = Mass of Structure times acceleration created by the earthquake.)

Hence, the main objective of the analysis is to determine the displacement 'u' (which is the primary unknown).

3.8.2.1.Procedures to solve for displacement, u

Primarily, we need to integrate the equation (3.16) above with respect to time. In this procedure, we can use the finite difference scheme, like ($\Delta t = t_{(n+1)} - t_n$). Where, n is the number of step and (Δt) is time increment at the end of the time step minus the start of the time step. Here, it is recognized that we have the time stepping procedures. In numerical methods, this is called 'the direct integration scheme'. In this scheme, we have to write 'u' in terms of the displacement at the end of the time steps and the beginning of the time steps. It is known that the displacement, u at the beginning of the time step is known from the previous time step (QUAKE/W, 2018).

Ultimately, the finite element equation takes the form shown below and this form of equation is identical to the form that is in other Geo-Studio Finite element analyses (Quake/W, 2018).

$$[\mathbf{K}]\{\mathbf{d}\} = \{\mathbf{F}\} - - - - - - - - (3\text{-}22)$$

Where;

[K] = Characteristics of the element, $\{d\} =$ Displacement and $\{F\}$ is driving force

To solve this equation, initially the earthquake shaking has to be specified either as displacement versus time boundary condition or as forcing body load. Here we can specify one of the two options, not both at a time. In Quake/W analysis, we use the second option (i.e., we specify the force on the right hand side of equation 4.7 and seek to compute the displacement, d).

3.8.2.2.Quake/W Implementations

Step1: Boundary is fixed;

- x-y is fixed at the base of the problem
- Only y or x is fixed at the side or ends of the problem (Problem dependent)

Step 2: An earthquake inertial force is specified as a body load (mass times earthquake acceleration)

Step3: We determine the mass of each element (i.e. mass is multiplied by the specified acceleration from earthquake record). These are the driving forces applied on each element nodes. Generally, in Quake/W dynamic finite element analysis, we apply a force and then compute displacements relative to fixed base.

Dynamic finite element solution gives us the motion relative to the fixed base. Because, only relative motion induces dynamic shear stresses, which is responsible for the generation of excess pore water pressure. Therefore, in engineering point of view, we are interested in relative motion rather than solid body motion in which generation of the excess pore water pressure cannot be occurred.

3.8.3. Data Collection

One of the most important challenges in dynamic analysis is access to input data. The primary inputs are material properties and earthquake data. Total unit weights, Poisson's ratio, maximum shear modulus at low strain (G_{max}), shear modulus reduction function (G/G_{max}), and damping ratio with shear strain are all fundamental material properties required for dynamic response analysis, using Equivalent linear soil model.

These material properties were collected from the geotechnical investigation and final design reports of the Kalid Dijo dam project, prepared by (ECDSWCo.); and the remaining were adopted from various geotechnical literatures and estimated using empirical relationships.

3.8.4. Constitutive (material) models in dynamic analysis

There are four different material models to choose from, when using Quake/W of Geo-Studio (QUAKE/W, 2018). These are;

- None model: - Used for detached portion of a model in an investigation.
- Linear-Elastic model
- Equivalent Linear model and
- Non-Linear model

Linear-Elastic Model

The simplest constitutive model is where the stress is directly proportional to the strain and the constant of proportionality is Young's modulus E. In equation form:

$$\boldsymbol{\sigma = E\varepsilon} \quad (3\text{-}23)$$

This is a linear r/n ship and is not related to the strength of the material. No iterative procedures are obligatory in a numerical analysis, and thus, there are no convergence issues. The linear-elastic model is not very suitable for real field problems, since in reality the stress-strain relationship is non-linear (QUAKE/W, 2018).

Equivalent Linear Model

The Equivalent Linear Model is like to the linear-elastic model, with the key variance being that the soil stiffness G is adjusted in response to calculated strains.

Non-linear model

It has long been understood that the creation of excess pore-pressures during earthquake shaking has a significant impact on the dynamic response at a specific site. To capture this behavior in a numerical model, a genuine nonlinear analysis is necessary, in which excess pore pressures are estimated and soil properties are modified during the shaking. The increase in pore-pressures alters the effective stresses and hence the soil properties; thus, this is known as a dynamic effective stress analysis.

However, the Non-linear model requires additional material parameters such as MFS (Martin Finn Seed) pore-pressure models (Recoverable modulus, MFS pore-pressure function), separate damping ratio and maximum damping ratio etc.). Hence, it is difficult to handle in this study.

The Equivalent Linear Constitutive Material Model was used to perform dynamic analysis in this research. The key characteristic to understand here is that G is a constant while stepping through the earthquake record, and it changes with each pass through the record, but it remains constant throughout one pass. Figure 3-22 depicts this graphically. The straight lines show that G remains constant over one iterative loop through the earthquake record. The change in slope represents the reduction in G between repetitions. This model requires the following material properties:

- Unit weight, Poisson's ratio, C′ and Ø′,
- Damping ratio constant or function,
- Ka and Ks functions,
- Pore-water pressure function
- G reduction function,
- G_{max} constant or function,
- Steady state strength and collapse surface angle (for liquefied zones)

Figure 3-22: G changes with each iteration of the earthquake.

The Equivalent Linear method computes excess pore pressures founded on peak dynamic shear stresses. Nevertheless, since the peak values are unknown until the termination of the dynamic analysis, the effective stresses cannot be changed during shaking. Excess pore pressures can only be calculated once the dynamic portion of the analysis is completed.

3.8.5. Earthquake Data/Input Motion

Ground motion intensity associated with an earthquake can be measured using peak ground acceleration. This is derived from the acceleration time history, modifications, and

base line correction, which are critical for determining the dynamic stability of embankment dams.

3.8.5.1. Peak Ground Acceleration (PGA)

The International Commission on Large Dams (ICOLD) states that the following three types of earthquakes must be addressed while planning a dam:

a) Maximum Credible Earthquake (MCE)

A Maximum Credible Earthquake (MCE) is the largest plausible earthquake size that is believed conceivable along a recognized fault or inside a geographically defined tectonic province, using the currently known or presumed tectonic framework. MCE ground motion is the most severe ground motion that happens at a dam site because of an MCE event (ICOLD, 2010).

b) Safety Evaluation Earthquake (SEE)

The Safety Evaluation Earthquake (SEE), also known as the maximum design earthquake (MDE) or the design base earthquake (DBE), is the greatest degree of ground motion for which a dam should be planned or studied (ICOLD, 2010).

c) Operating Basis Earthquake (OBE)

The Operating Basis Earthquake (OBE) refers to the amount of ground motion at the dam site that is acceptable for little damage. The dam, its supporting structures, and machinery must remain operational, and any damage caused by seismic shaking should be quickly repaired. (ICOLD, 2010).

The PGA values for varying annual frequency of exceedances for the dam in question were obtained from uniform hazard spectra. The PSHA study refer to a PGA value of 0.45g for a 2500-year return period. The study does not, however, offer PGA values for longer return periods; instead, uniform hazard spectra (UHS) are used for estimation (ECDSWCo., 2020).

Table 3-16: Peak ground acceleration for the Dalucha (Kalid-Dijo) Dam site (based on UHS estimates) (ECDSWCo., 2020).

Return Periods (Yrs.)	Rock Site		Soil Site	
	SA (Peak)	PGA	SA (Peak)	PGA
100	0.1504	0.11	0.1599	0.11
500	0.3154	0.23	0.3348	0.23
1,000	0.4112	0.31	0.4276	0.31
2,500	0.5116	0.45	0.5372	0.45
10,000	0.712	0.63	0.7587	0.63

3.8.5.2.Return Periods

Earthquakes must be defined analytically in order to establish acceptable seismic evaluation criteria. ICOLD Bulletin 72 defines the Safety Evaluation Earthquake (SEE) as an alternative to the Maximum Design Earthquake (MDE), Operating Basis Earthquake (OBE), and Maximum Credible Earthquake (MCE).

According to the seismic hazard evaluation report for the Kalid-Dijo dam and irrigation project, PGA values for 2500 years return period can be used to safety evaluation earthquake (SEE) based on Germany's experience. The ICOLD 72 Bulletin also suggests looking into a very long return term, such as 10,000 years, but does not specify a specific period for MCE; therefore, given the scope of the project, a 2500-year return period for SEE and a 500-year return period for OBE were considered for the current study.

Hence, for dynamic and stress deformation analysis of the Kalid-Dijo dam, the PGA values indicated Table 3-16 shall be used directly; i.e. α_h = 0.45g and 0.23g for SEE and OBE evaluations, respectively.

3.8.5.3.Acceleration Time History (ATH)

Horizontal acceleration time histories are critical input parameters in the dynamic analysis of embankment dams using QUAKE/W; the Finite Element Method. As a result, site-specific horizontal ATHs for the Kalid-Dijo dam should be computed utilizing peak accelerations and seismic data. However, because there is no ATH data exist at the dam site or project region, it is common alternative to scale real accelerographs collected elsewhere into the PGA magnitudes of the embankment dam model being considered. The

major criteria for picking time history data are the magnitude of the earthquake and the hypocentral distance.

Tensay G. (2010) on his work on Tendaho dam, stated that 'as there is no acceleration time history in / or around the area, the commonly used acceleration time history for earthquake resistant design is the 1940 El Centro (California) earthquake'.

Based on these facts, three recorded data elsewhere having their own different unique features are selected and used in the dynamic analysis of the dam under study.

- The 1940 El Centro Record, USA (M=6.7, H=11 km, R=11.5 km),
  - ✓ Several peaks in a short span of time, rich in frequency.
- 1995 Kobe JMA record, Japan (M=7.2, H=14.3 km, R=19 km)
  - ✓ Short duration, big pulse
- The 1968 Hachinohe record from Japan (M=7.9, H=0 km, R=200 km)
  - ✓ Longer duration

Where M represents ground motion magnitude, H represents focal depth (the distance from the epicenter to the focus), and R represents epicentral distance (the distance from a point of interest to the epicenter) from a nearby source (Haile, 1996).

a) ATH Data Modification

Once the data taken to QUAKE/W, it can be modified to meet the needs of a specific site or analysis (QUAKE/W, 2018). It is possible to set the peak acceleration and duration. Following that, the record is scaled to the given values. The record's form remains unchanged; only the amplitudes have been adjusted.

b) Deconvolved ATH

So as to remove site and path effects, Messele Haile (1996) has done extensive work on his doctoral thesis and the deconvolved ATH developed by him for the 1940 El Centro Record, USA (M = 6.7, H = 11 km, R = 11.5 km), the 1995 Kobe JMA Record, Japan (M = 7.2, H = 14.3 km, R = 19 km), and the 1968 Hachinohe Record, Japan (M = 7.9, H = 0 km, R = 200 km), which is the basis for the dynamic analysis of some of the research

works done in our country, like Hadush et al. (2010), Tensay G. (2010), Mohammed Abdulkadir Abdurahman, and Leulseged Abayneh Seifu (2017).

c) Baseline Correction

Data in earthquake recordings is sometimes distorted. This has little effect on a structure's dynamic response analysis, but it does produce an incorrect picture of displacement estimated from the acceleration record's double integration. QUAKE/W can update the baseline to eliminate this drift (QUAKE/W, 2018). QUAKE/W baseline correction is calculated using basic linear regression. The objective is to maintain the area of curve constant above and below the zero acceleration axes (that is, the slope of the modified linear regression line is zero). This does not imply that a double integration displacement curve near the end of the recording will always converge to zero. Even, the curve may exhibit a cumulative shift. Unnecessary displacement offsets can be further reduced by eliminating as much redundant data as possible from the start.

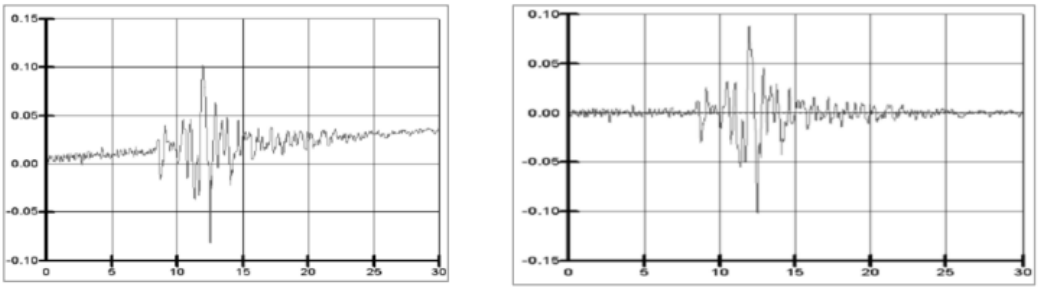

(a) (b)

Figure 3-23 (a) An earthquake record with some drift in the data, (b) An earthquake record with a baseline correction (Quake/W, 2018).

d) Time Stepping

The QUAKE/W formulation's direct integration approach requires stepping through the acceleration time history. Because of the dramatic, exceptionally fast changes in motion, it is required to progress through time history in short stages. Earthquake shaking typically lasts a few seconds, and time increments must be fractions of a second in order to capture all of the motion's features. The usual value is two hundredths (0.02) of a second. This leads to a significant number of time steps. Smaller time increments are more precise, but they take significantly more computation time and can generate significantly more data.

As with other numerical analyses, it is critical to strike a balance between numerical aims and practical repercussions such as computation time and data volume (QUAKE/W, 2018).

No guidelines for selecting time step extents. Theoretically, the time increments should be selected so that the bulk of the peaks and quick shifts are roughly recorded. To assist in establishing an appropriate time integration sequence, QUAKE/W includes a tool that allows you to generate a time integration scheme from earthquake data. This is a highly useful feature, and the preferable strategy, unless there is a compelling need to use an alternative time stepping sequence. The stated change in time (time step) integration should not exceed the time interval in the earthquake record (QUAKE/W, 2018).

In general, the scaled ATH values from three other records, 1940 El Centro, 1968 Hachinohe, and 1995 Kobe JMA, were employed for comparison in the dynamic analysis of the project under review. As a result, figures from Figure 3-24 to Figure 3-29 show the ATH data scaled to the horizontal SEE and OBE PGA values of 0.45g and 0.23g, respectively.

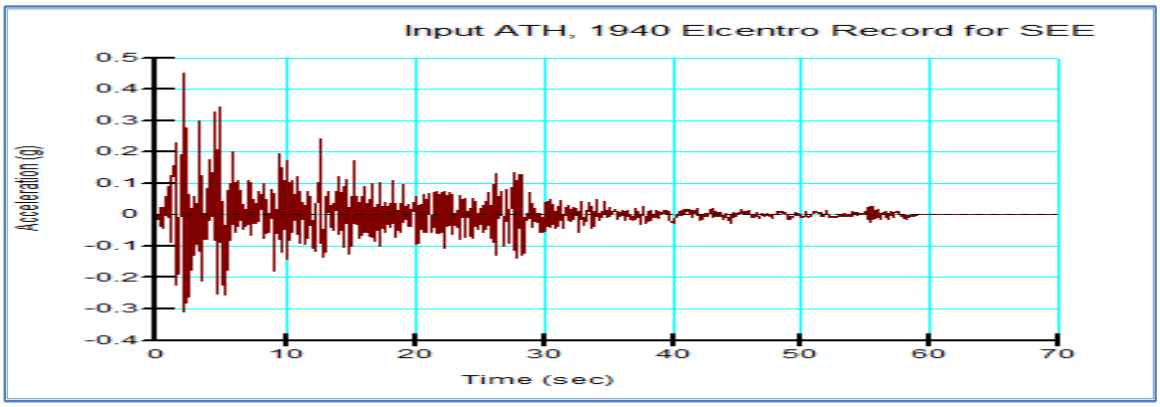

Figure 3-24: Modified input acceleration time histories for El Centro SEE

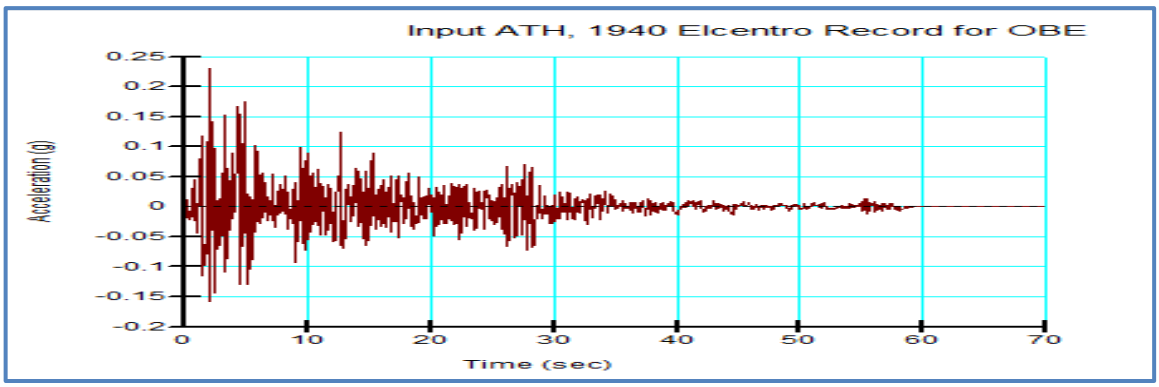

Figure 3-25: Modified input acceleration time histories for El Centro OBE

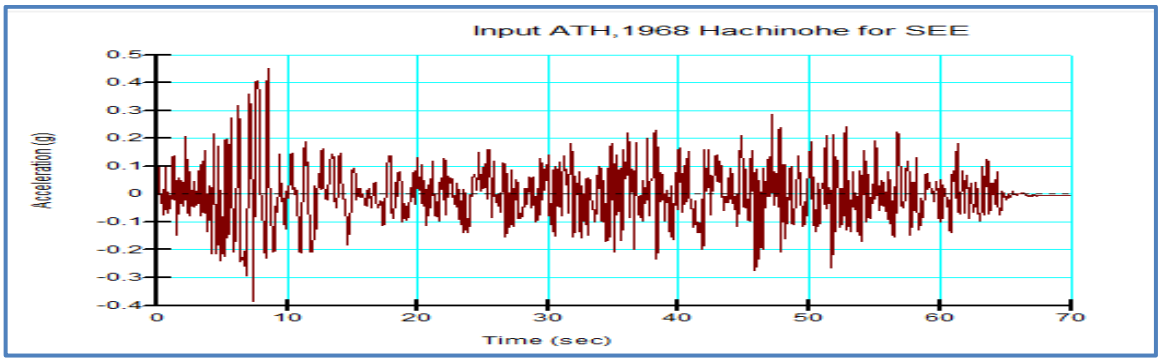

Figure 3-26: Modified input acceleration time histories for Hachinohe SEE

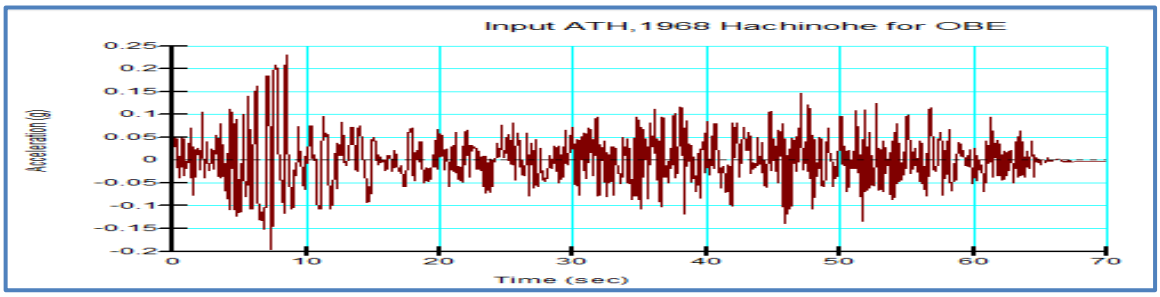

Figure 3-27: Modified input acceleration time histories for Hachinohe OBE

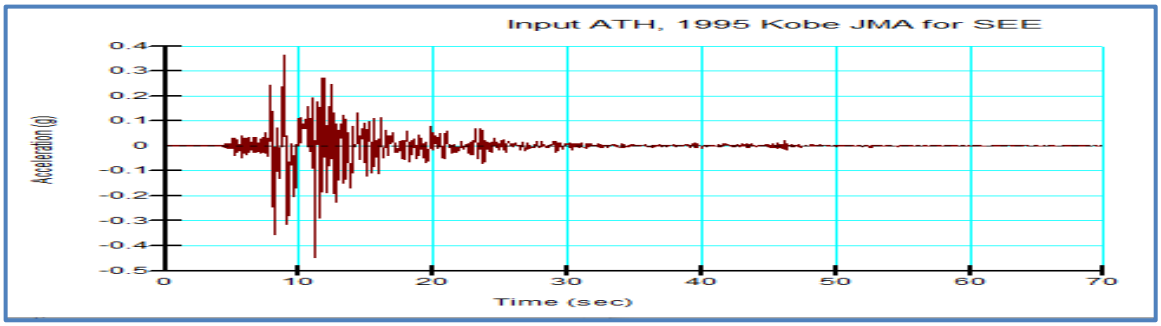

Figure 3-28: Modified input acceleration time histories for Kobe SEE

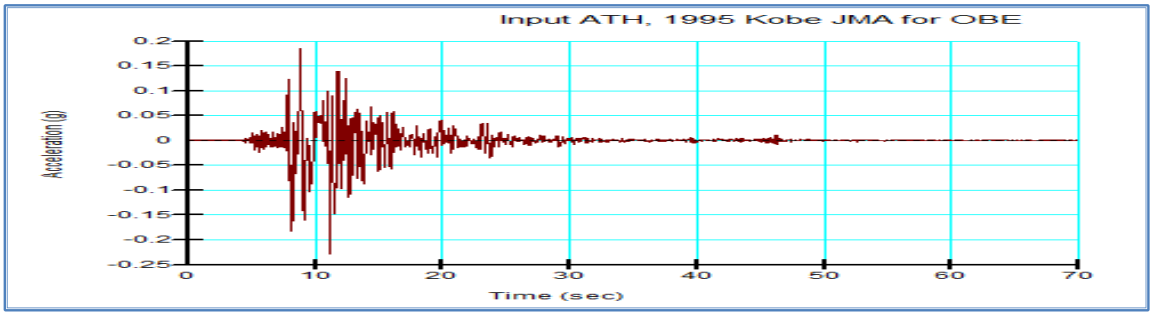

Figure 3-29: Modified input acceleration time histories for Kobe OBE

3.8.6. Boundary conditions

QUAKE/W, like all other finite element products in Geo-Studio, is a boundary valued analysis; that is, the problem consists only of a small portion of the real domain and consequently it is necessary to specify conditions along the boundaries where the analysis section has been lifted out of the actual field domain. Besides, it is necessary to specify the excitation forces acting on the body of the problem; that is, forces such as gravity and inertial forces associated with earthquake shaking. (QUAKE/W, 2018).

3.8.6.1.Boundary condition basics

For the dynamic finite element equation given in equation (3.21) and (3.22), the primary unknown is displacement, d. To solve for this equation (3.22), it is necessary to specify, d somewhere in the domain; that is, a displacement boundary condition must exist at some nodes in the problem. Usually the displacement is specified as zero somewhere along the boundary and the motion is then computed relative to this specified displacement boundary condition.

Another important aspect to remember here is that all boundary conditions eventually fall to one of two types: displacement or force. There are just two alternatives available.

3.8.6.2.Boundary condition locations

Boundary conditions (BC) in Quake/W need be applied directly to geometry objects such as region faces, region lines, free lines, and free points. A BC cannot be applied exactly to an element's edge or node. Linking the BC to the geometry has the benefit of making it independent of the mesh, which may be altered if required without disturbing the boundary condition arrangement (QUAKE/W, 2018).

3.8.6.3.Nodal force boundary conditions

Forces may be assigned to any node in a finite element mesh by introducing a geometry point at the area of interest, however the forces are seldom known in a dynamic analysis, hence this sort of boundary condition is rarely employed, particularly in earthquake analysis. Nonetheless, the function exists for unique scenarios and to ensure that a stress-based analysis is thorough (QUAKE/W, 2018).

3.8.6.4. Nodal displacement boundary conditions

Nodal displacements are most commonly supplied to provide a frame of reference- usually the displacement is zero. Figure 3-30 shows an example in which the displacement at the problem's base is set to zero. This means that the computed motion will be relative to the base being fixed in both x and y directions (QUAKE/W, 2018).

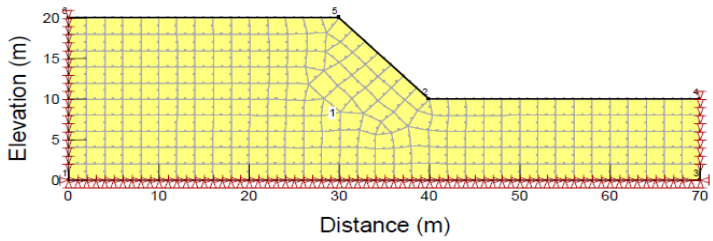

Figure 3-30: Examples of fixed boundary conditions (QUAKE/W, 2018).

In this problem, it is deemed appropriate to allow horizontal motion at the ends of the problem, but not vertical motion. The reasoning is that the horizontal motion beyond the ends of the problem will be the same as at the ends of the mesh. Another way of viewing this is that beyond the ends of the mesh there is no resistance to lateral motion. Shear in the soil will, however, prevent, or keep to a minimum, the vertical displacement at the ends of the problem. Consequently, only the vertical displacements are specified at the ends of the problem (QUAKE/W, 2018).

The specifying zero vertical displacement at the ends is not strictly correct, but the boundary is far enough away from the slope that a zero-displacement boundary has no significant effect on the dynamic shear stresses in the slope, which is the primary goal of this analysis (QUAKE/W, 2018).

As a result, the vertical boundary condition was fixed more than twice the dam height away from the base of the dam's slope, and the nodal displacement boundary condition type was used in the present study based on this concepts.

3.8.7. Analysis types

There are three types of analyses available in QUAKE/W, 2018. They are;

- Initial Static
- Equivalent Linear Dynamic •
- Nonlinear Dynamic

The "initial static" analysis takes into account the dam's initial stress. However, “Equivalent Linear Dynamic" and "Nonlinear Dynamic" analyses are used for dynamic analyses. "Non-linear dynamic" analysis necessitates additional material properties and/or parameters, making it challenging to define in this study. Out of the three analysis alternatives in Quake/W, the current study employs initial static and equivalent linear dynamic analysis, which is discussed further below:

1) Initial Static analysis

Before doing a QUAKE/W dynamic analysis, the starting stresses must be determined. The effective stresses in the ground often dictate material properties like shear modulus (G). Other factors, such as the Cyclic Stress Ratio, rely on the initial effective stresses. As a result, before commencing the dynamic analysis, the initial condition of stress in the ground need to be established.

QUAKE/W's "Initial Static" study focuses on determining initial stresses. A SIGMA/W analysis may also be used to determine starting stresses. The initial static approach is the same as the SIGMA/W in-situ method. The SIGMA/W analysis contains a boundary constraint that limits horizontal displacements to zero on both the left and right boundaries. Furthermore, the bottom border of the analysis is limited by both zero vertical and horizontal displacements. In the current investigation, the SIGMA/W in situ stress technique was applied for the first in situ stress analysis.

2) Equivalent Linear Dynamic

The primary goal of using QUAKE/W is to conduct dynamic analyses. It is the portion of the analysis that simulates an earth structure's reaction to an osculating or sudden impulse force, such as that caused by earthquake shaking or blasting. The shear stresses caused by self-weight, pore pressure, hydrostatic pressure, and cyclic shear stress are computed using dynamic analysis. The specific dynamic shear stress is calculated by subtracting the initial static stress from the dynamic analysis stress, resulting in deformations and slope instability (QUAKE/W, 2018).

To compute a solution in any QUAKE/W analysis, displacements must be given as a boundary condition. If no displacements are supplied, a finite element solution cannot be obtained numerically. The foundation's left and right borders are confined vertically to allow for horizontal free movement of the soil along with ground motion, while the bottom is fixed during this study.

3.8.8. Mesh Generation

Discretization, often known as meshing, is one of the three main components of finite element modeling, alongside material attributes and boundary conditions. Discretization is the process of determining geometry, length, area, and volume. It is the component responsible for the domain's physical dimensions. (Rao, 2004).

Geo-Studio (2018) handles all meshing automatically. A geometric area or line is originally drawn unmeshed. When the Draw-Mesh Properties command is initially used, a default mesh for the soil areas is created, with the ability to modify it. Mesh density can be defined as a real-length unit, a ratio of global mesh size, or the number of divisions along a line edge. In general, however, it is advised to confine mesh changes to adjusting global density and, if necessary, at a few limited regions where finer or coarser density is required (QUAKE/W, 2018).

The Geo-Studio packages include five (5) mesh types and patterns, which are:

- Structured mesh,
- Unstructured quad and triangle mesh,
- Unstructured triangular mesh,

- Triangular grid regions and
- Rectangular grid of quads

Out of these types, structured mesh and unstructured quad & triangle mesh types were considered in the current study.

Structured mesh

It is known as structured mesh because the components are organized in a regular pattern and only come in two forms and sizes. A structured mesh for a non-symmetrical geometric design demands the construction of many soil areas, with meshing regulated within each zone. This will almost probably result in increased work but no significant improvement in results. A structured mesh consists of a rectangular grid of quads or a triangular grid of quads/triangles (GEOSLOPE, 2018).

Unstructured quad and triangle mesh

A highly structured mesh may require multiple regions to be created in order to retain structure and allow for detailed meshing control. Geo-Studio provides a meshing pattern that generates a well-behaved unstructured pattern of quadrilateral and triangular parts automatically. The Geo-Studio documentation recommends that this mesh option be chosen initially since it will meet the demands in the vast majority of instances. (GEOSLOPE, 2018).

Given the dam's design, an unstructured quad and triangle mesh was utilized for this investigation, as seen in the picture below.

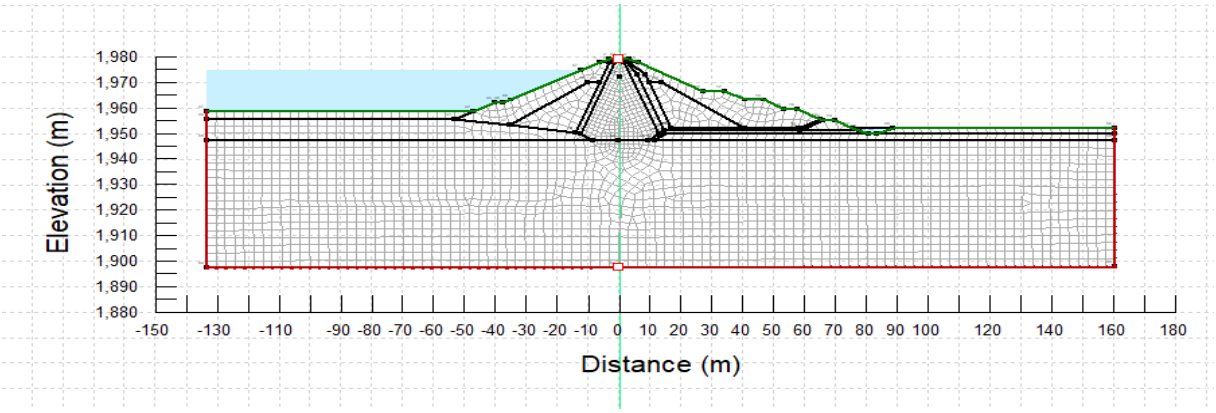

Figure 3-31: QUAKE/W Mesh

An effective finite element mesh is problem-dependent; hence, there are no set of procedures for constructing one. Furthermore, the type of mesh created for a specific problem will be determined by the user's experience and creativity. The size of an element has a direct impact on the solution's convergence and must therefore be carefully chosen. Although more features normally imply further precise findings for every agreed problem, there will be a limit to how many elements can be added without significantly increasing accuracy. Furthermore, using smaller elements will require more computing time because more elements imply more degrees of freedom in the process, which necessitates more computer memory (Rao, 2004).

It is suggested to start an analysis with as few elements as feasible. There is no specific mesh size limit in QUAKE/W, however for practical reasons; meshes should not be much larger than roughly 1000 elements (QUAKE/W, 2018).

3.9. Staged/multiple analysis in Geo-Studio

The integration of numerous Geo-Studio software packages allows us to merge many studies completed using different products into a single modeling project. Creating new analyses is as simple as cloning a current one and altering its characteristics. When the model is ready to be examined, Geo-Studio performs the analyses in the right order. The results of one analysis can be used to another. This approach may be used to model construction processes, generate initial conditions, run sensitivity analyses, model complicated time sequences, and execute more manageable studies (GEOSLOPE, 2018). Geo-Studio 2018 has seven packages that may be linked together; four were used in this investigation.

Hence, a clear and systematic process was shown in Figure 3-32 below.

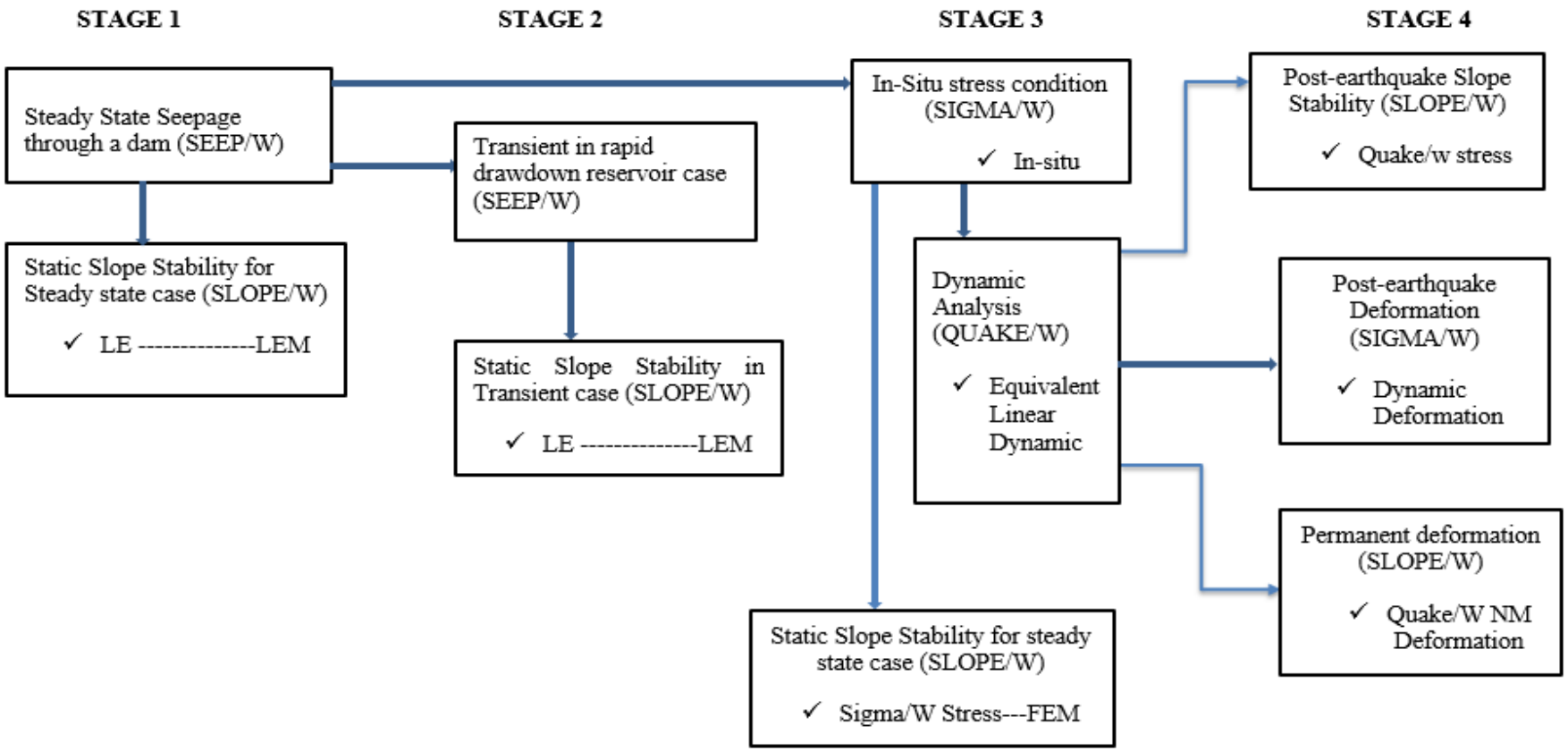

Figure 3-32: Diagram depicting the sequence of analysis used in this study.

CHAPTER 4 ANALYSIS RESULTS AND DISCUSSIONS

(CASE 1: THE DAM WITHOUT GEOSYNTHETIC REINFORCEMENT)

Case 1A: The Dam with Rock Fill Zone (As Previously Designed By ECDSWCo.)

4.1. General

4.1.1. Embankment type and geometry

According to the methodology part (Chapter 3), the Kalid-Dijo dam is a zoned earth-rock fill dam. Table 4-1 presents the design geometry data.

Table 4-1: Geometric records of the Kalid-Dijo Zoned Earth-Rock Fill Dam

Upstream Slope					Downstream Slope				
RL	Berm Width (m)	Remarks	Slope (H:V)	Elevation(m)	RL	Berm Width (m)	Remarks	Slope (H:V)	Elevation(m)
1958.63		GL	1:2.0	1956.68 to 1979.00	1952.00		GL	1:1.9	1952.0 to 1955.0
1963.0		MOL			1955.0	4.0	Rock toe Crest	1:1.9	1955.0 to 1959.5
1962	3.0	Berm			1959.5	4.0	Berm	1:1.9	1959.5 to 1963.0
1974.50		FRL			1963.0	6	Berm	1:1.9	1963.0 to 1966.5
1976.10		MWL			1966.5	7.10	Berm	1:1.9	1966.5 to 1977.5
1977.50		CCCL			1977.50		CCCL	1:1.9	1977.5 to 1979.0
1979.00		DCL			1979.0		DCL	1:1.9	1979.00

4.2. Static Stability Analysis for the dam without Geosynthetic Reinforcement

Prior to earthquake shaking, it is a good idea to check for stability under static conditions. The finite element analysis method produces results for both upstream and downstream slope stability analysis performed prior to an earthquake to ensure static stability.

4.2.1. Loading condition and minimum factor of safety

The stability of an embankment is determined by the qualities of the foundation and fill materials, the geometry of the embankment section, and other elements such as water present, loading circumstances, shear strength parameters utilized in the study, and pore pressure characteristics. Tables 4-2 and 4-3 indicate the minimal safety factor needed for the study, in different loading circumstances and standard requirements.

Table 4-2: Loading conditions and the required minimal factor of safety (as specified by USACE and adopted globally).

Cases	Loading Situation	Slope	Least F.S (F O $S_{Min.}$)
Case I	At period of Construction	U/S	1.30
		D/S	1.30
Case II	Completion of Construction	U/S	1.30
		D/S	1.30
Case III	Rapid Drawdown	U/S	1.25
Case IV	Steady-state seepage	D/S	1.50
Case V	Steady state seepage with Earthquake	D/S	1.10

Table 4-3: Minimum safety factors (derived from USBR Design Standards No. 13.

Loading Situation	Shear strength parameters	Pore pressure features	Least Factor of Safety
Steady-state seepage	Effective	Steady-state seepage in the active conservation pool	1.50

Operational condition	Effective or Un-drained	Rapid descent from the regular water surface to the inactive water surface	1.30

4.2.2. Slope Stability Analysis Prior to Earthquake shaking

As previously stated, the Kalid Dijo Dam Project is located on the rift valley's escarpments, necessitating earthquake-resistant design methods. As a result, the primary focus of this thesis will be dynamic analysis; however, static analysis under various loading conditions has been performed and reported to ensure static stability.

4.2.2.1. Model of the Kalid-Dijo zone, Earth-Rock fill dam

The dam has been modeled using SLOPE/W, Geo-Slope International Ltd. and shown in Figure 4-1 below.

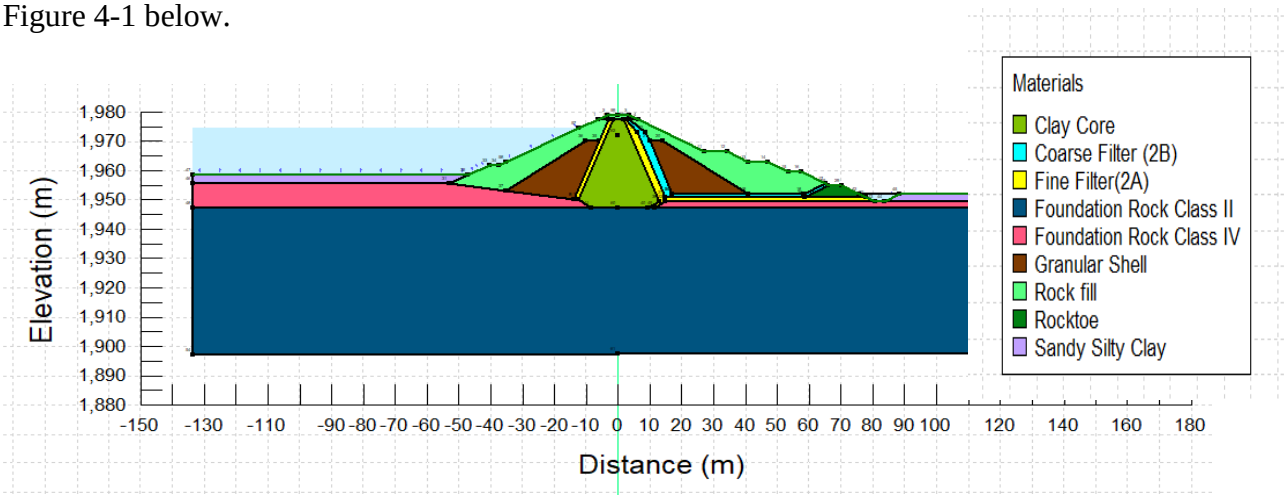

Figure 4-1: Kalid-Dijo Dam Model (Geo-Slope, 2018).

4.2.2.2. Downstream Steady State Seepage Analysis using SEEP/W

Before studying stability, the pore pressure situation must be understood. This may be performed by seepage analysis with SEEP/W, as explained in the next section.

4.2.2.2.1. Seepage analysis results from SEEP/W

SEEP/W uses the finite element approach to model two-dimensional Darcy's flow in saturated and unsaturated soils. The main features of water flow in unsaturated soil are:

- In unsaturated soils, the coefficient of permeability is not a constant but rather a function of the degree of saturation or matric suction.

- The volumetric water content of unsaturated soil varies with time.

SEEP/W-generated pore pressure is sent to SLOPE/W for stability analysis. The analysis results are given in the figures below after modeling the dam with SEEP/W and applying the appropriate material characteristics.

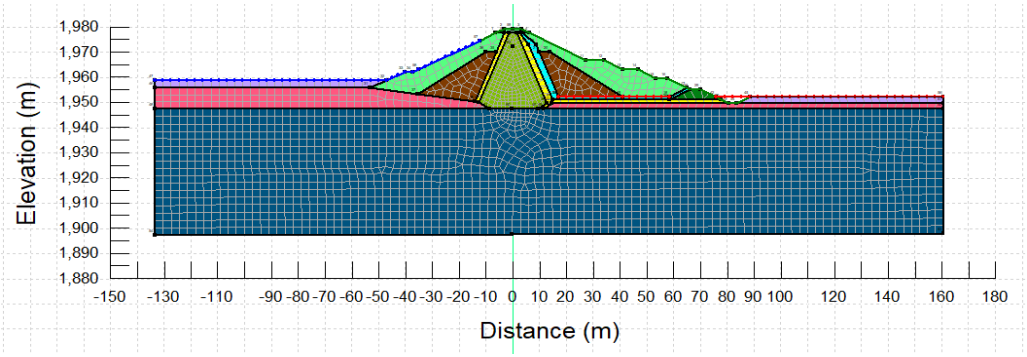

Figure 4-2: Seep/W's finite element model for seepage analysis.

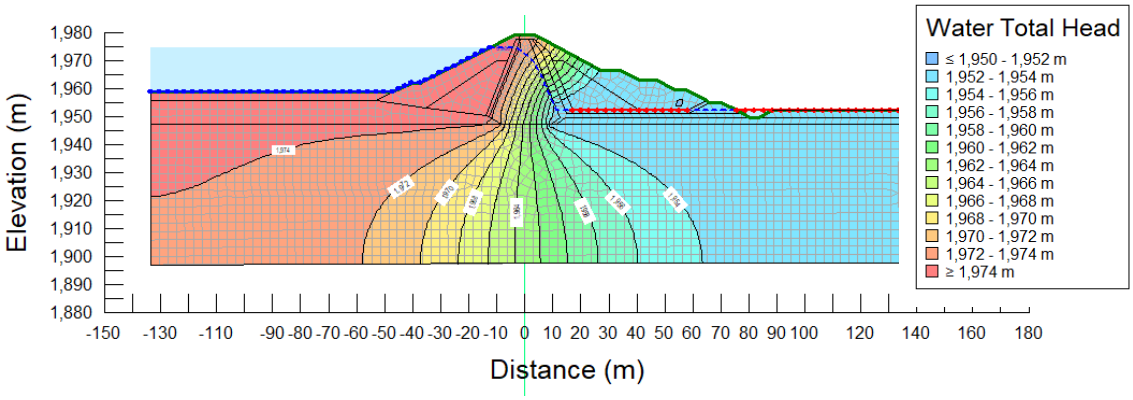

Figure 4-3: Contour of Isopotential lines (total head).

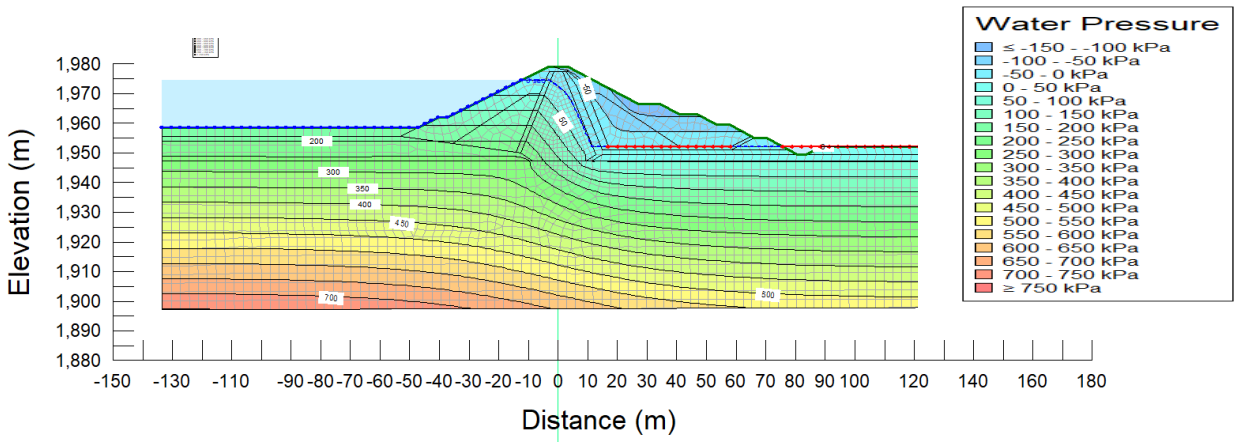

Figure 4-4: Contour of Pore Water Pressure (in kPa)

4.2.2.3. Transient analysis using SEEP/W

When the pore water pressure and exposure conditions in the system change over time, a time-dependent seepage analysis is required. This kind of study is known as transient analysis. It refers to something that is always changing. It is evolving because it considers how long it takes for the soil to respond to the user-defined boundary conditions. One example is when a reservoir upstream from a dam is unexpectedly depleted (SEEP/W, 2018).

4.2.2.3.1. Initial condition

To conduct a transient analysis, the opening (beginning) total head at all nodes must be defined. The initial condition was determined from the previous steady-state seepage analysis.

Furthermore, the components necessary for steady-state analysis, transient analysis requires an extra component: a time-dependent border condition. In other words, steady-state analysis assumes that the boundary condition is consistent across time. Transient analysis, alternatively, involves changing the boundary conditions throughout time. The analysis lasts 20.5 days and involves ten time phases.

Hydraulic conductivity and volumetric water content are two key hydraulic property functions. These functions are generated using the system's matric suction. Therefore, the hydraulic conductivity and volumetric water content functions employed in the study for different materials are depicted in the figures below.

There are two estimating strategies available: estimation based on grain size distribution and estimation using sample function. Based on the available data, this study used estimation from sample function. A similar approach has been used to estimate the volumetric water content function.

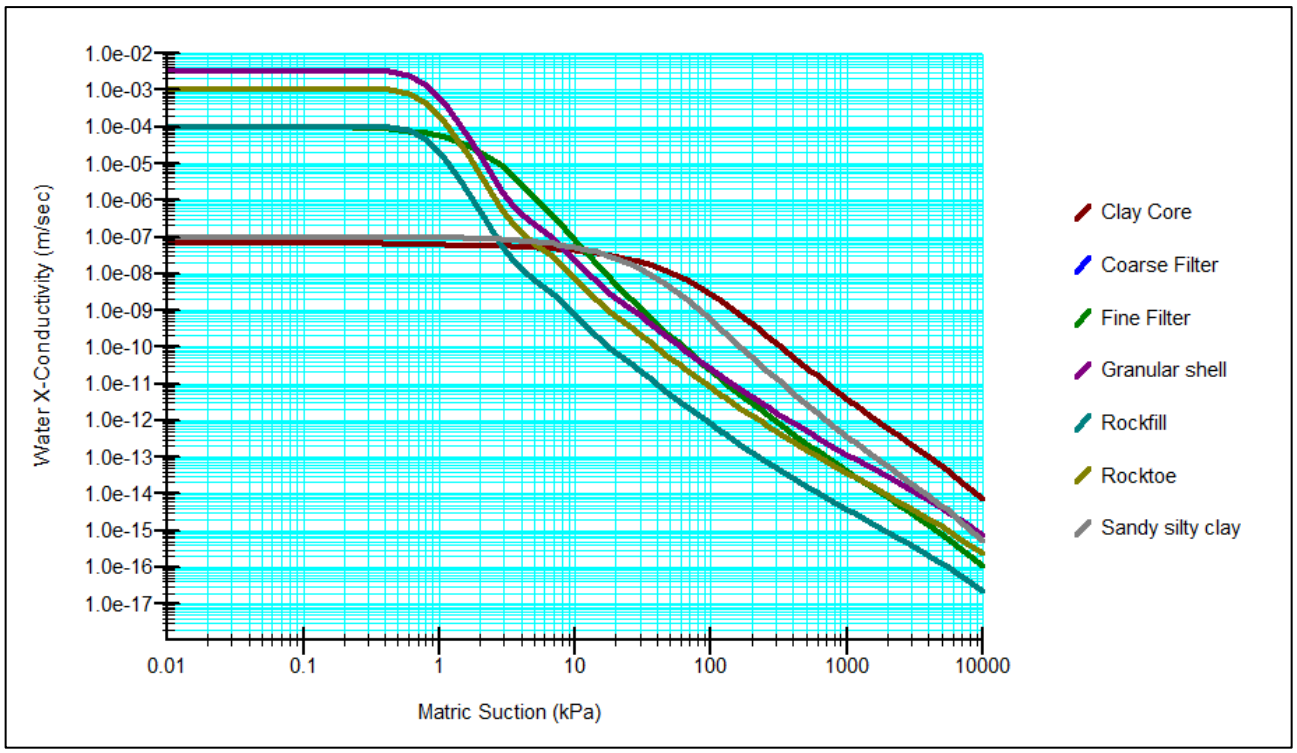

Figure 4-5: Hydraulic conductivity function for all dam materials and foundation

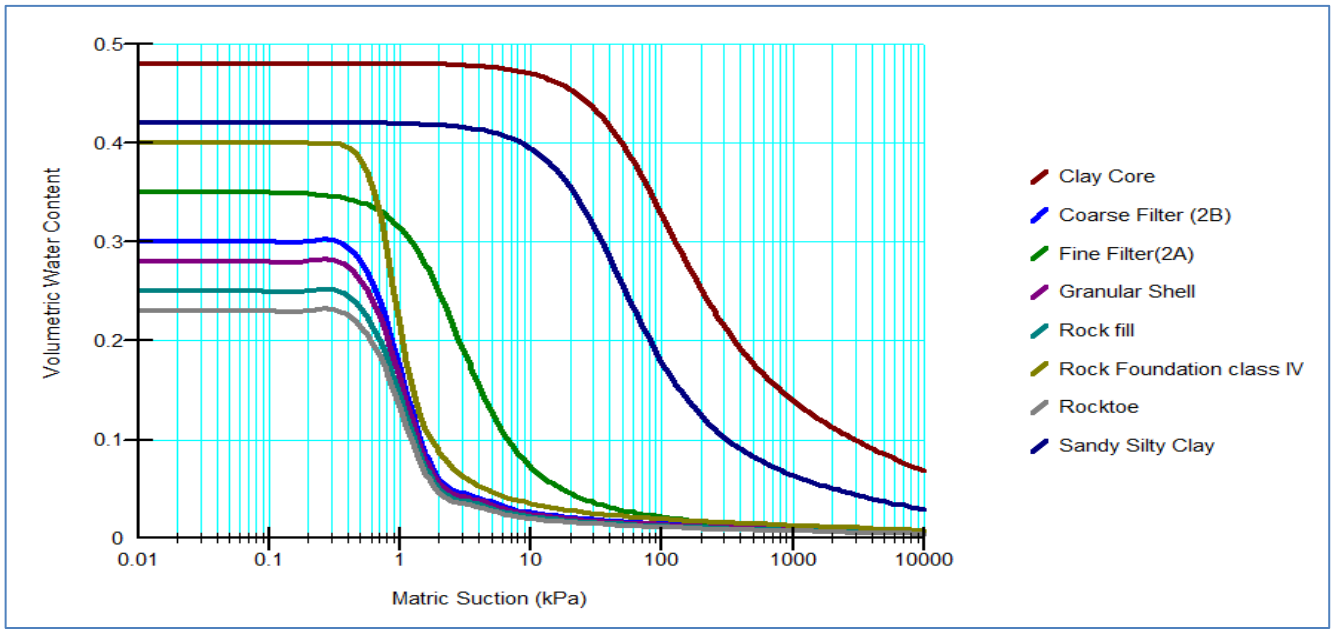

Figure 4-6: The volumetric water content function applies to all dam materials and foundation.

As previously stated, the steady-state analysis will serve as the starting point for the transient analysis. The transient analysis was performed under conditions of rapid

drawdown for a duration of 20.5 days and 10 steps. The results are saved every three days, as shown below.

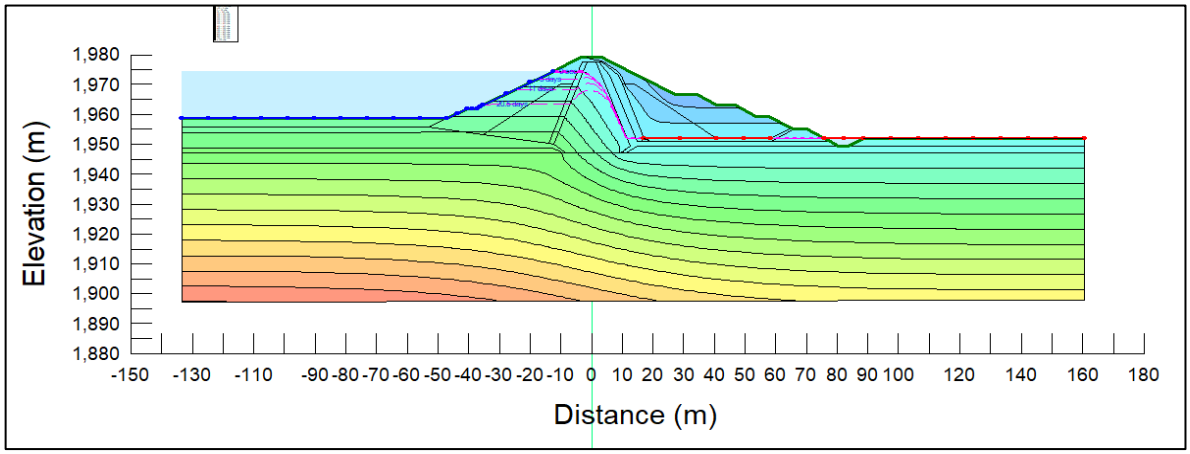

Figure 4-7: Isoclines (zero pressure line) for 20.5 days draw down

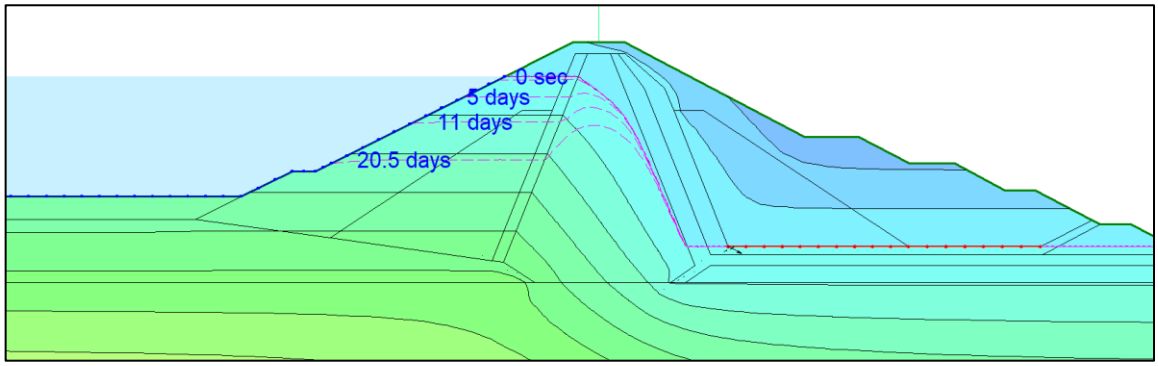

Figure 4-8: Isoclines (zero pressure lines) for various days

4.2.2.4. Initial Static stress analysis results from SIGMA/W

This analysis was conducted using the elastic-plastic constitutive material model. To restrict horizontal movement, a boundary condition is specified for both the left and right vertical ends of the SIGMA/W model. The lower border of the analysis is constrained both vertically and horizontally. Figure below depicts the outcome of effective stresses in the embankment zone as a labeled contour.

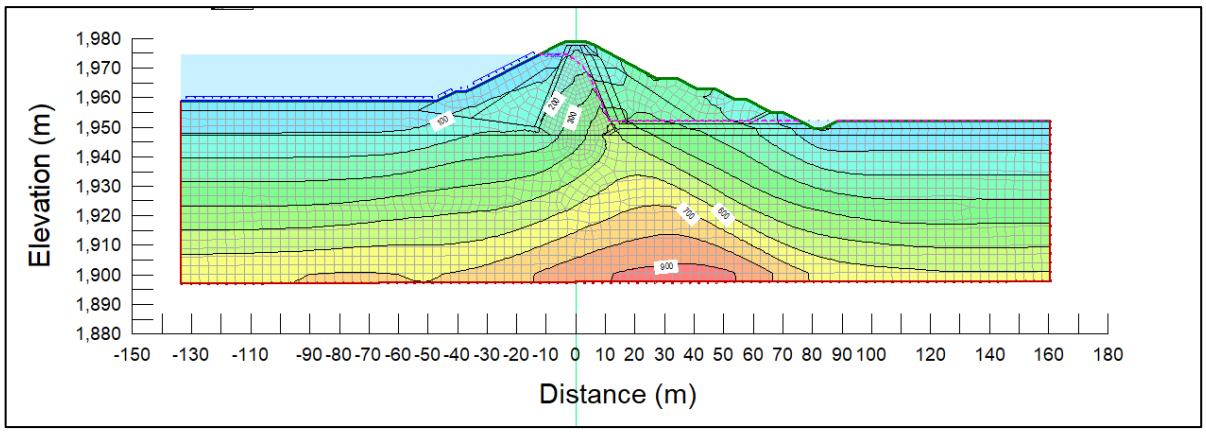

Figure 4-9: Effective stress distribution in the dam

The graph depicts the maximum effective stress (900kPa) measured at the bottom of the clay core's downstream toe. The effective stress is calculated by subtracting pore water pressure from total stress. Because of the stored-water pore pressure, the upstream face has the least effective stress.

4.2.2.5. Slope stability study findings prior to Earthquake shaking

The upstream slope's determined factor of safety in slope 1V to 2.0H is 1.760 and 1.658 against slope instability for steady state and rapid drawdown cases, respectively. For the downstream slope, the calculated factor of safety in slope 1V to 1.9H is 1.912 against slope instability as shown in figures (Figure 4-10, Figure 4-11 and Figure 4-12 respectively.

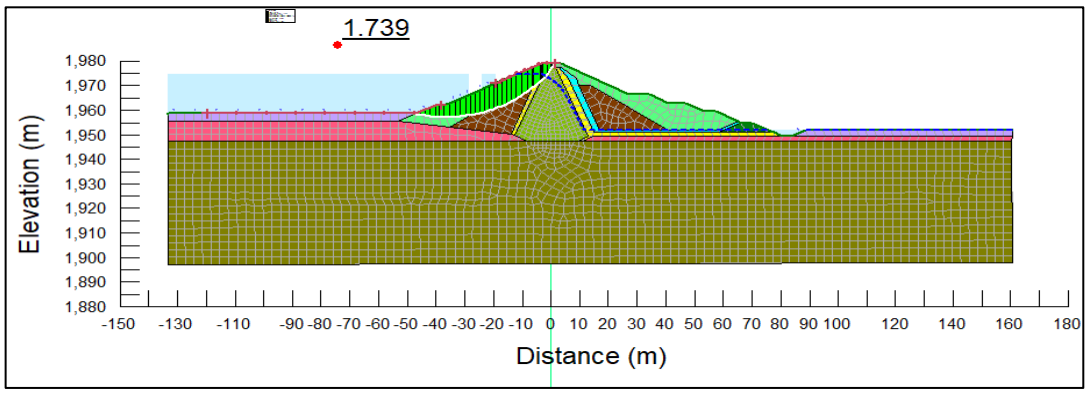

Figure 4-10**:** 1V to 2.0H Upstream slope Finite element static stability (Steady State Case)

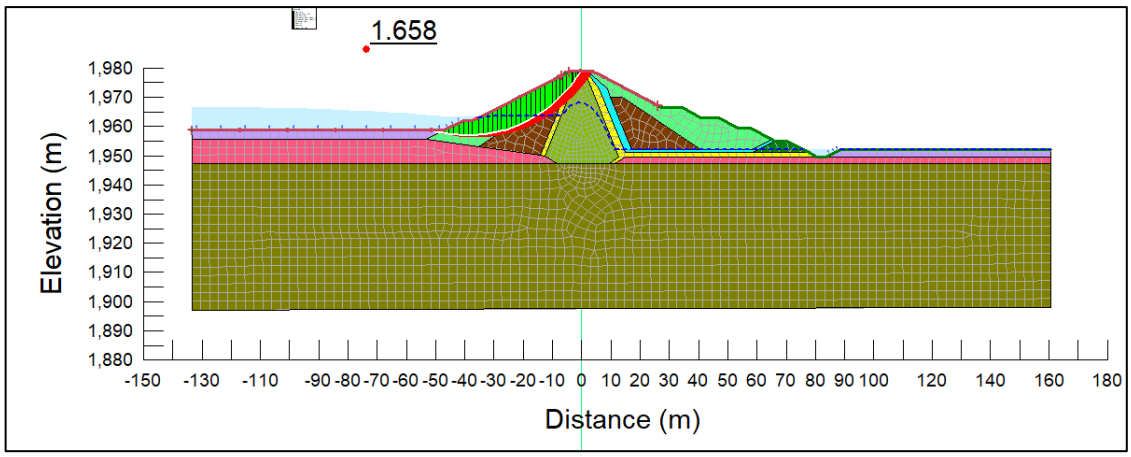

Figure 4-11: 1V to 2.0H Upstream slope Finite element static stability (Rapid draw down case)

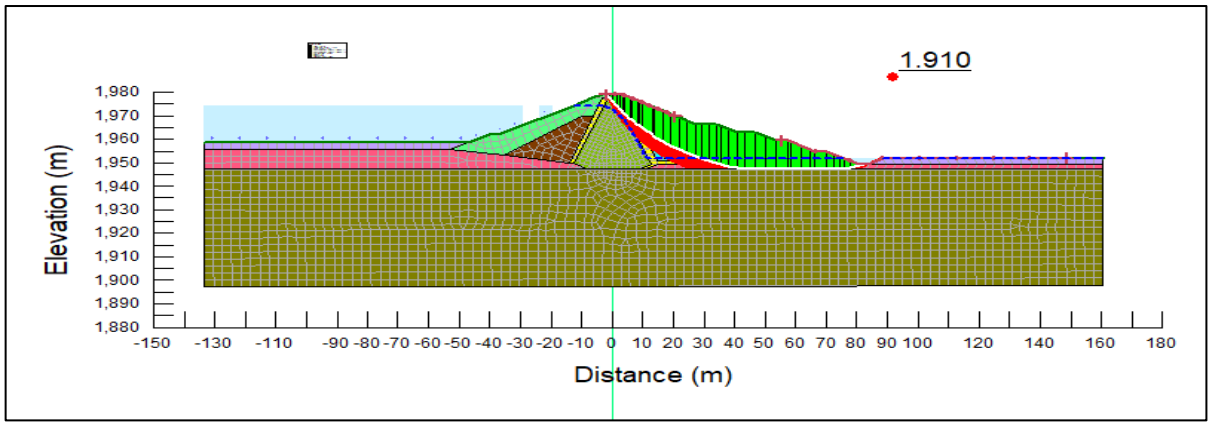

Figure 4-12: 1V to 1.9H Downstream slope Finite element static stability

The dam's upstream slope of 1V to 2.0H and downstream slope of 1V to 1.9H met the minimum requirements under static loading conditions, as determined by the marginal safety factors for both upstream and downstream slopes.

4.3. Dynamic Stability Analysis for the dam without Geosynthetic Reinforcement

4.3.1. General

The dam under study's finite element dynamic analysis was carried out utilizing state of art software QUAKE/W (Geo-Slope International Ltd).The program is a two-dimensional dynamic finite element model with comparable linear strain-dependent modulus and damping properties. The software employs an iterative approach to estimate nonlinear strain-dependent features. The shear modulus and damping ratios for each element in the

finite element model are first computed, and the system is then assessed using these starting values. Following each cycle, the effective shear strain values for each element are calculated, and the corresponding modulus and damping characteristics at the computed strain level are compared to the estimated values from the previous iteration. The method is repeated until convergence has been obtained.

4.3.2. The Finite Element Model

The finite element model was done by placing the dam foundation in the rock classes II and IV after removing the sandy silty soil layers under the main dam. Figure 4-13 depicts the finite element model used for the dynamic study of the Kalid-Dijo rock-earth fill dam. The model is created using the QUAKE/W software for the dam's maximal cross-section. This model comprises of 2464 nodes for checking equations and 2371 elements for extracting material attributes. Using an assumed global element size of 3m. The quadrilateral and triangular element geometries were chosen for their suitability in an unstructured mesh.

To reduce the disruption caused by boundary and wave reflection in dynamic studies, the side borders were expanded by 80m (more than three times the dam height) in both left and right directions. The model's bottom boundary was identified in foundation rock class II (welded tuff) 50m below the dam cut-off level.

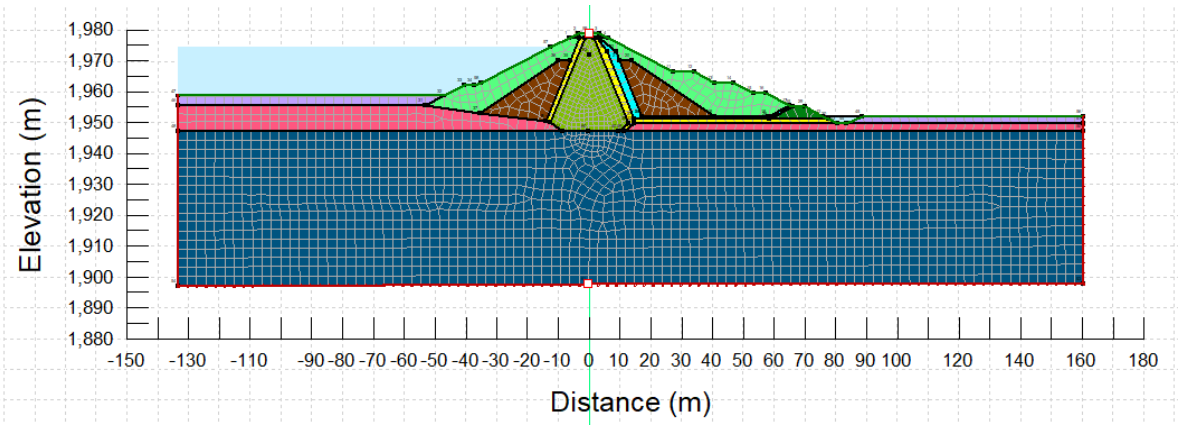

Figure 4-13: QUAKE/W Finite element model to show mesh elements and nodes

4.3.3. Dynamic analysis results and discussions

Figure 4-14 shows a sample output for the horizontal maximum acceleration. Figure 4-14 depicts a sample output for the horizontal maximum acceleration. The dam is 25.5 meters tall and is built on weathered, pyroclastic deposit (welded tuff) or Rock class II foundations

that experience El Centro ground motion with an amplitude of 0.45g. The dam's side slopes are 2H: 1V upstream and 1.9H: 1V downstream, with a core side slope of 0.4H: 1V. This section discusses the maximum horizontal acceleration at the top of the foundation and within the dam.

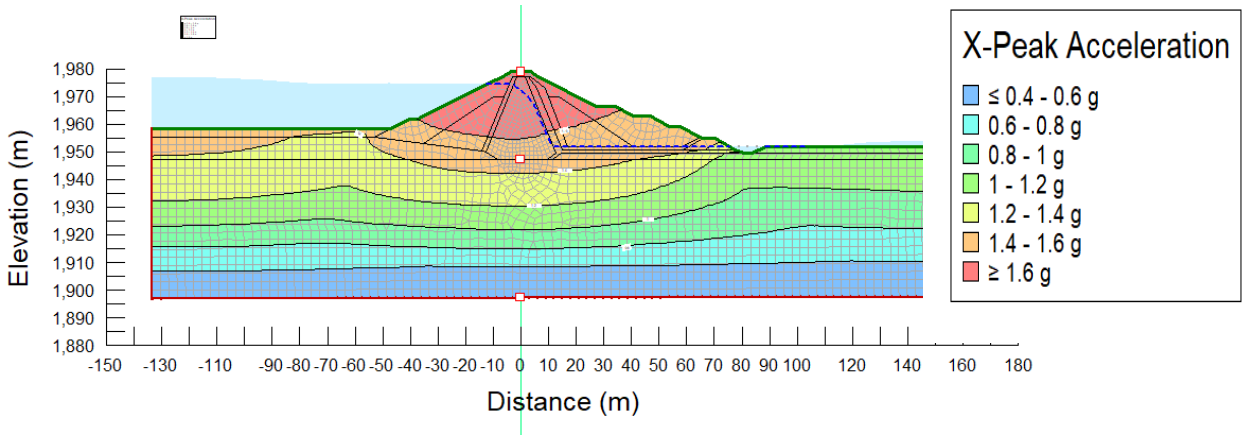

Figure 4-14: Sample FE software output for x-peak acceleration.

4.3.3.1. Acceleration Response at the dam Crest

Figure 4-15 and Figure 4-16 illustrate the acceleration response at the dam crest for the Hachinohe earthquake, corresponding to the site specific SEE and OBE horizontal PGA, respectively, compared to the input ground motion. Figures 4-15 and 4-16 demonstrate that the estimated ground accelerations at the dam crest are 1.74g and 0.85g for horizontal SEE and OBE Hachinohe accelerations, respectively. Peak ground accelerations are expected to be increased from 0.45g at the model's base to around 1.74g at the crest for the Kalid-Dijo dam for the Hachinohe earthquake safety evaluation record. This relates to an amplification value of approximately 1.29. Outcomes for other earthquakes shall be given in Appendices at the end of the reports.

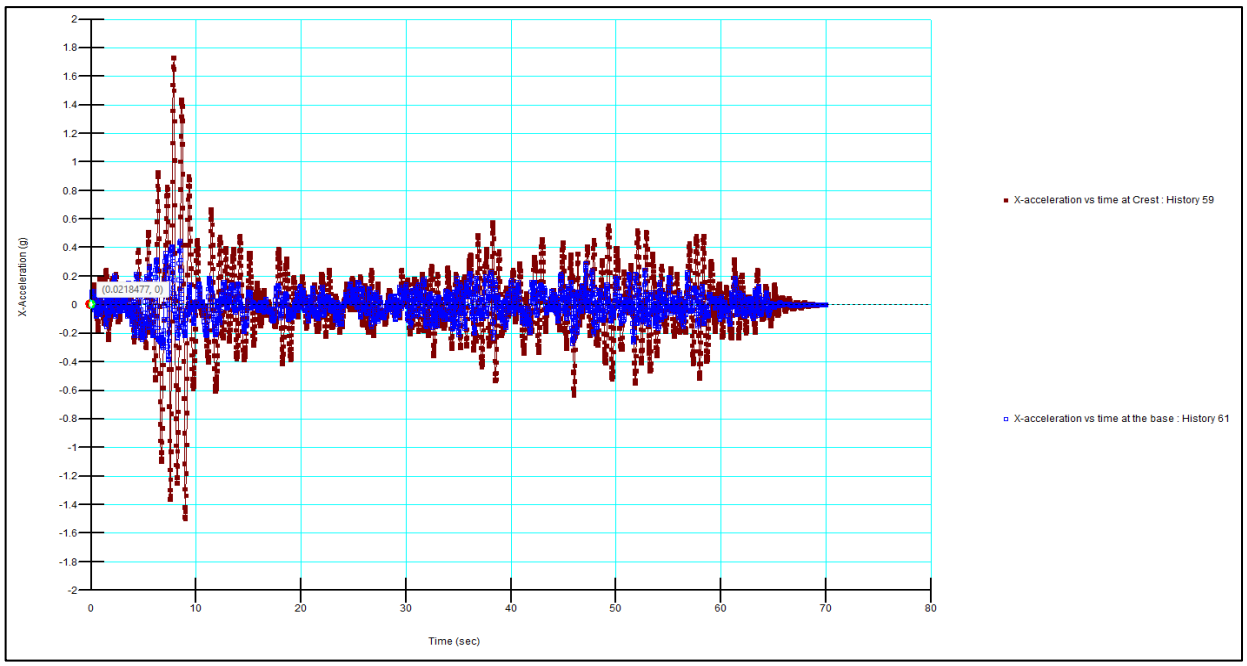

Figure 4-15: X-acceleration response near the dam crest and input motion at the base for Hachinohe Safety Evaluation Earthquake (SEE).

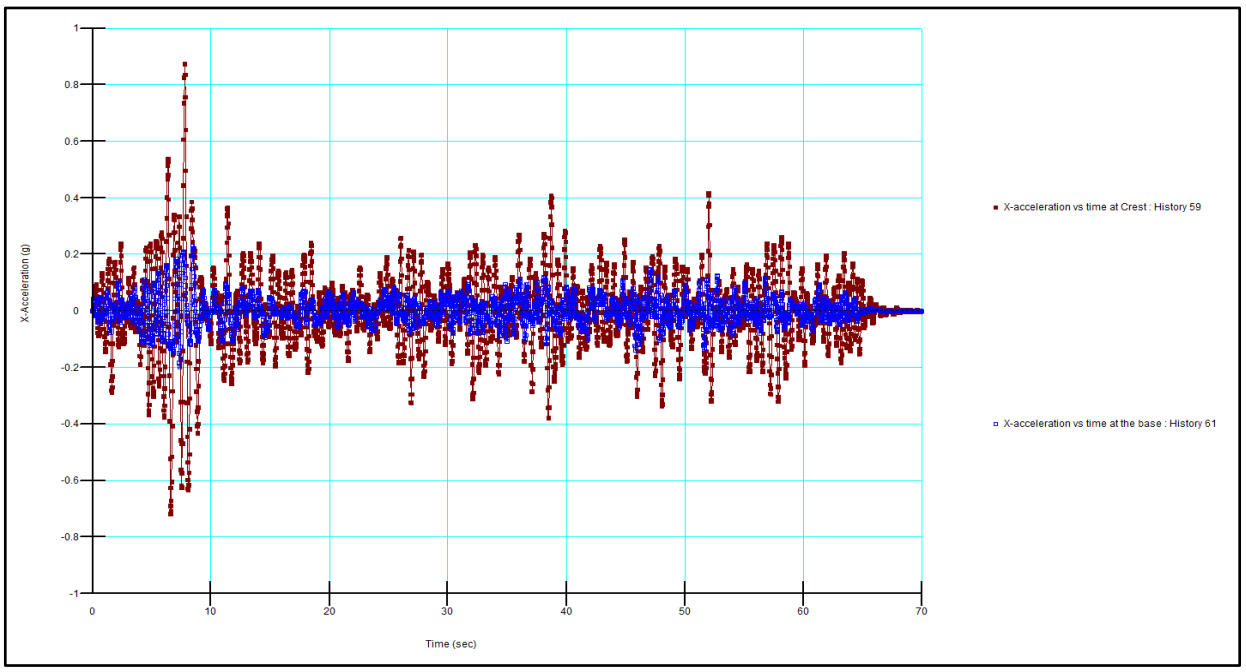

Figure 4-16: X-acceleration response at dam crest and input motion at the base for Hachinohe, Operating Basis Earthquake (OBE).

4.3.3.2. Spectral response at dam crest

Figure 4-17 shows that the dam's peak spectral reaction to a Safety Evaluation Earthquake (SEE) occurs at a period of 0.57 seconds (frequency of 1.75 cycles per second); Similarly,

in the event of an Operating Basis Earthquake (OBE), as shown in Figure 4-18, the highest spectrum response occurs at 0.49sec (2.04 cycles per second), which is also within the range of the natural period or frequency for embankment dams (0.5 Hz to 10 Hz).

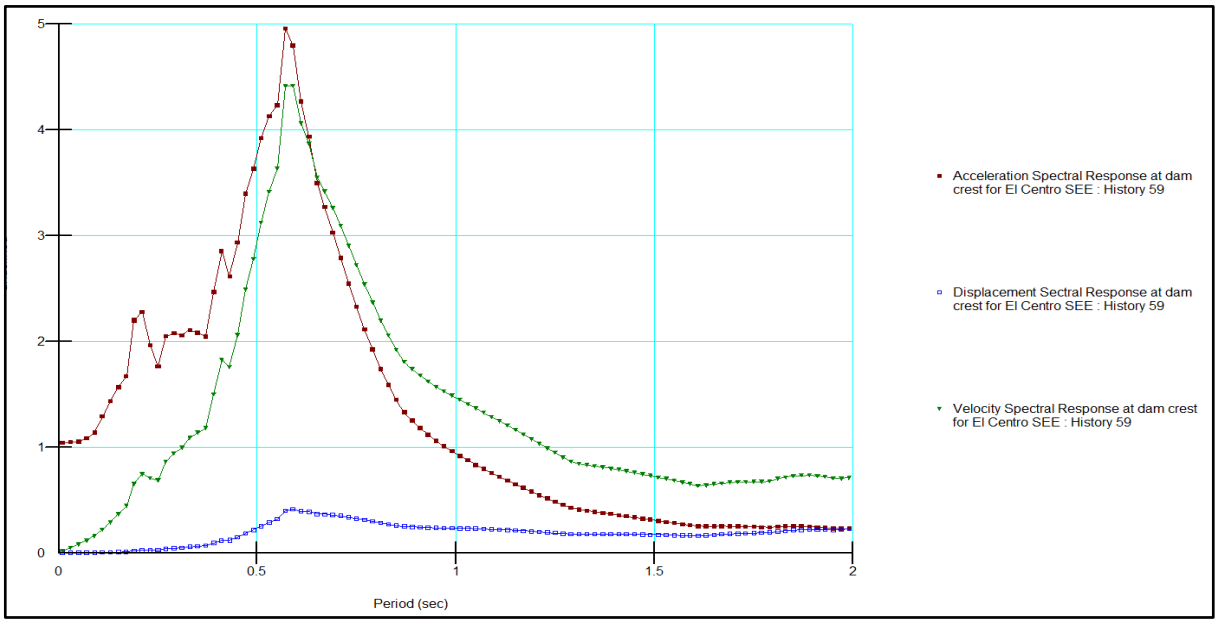

Figure 4-17: Horizontal Spectral Response at Dam Crest Corresponds to SEE (El Centro)

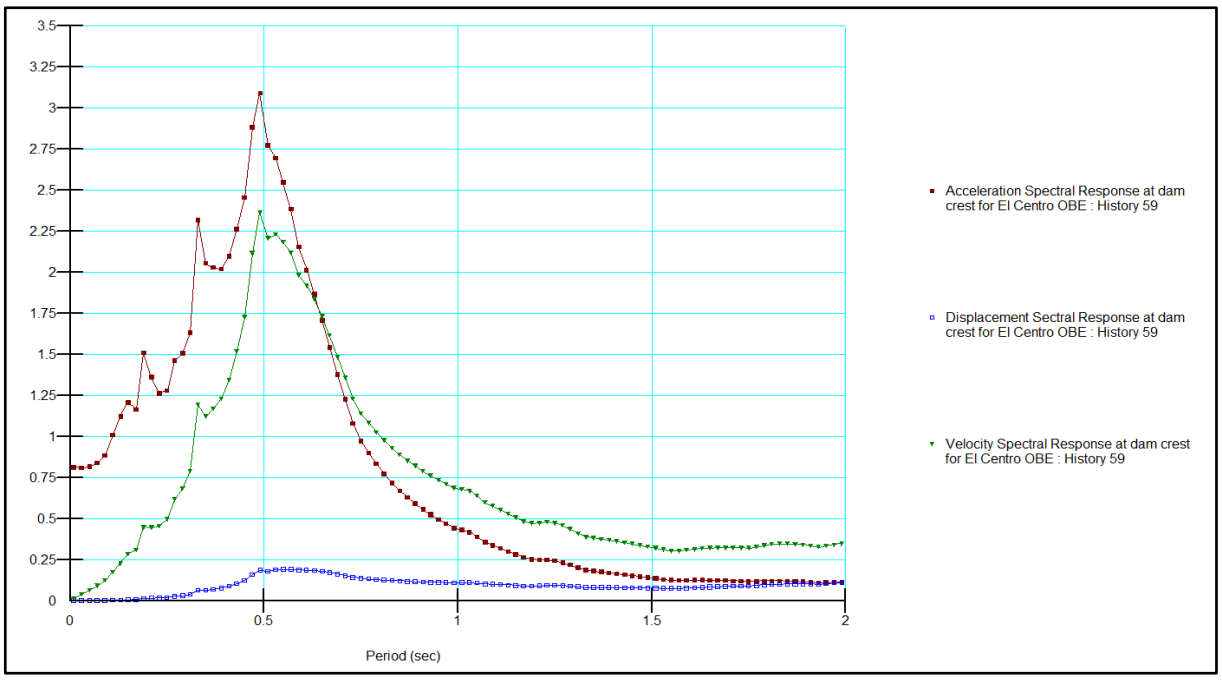

Figure 4-18: Horizontal Spectral response at dam crest corresponding to OBE (El Centro)

4.3.3.3. Post-Earthquake Stability

This was conducted to assess the dam's stability following the earthquake shaking. The analysis was carried out with the Finite element method analysis part of the SLOPE/W Geo-Studio product, Quake/W Stress analysis type. This is performed by using post-earthquake pore pressure from the QUAKE/W dynamic analysis results.

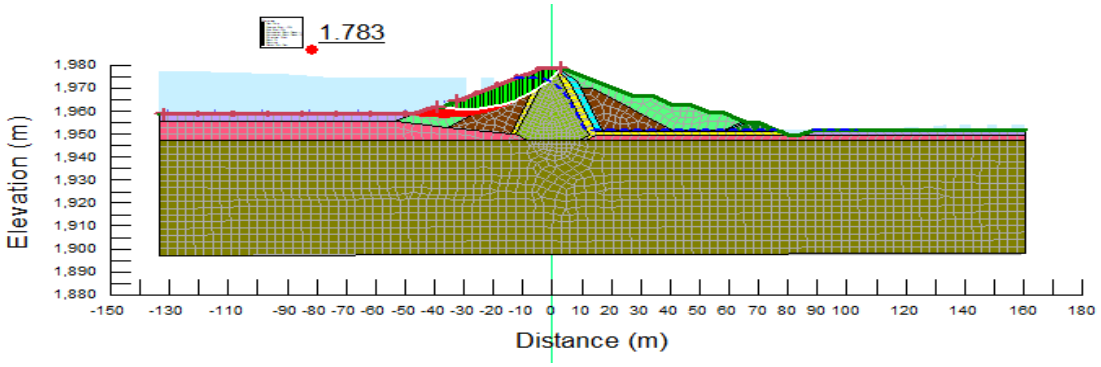

Figure 4-19: U/s slope stability after an earthquake

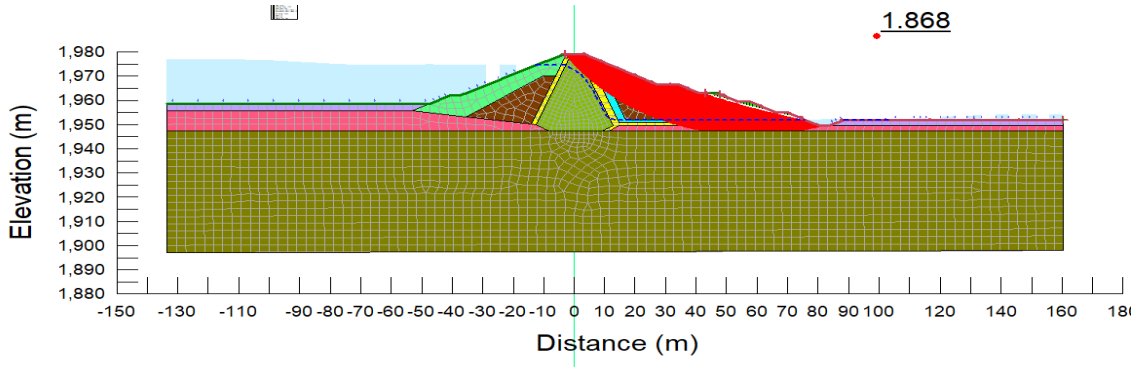

Figure 4-20: D/s slope stability after earthquake.

4.3.3.4. Post-Earthquake Deformation

One of the most significant components of dynamic analysis is doing deformation analysis after an earthquake has passed. This is the ability to connect SIGMA/W with the findings of a QUAKE/W dynamic analysis. The maximum vertical displacement of 1.70m was observed. Figure 4-21 depicts the dam's distorted configuration following the earthquake.

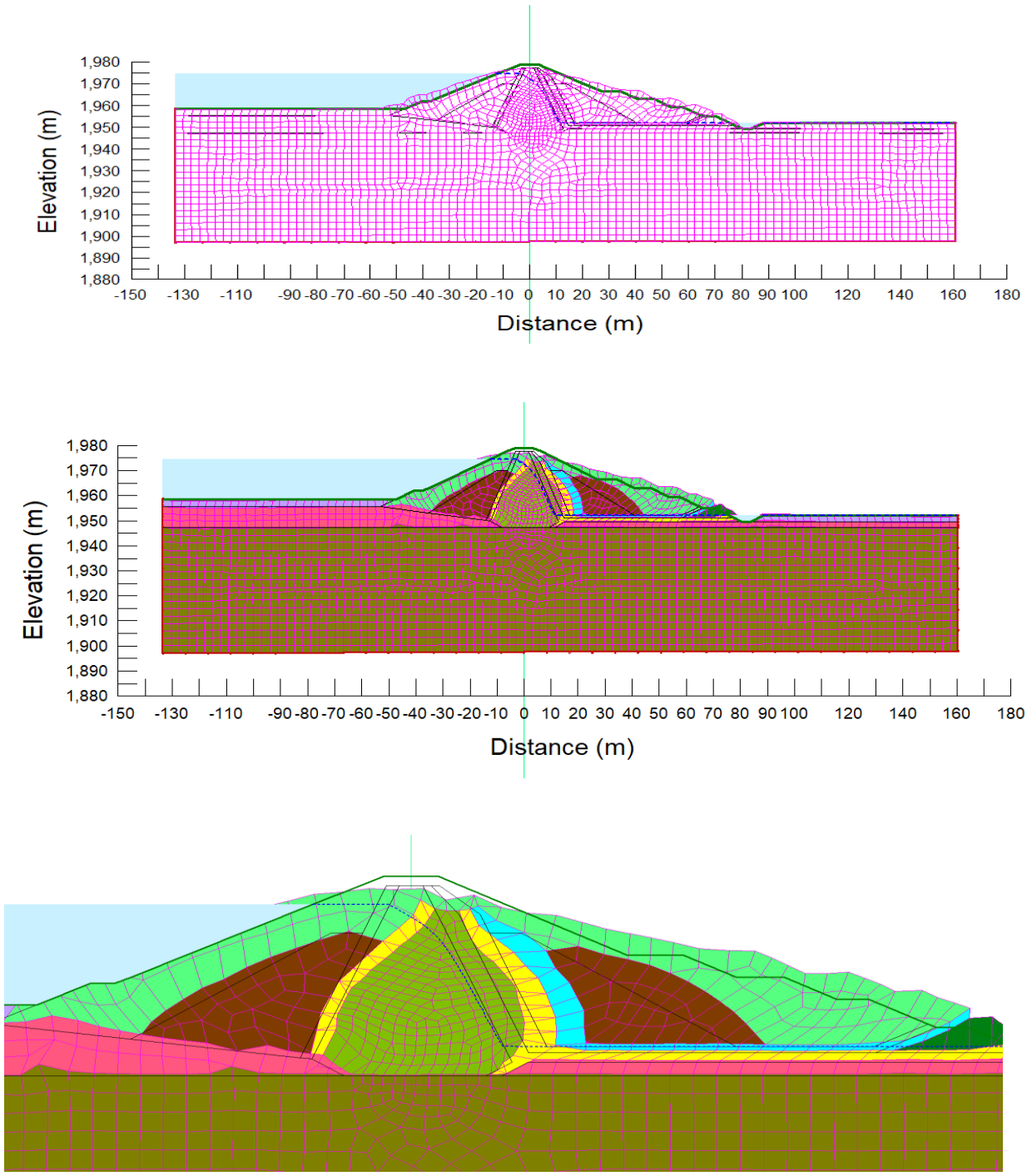

Figure 4-21: Post Earthquake deformation/Deformed mesh

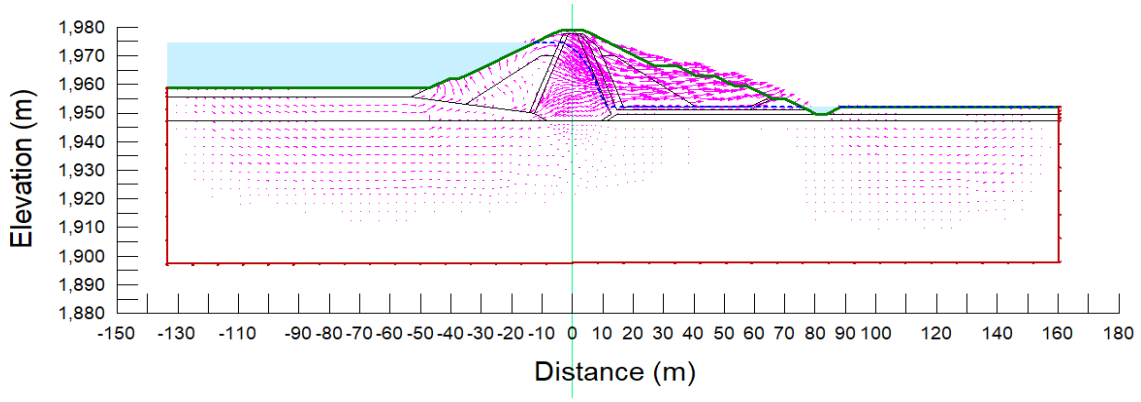

Figure 4-22: Displacement field vectors

4.3.3.5. Liquefaction analysis results for the dam without reinforcements

One purpose of the dynamic analysis is to determine the excess pore-pressures that may develop, and identify zones where the soil may have liquefied or where the soil strength may have dropped down to the steady-state strength. The computed liquefied zones at the end of earthquake duration are shown in Figure 4-23 as can be seen from the yellow shaded zones, the Sandy Silty Clay soil is liquefied during earthquake shaking.

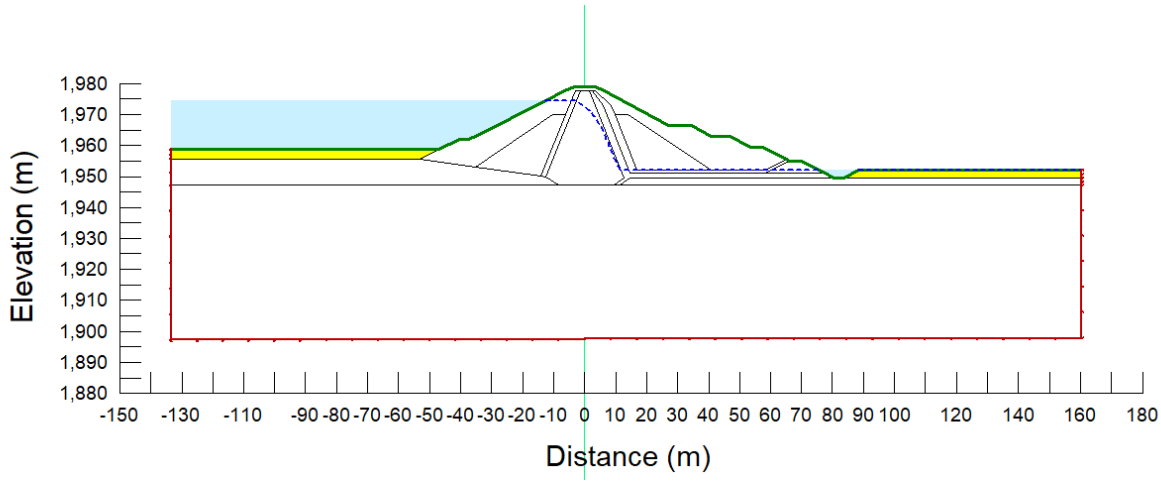

Figure 4-23: Liquefied zone of Kalid Dijo dam without reinforcement, corresponding to SEE (Based on El Centro Records)

4.3.3.6. Deformation Analysis by Newmark

The shaking caused by earthquakes generates inertial forces. These inertial forces cause the tensions in the earth to change throughout time. The mobilized shear strength of a prospective slip surface increases and decreases in response to inertial forces. During the shaking, the mobilized shear strength may surpass the available shear resistance, causing

a brief loss of stability. If the factor of safety is less than one, the earth may shift somewhat. These displacements accumulate and cause irreversible deformation (QUAKE/W, 2018).

Examining the permanent deformations caused by dynamic inertial forces is an essential component of dam dynamic analysis. SLOPE/W in the Geo-Studio program performs earthquake-induced permanent deformations in dams by combining the QUAKE/W calculated results with the Newmark sliding block idea. The Newmark technique is based on the concept that a prospective sliding mass behaves like a rigid body, moving down a slope whenever the total (static and dynamic) driving force exceeds the available resisting force. The yield acceleration is the crucial value of the resultant acceleration, which causes the sliding mass to move. It denotes the resulting (average) acceleration for which the factor of safety against sliding is 1.0.

4.3.3.6.1. Numerical Procedures to estimate permanent deformation

The stresses from QUAKE/W are the sum of the static plus dynamic stresses. The static stresses are known from the specified initial in-situ stresses. Subtracting the initial static stresses from the QUAKE/W stresses therefore gives the dynamic stresses. In equation form:

$$\sigma_{\text{dynamic}} = \sigma_{\text{Quake}} + \sigma_{\text{Static}} \text{----------} (4\text{-}1)$$

The dynamic stress may be estimated at the base of each slice. Total dynamic mobilized shear is calculated by integrating throughout the whole slip surface. This is the increased shear created by the earthquake shaking. Average acceleration is calculated by dividing total mobilized dynamic shear by potential sliding mass. This value is calculated for each time integration step during the shaking and displayed against the relevant safety factor, as illustrated in Figure 4-24.

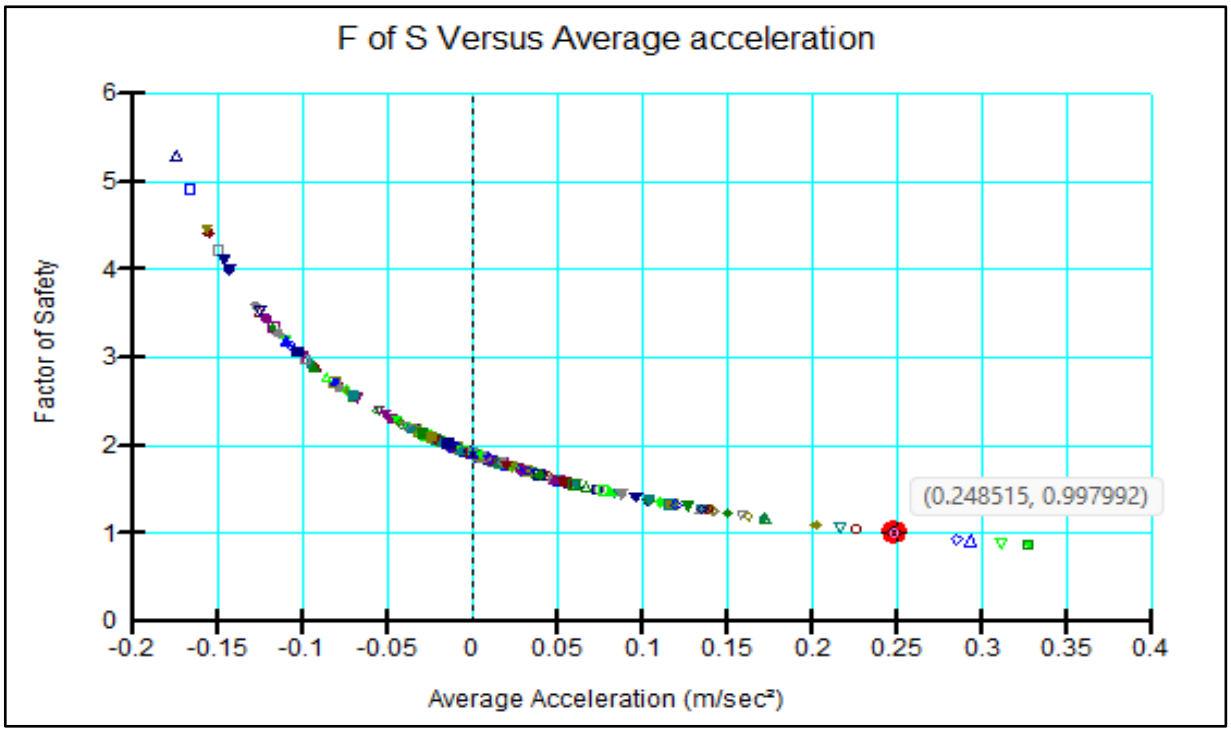

Figure 4-24: Average acceleration vs. Factor of Safety

The average acceleration corresponding to a factor of safety of 1.0 is known as the yield acceleration, a_y. The sliding mass will fail or move if the total average acceleration is greater than zero. In this case, a_y is around 0.25. Figure 4-25 shows a plot of the average acceleration produced at each integration step over time.

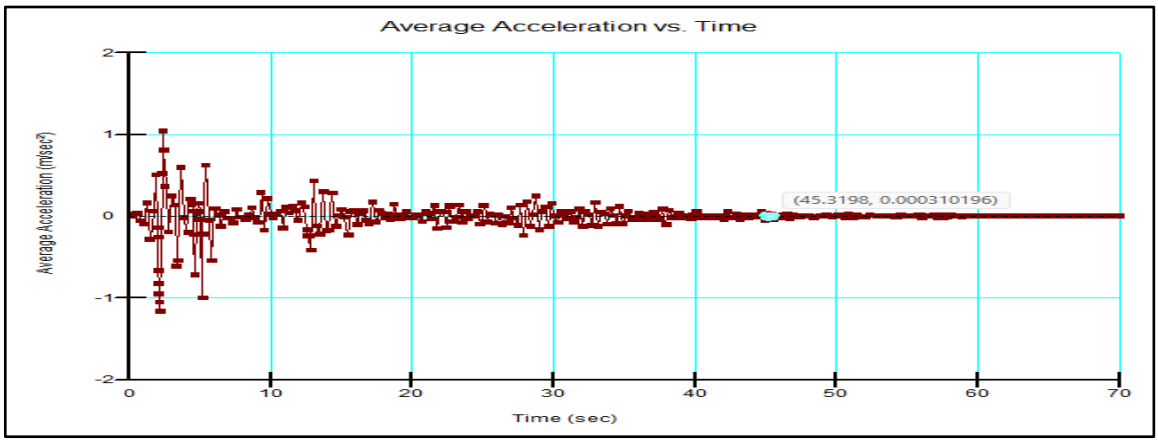

Figure 4-25: Average acceleration versus time during the shaking

The slope will change when the average acceleration reaches a_y. In the QUAKE/W analysis, the average acceleration is the sum of the horizontal and vertical applied accelerations.

The velocity of the sliding mass during movement is calculated by integrating the area under the average acceleration versus time curve when the acceleration exceeds a_y, as illustrated in Figure 4-26.

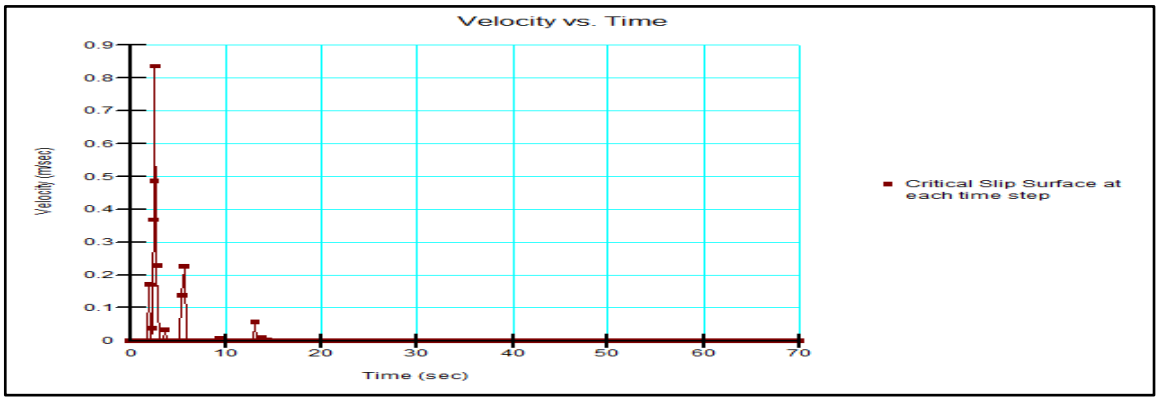

Figure 4-26: Velocity versus time

Integrating the area under the velocity versus time curve gives the cumulative movement during the shaking as seen in Figure 4-27. Based on this figure**,** the maximum earthquake induced Newmark's permanent deformation is about 0.45m.

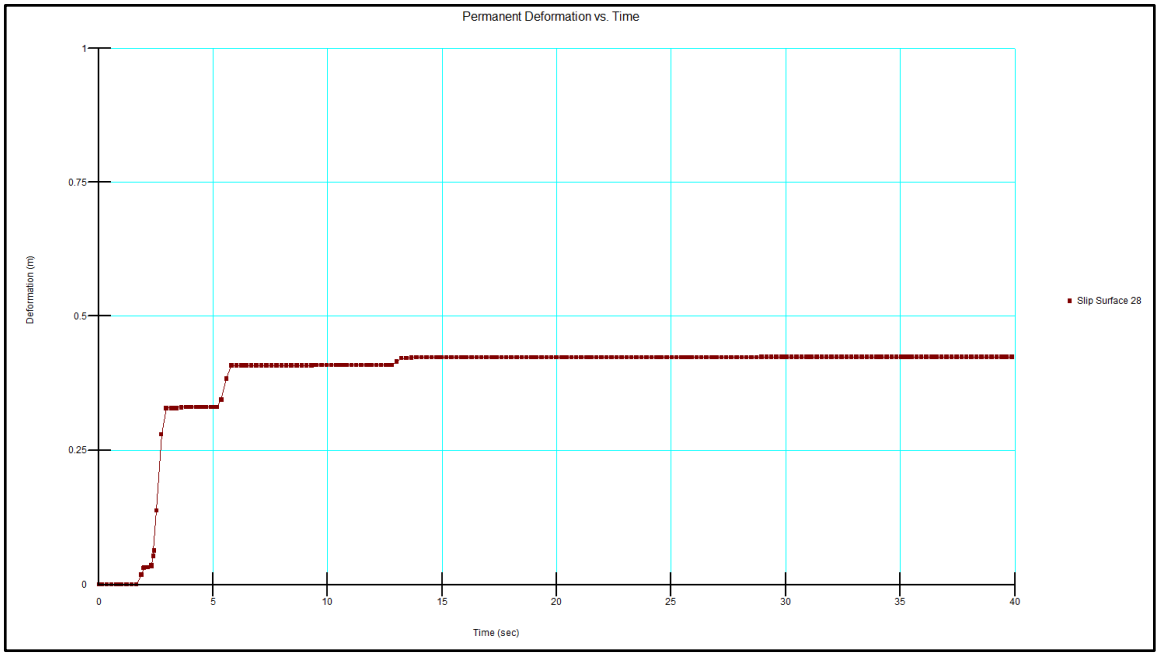

Figure 4-27: Cumulative movement during the shaking

The movement occurs parallel to the slip surface. The movement might thus be both rotational and translational.

SLOPE/W does this sort of computation for each trial slip surface, allowing to determine which trial slip surface has the most potential movement. To make things easier, the experimental slip surfaces can be sorted by deformation rather than safety factor to find the one with the most movement (SLOPE/W, 2018).

Case 1B: The Dam without Rock Fill Zone and Without Geosynthetic Reinforcement

In this case, the dam was re-analyzed by replacing the rock fill zone by granular shell fill without geosynthetic reinforcement. This is to check the static and dynamic stability of the dam without rock fill zone.

4.3.4. Static Stability Analysis for the dam without Geosynthetic Reinforcement and without rock fill zone.

4.3.4.1. Slope Stability Analysis before Earthquake Shaking

Static stability study was performed and reported under various loading circumstances to ensure static stability.

4.3.4.2. Model of zoned, Earth fill dam

The dam modeled by SLOPE/W has been shown in Figure 4-28 below

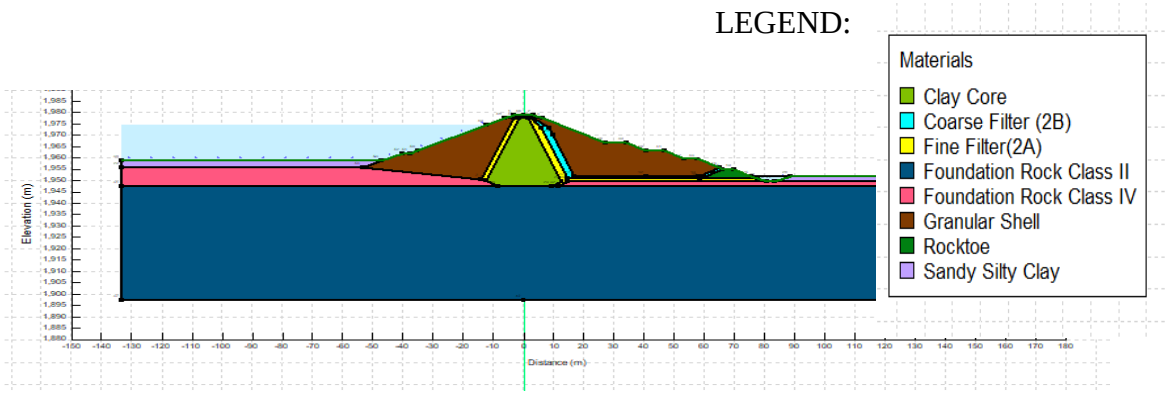

Figure 4-28: Model of the Kalid-Dijo Dam without rock fill zone, from SLOPE/W

4.3.4.3. Downstream Steady State Seepage Analysis using SEEP/W

The dam was modeled in SEEP/W, 2018 and it was illustrated in Figure 4-29.

4.3.4.3.1. Seepage analysis results from SEEP/W

Analysis findings have been shown in Figure 3-30 and Figure 4-31 below.

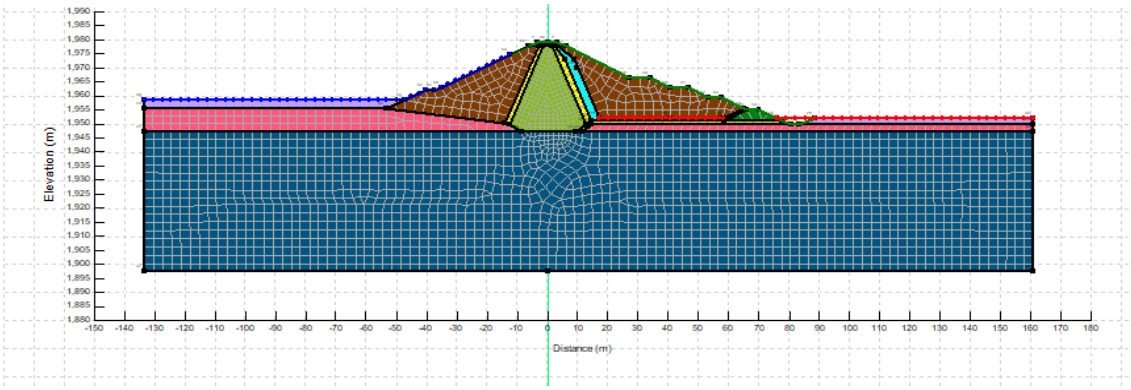

Figure 4-29: SEEP/W's finite element model for seepage analysis.

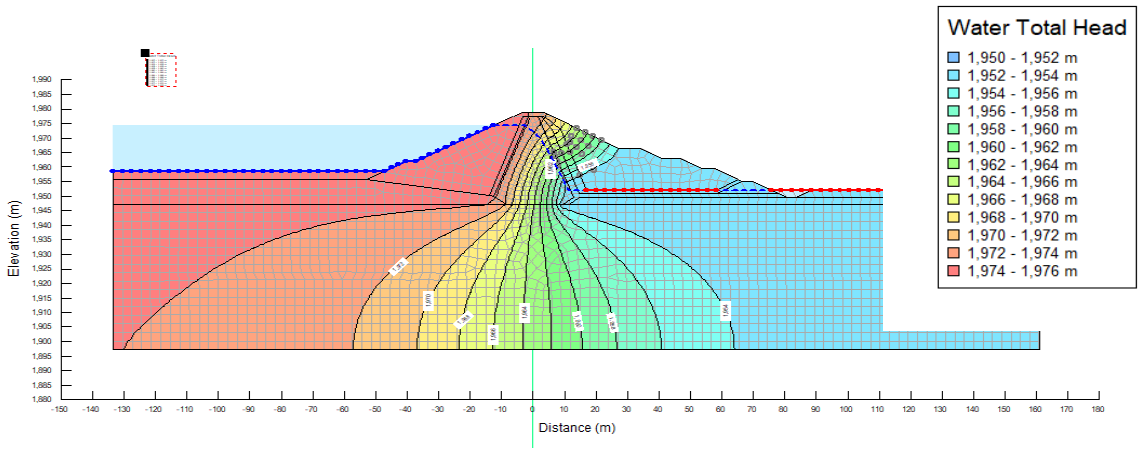

Figure 4-30: Isopotential lines (total head) contour

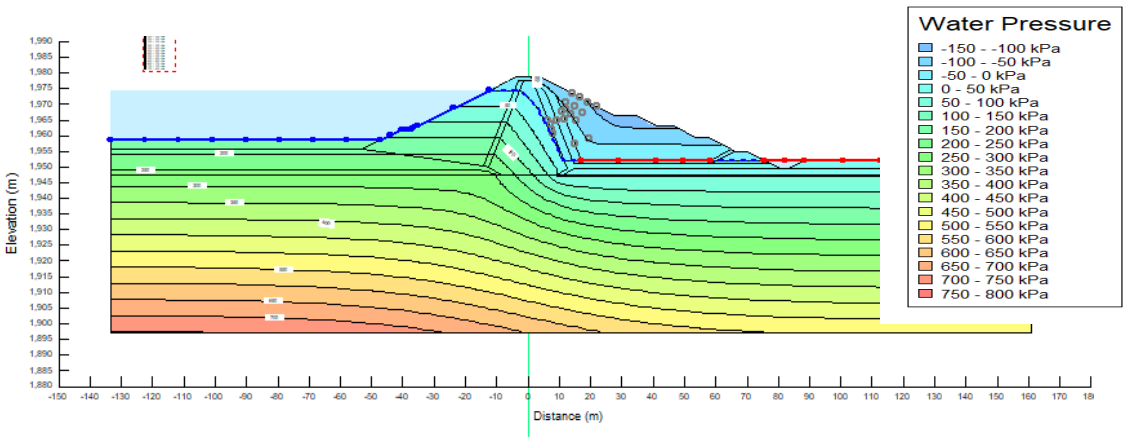

Figure 4-31: Pore Water Pressure Contour (kPa)

4.3.4.4. Transient analysis using Seep/W

4.3.4.4.1. Initial condition

Initial condition has been specified from steady state seepage analysis results above; as stated in section 4.2.2.3. Hydraulic conductivity and volumetric water content functions used for different materials in the analysis have been adopted as presented in the previous sections under case 1A.

4.3.4.5. Initial Static stress analysis results from SIGMA/W

The outcome of effective stresses in the embankment zone is depicted with a labeled contour below in Figure 4-32.

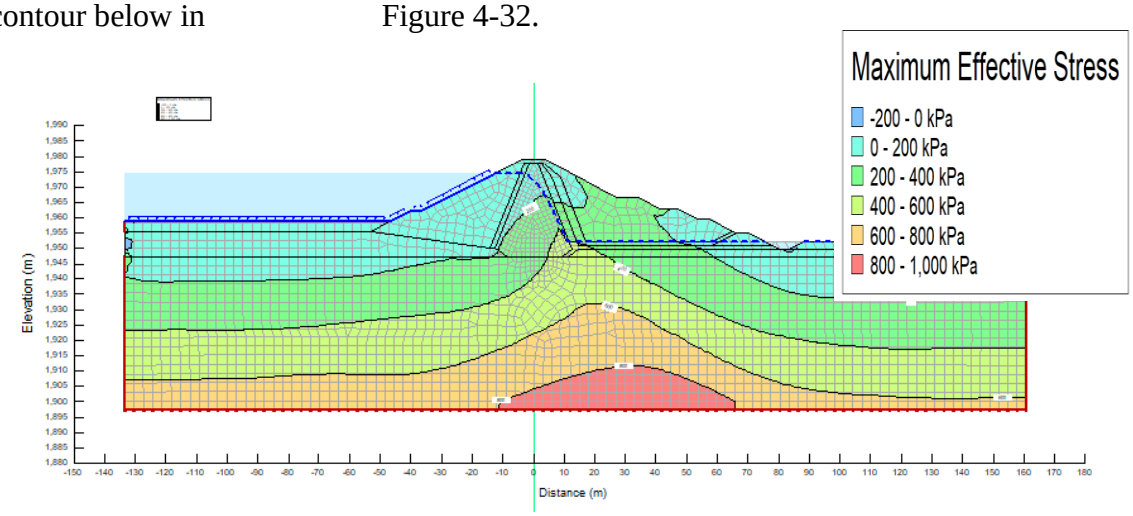

Figure 4-32: Effective stress distribution in the dam

Maximum effective stress (800kPa) is measured at the bottom of the clay core's downstream toe, as seen in the graph. Because of the stored-water pore pressure, the upstream face has the lowest effective stress.

4.3.4.6. Slope Stability Analysis results before the Earthquake Shaking

4.3.4.6.1. For Steady state and Transient situations

The Finite element method, Sigma/W Stress analysis type is selected from the SLOPE/W package, and the analysis results are discussed as follows.

For the upstream slope, the calculated factor of safety for the slope of 1V to 2.0H is 1.314 against slope instability for steady state condition and 1.313 for rapid draw down case (which is the worst condition for upstream slope).

For the downstream slope, the estimated factor of safety for the slope 1V to 1.9H is 1.325 against slope instability, for steady state case (Which is worst condition for downstream slope) as shown from figures 4-33 to 4-35.

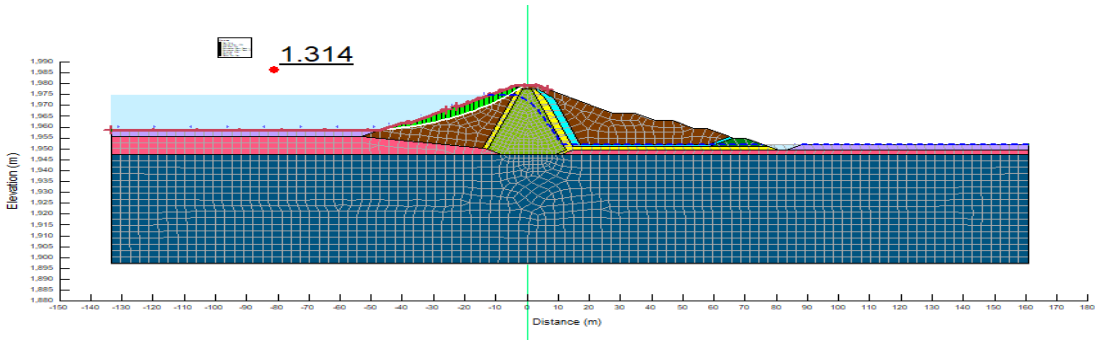

Figure 4-33**:** 1V to 2.0H Upstream slope Finite element static stability (steady state case)

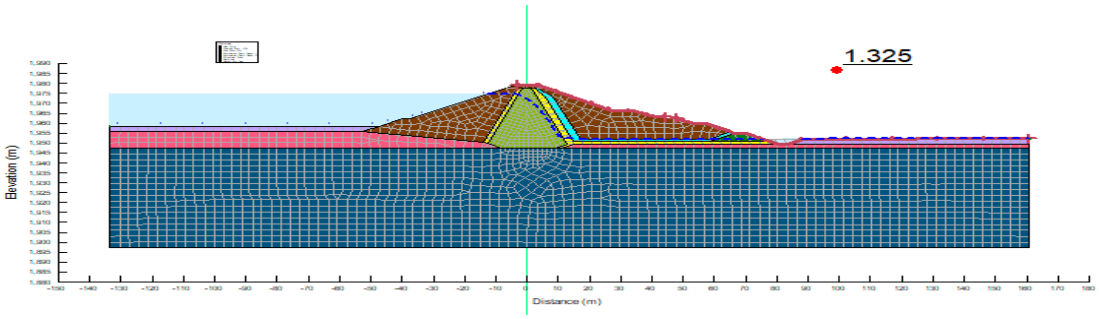

Figure 4-34: 1V to 1.9H Downstream slope Finite element static stability ((steady state case)

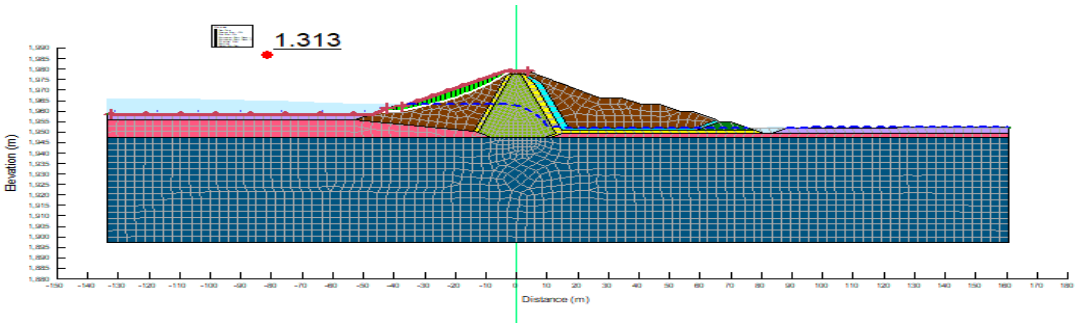

Figure 4-35: 1V to 2.0H Upstream slope Finite element static stability (Transient case)

Despite the fact that all of the slopes have a factor of safety greater than one (1.0), the lowest required factor of safety for a static scenario is 1.5. As a result, the minimum need for both upstream and downstream slopes is not met for a steady-state situation, as seen in the figures above. Furthermore, in the transient (rapid drawdown reservoir), as example

for upstream slope's computed factor of safety against slope instability is 1.313 in the slope of 1V: 2.0H. This value is also at margin of the threshold for static stability.

- As a result, the dam's upstream and downstream slopes of 1V: 2.0H and 1V: 1.9H fail to fulfill the factor of safety minimum criteria for the proposed embankment fill materials (Case 1b), under static loading circumstances.

CASE 2: THE DAM WITH GEOSYNTHETIC REINFORCEMENT

4.4. General

In this case, the dam was re-analyzed by replacing the rock fill zone by granular shell fill and introducing geosynthetic reinforcement to upstream and downstream slopes of the dam. The dam's downstream and upstream slopes are thought to be strengthened (reinforced) by horizontal geotextile layers.

4.5. Static Stability Analysis for Geosynthetic Reinforced Dam

4.5.1. Slope Stability Analysis before Earthquake Shaking

Static stability analysis for different loading conditions of the reinforced dam has been performed for the assurance of the static stability before proceeding the dynamic analysis.

4.5.1.1. Model of the Kalid-Dijo zoned, earth fill dam with geosynthetic reinforcement

The dam was modelled using state of art, Finite element software, SIGMA/W of Geo-Slpope package, as demonstrated in Figure 4-36 below.

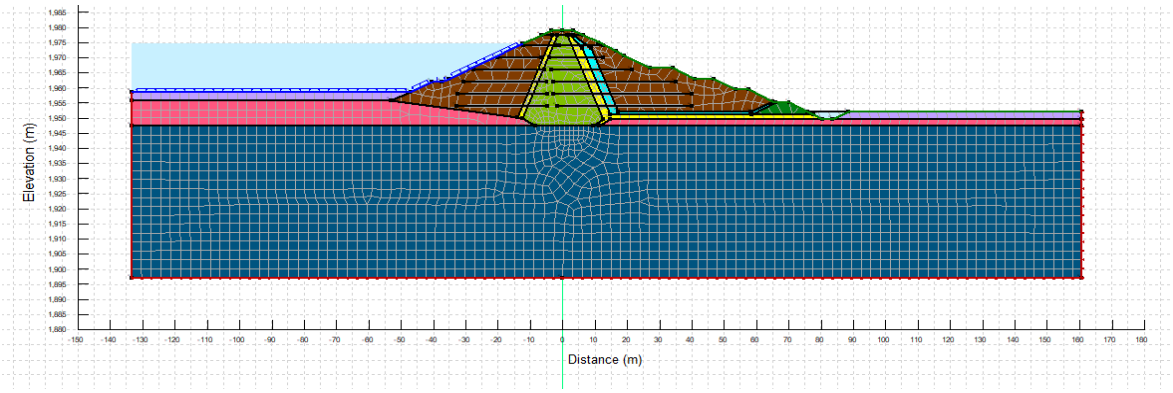

Figure 4-36: Model of the Kalid-Dijo Dam with Geosynthetic reinforcements from SIGMA/W, Geo-Slope International Ltd.

4.5.1.2. Reinforced dam Seepage Analysis

Figure 4-36 depicts the dam with reinforcement as modeled in SEEP/W. However, before testing for stability, the pore pressure condition must be determined. This may be achieved using seepage analysis as described in the next section.

4.5.1.2.1. Downstream steady state Seepage analysis results from SEEP/W

Figure 4-37, Figure 4-38 and Figure 4-39 illustrate the analytical findings after modeling the dam with seep/W and applying the relevant material characteristics.

Figure 4-37 depicts a finite element model with head boundary conditions for the dam's upstream and downstream sides.

Figure 4-38 depicts the total head contour for the specified boundary condition.

Figure 4-39 depicts the pore water pressure, which will be utilized as an input for stability analysis.

Thus, SEEP/W generated pore pressure is taken to SLOPE/W for stability analysis

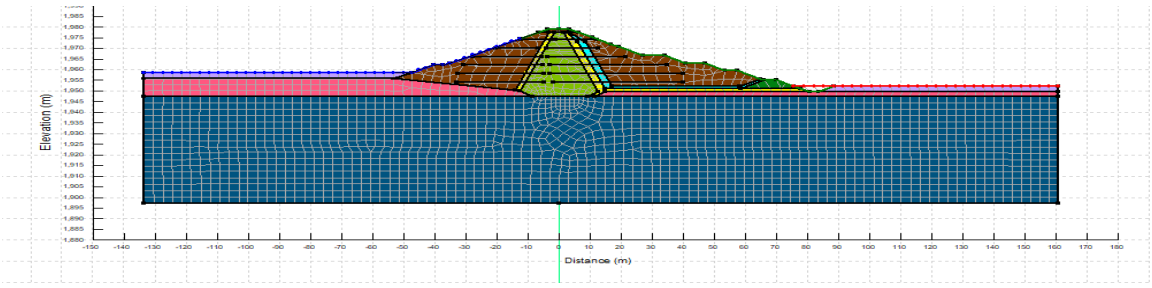

Figure 4-37: Finite element model of reinforced dam for seepage analysis (taken from SEEP/W)

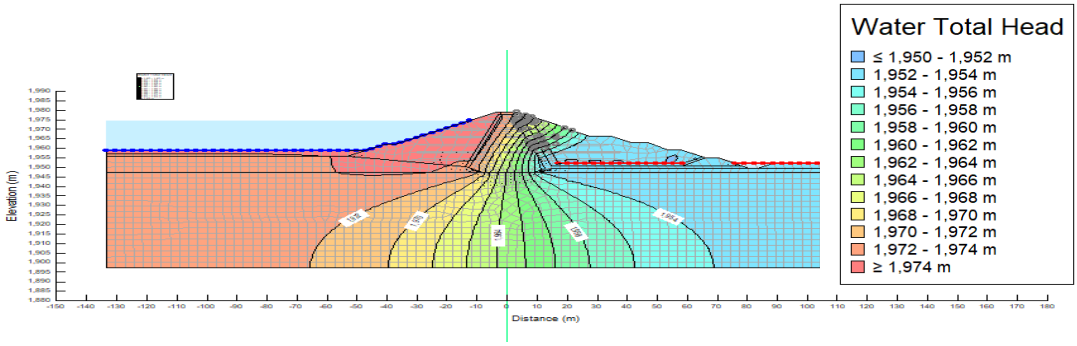

Figure 4-38: Isopotential lines (total head) contour

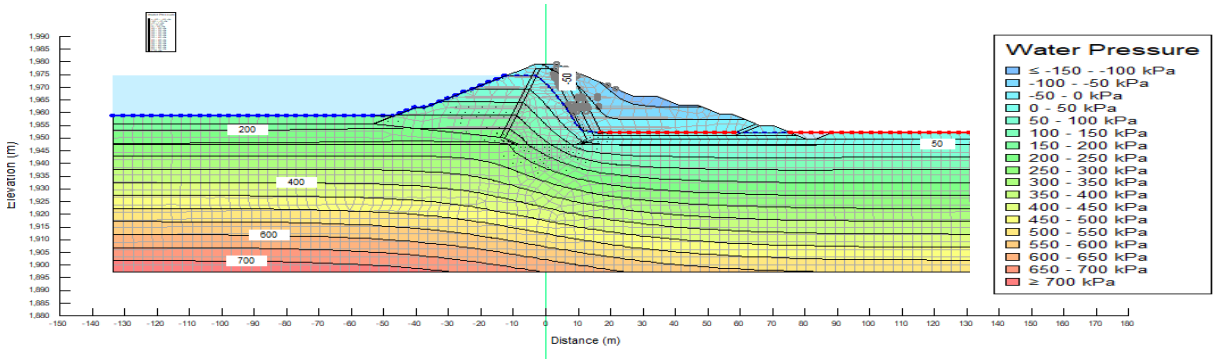

Figure 4-39: Pore Water Pressure Contour (kPa)

4.5.1.3. Transient analysis results using Seep/W

4.5.1.3.1. Initial condition

The initial condition was determined from the preceding steady-state seepage study (section 4.5.1.2.1). In transient analysis, the boundary conditions are time-dependent. As a result, the period of the analysis for this study has been set at 20.5 days with 10 time increments, as in prior examples.

The hydraulic conductivity and volumetric water content functions utilized for the various materials in the analysis are displayed in the figures below.

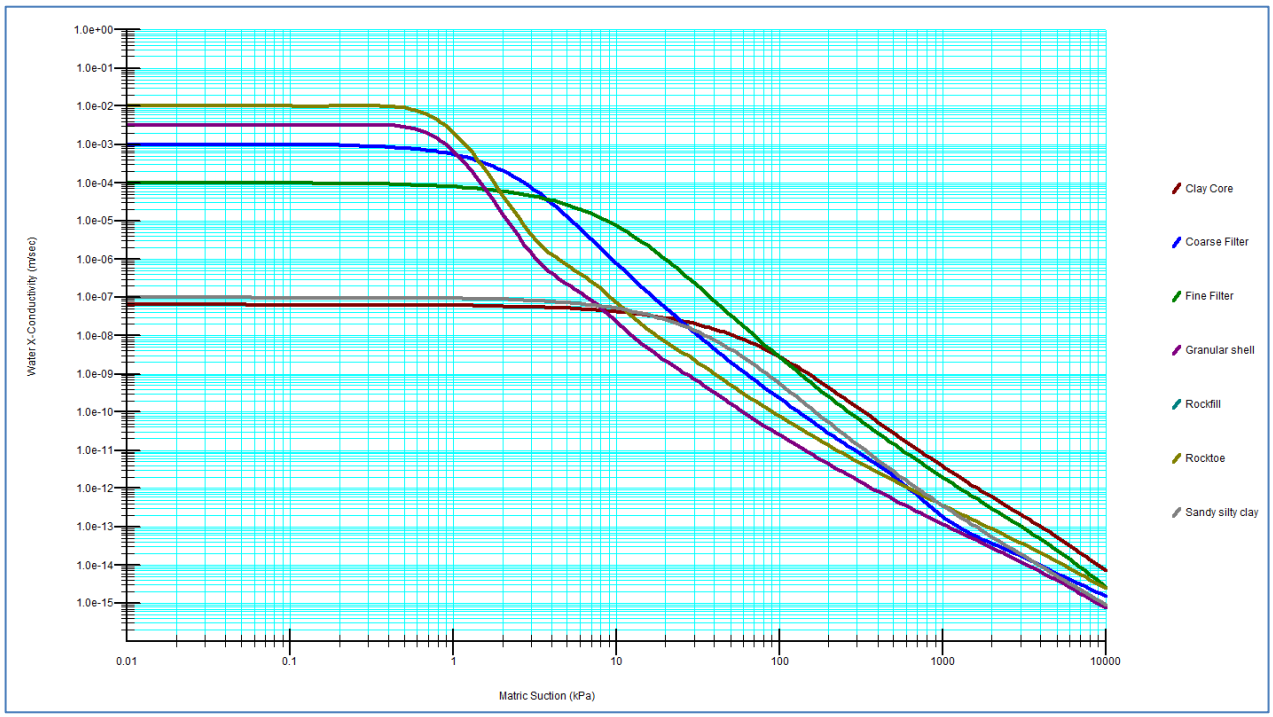

Figure 4-40: Hydraulic conductivity function for all dam materials and foundation

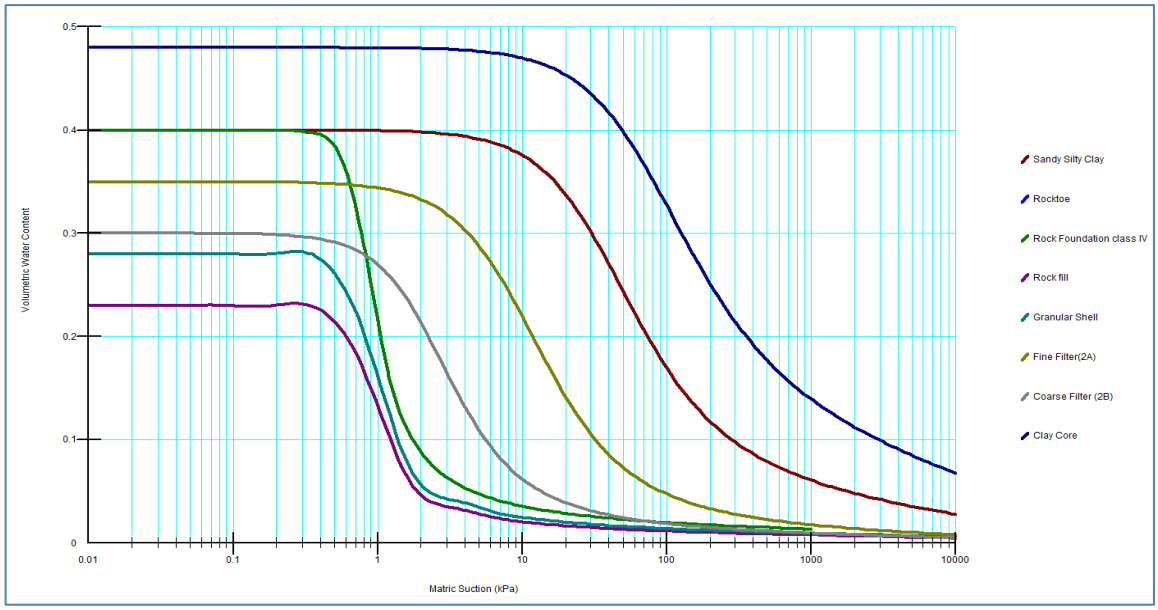

Figure 4-41: Volumetric water content function for all dam materials and foundation

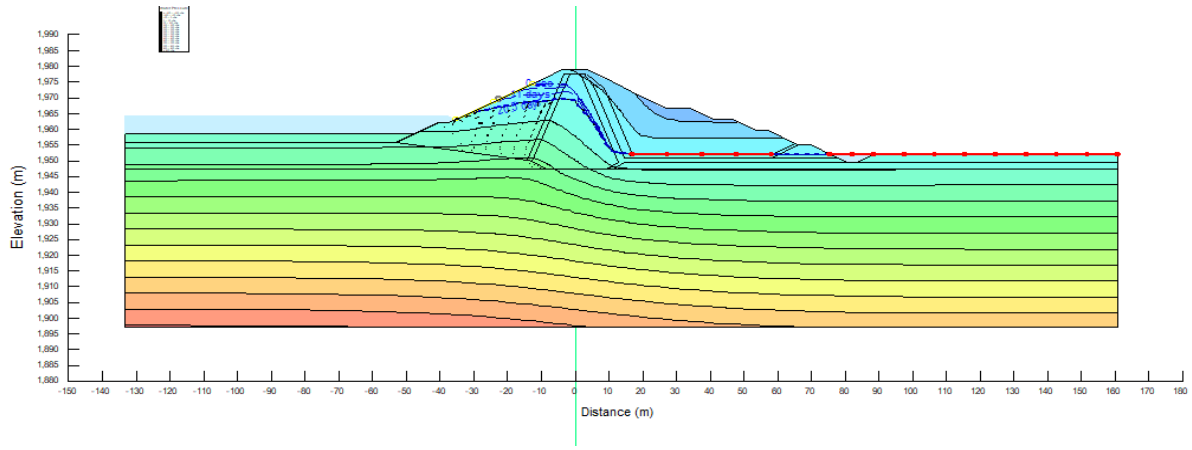

Figure 4-42: Isoclines (zero pressure line) for 20.5 days draw down

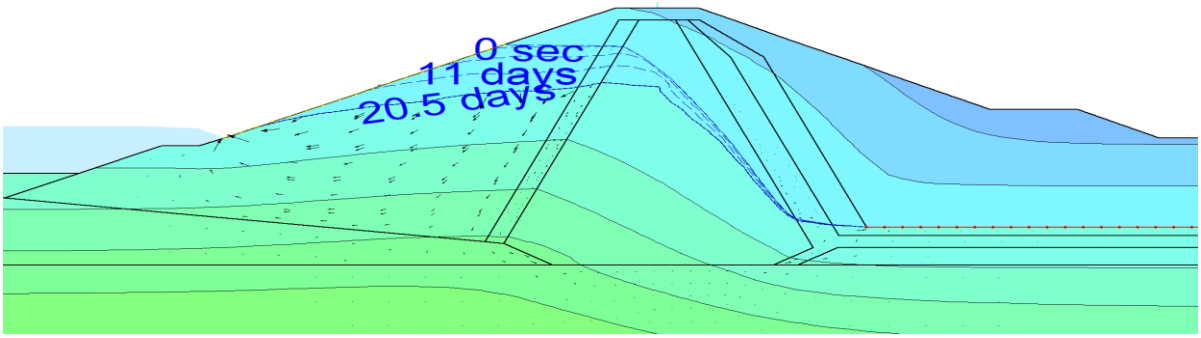

Figure 4-43: Detail of Isoclines (zero pressure lines) for different days

4.5.1.4. Initial Static stress analysis results from SIGMA/W

The elastic-plastic constitutive material model was chosen for this analysis. A boundary condition was specified to both the left and right vertical ends of the SIGMA/W model to restrict horizontal movement. The analyses' lower border is constrained in both vertical and horizontal directions. The outcome of effective stresses in the embankment zone was depicted with a labeled contour below in Figure 4-44.

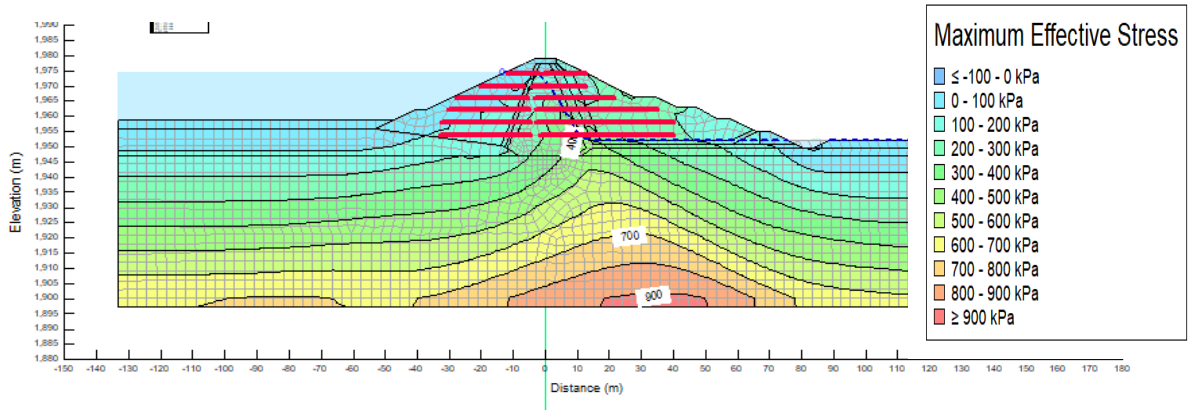

Figure 4-44: Effective stress distribution in the dam

Maximum effective stress (900kPa) was measured at the bottom of the clay core's downstream toe, as seen in the graph. Deducting pore water pressure from total stress yields effective stress. Because of the stored-water pore pressure, the upstream face has the lowest effective stress.

4.5.1.5. Slope Stability Analysis results before the Earthquake Shaking

During the static slope stability study of geosynthetic reinforced Kalid- Dijo earth fill dam, the downstream and upstream slopes of the dam were considered to be reinforced with horizontal geotextile layers independently under the worst loading situations. The static slope stability study was carried out with GeoStudio state of art software, which included both the limit equilibrium and finite element approaches.

4.5.1.5.1. Limit equilibrium method of reinforced dam stability analysis

The limit equilibrium technique of slices was originally designed for traditional slope stability assessments. Despite the early creators' worries, concentrated loads were gradually integrated into the approach, mostly to simulate machinery or other surcharge loading on the hill crest. Later, thinking on the issue evolved into the notion that if

concentrated point loads can be included in the approach, then other lateral concentrated point loads to indicate reinforcement may be incorporated.

GeoStudio includes various reinforcement types for 2D analysis, including anchors, nails, geosynthetics, and piles. In a limit equilibrium analysis, all reinforcement is represented as a concentrated point load. The concentrated point loads operate on the free body, or potential sliding mass, and must thus be included in the moment and force equilibrium calculations. Although there are several handy methods for determining the features of the reinforcement, the supplied parameters are eventually employed to generate a concentrated point load in factor of safety calculations.

There are two ways for calculating pullout resistance in geosynthetics like geotextiles and geogrids. The selection is dependent on the reinforcement's stress transmission method.

- If passive resistance is the major form of stress transmission (for example, geogrids), the pullout resistance might be defined explicitly.

- If frictional resistance is the dominant stress transfer mechanism (e.g., geotextiles), the pullout resistance may be computed using the overburden stress.

Hence, since geotextile reinforcement was considered for the current study, the second alternative of pullout resistance calculation is used.

The calculated pullout resistance option requires the following parameters;

- Interface adhesion (S_{IA}): When considering effective drained soil strengths, apparent cohesion (adhesion) is taken into account. The parameter can also be used to define the un-drained strength at the geosynthetic-soil interface (SLOPE/W, 2018). For current study, the value of interface adhesion 0kPa was considered as per stated in Table 3-10 (adhesion value of geotextile-gravel interface), since most of the reinforcement is applied to the granular shell fill material that is almost non-cohesive.

- Interface shear angle (δ): Soil-geosynthetic interface friction is an important parameter for designing a reinforced slope (Shukla and

Yin, 2006). Geotechnical literatures recommends different relationships of soil –soil interface shear angle and geotextile –soil interface shear angles as observed in section (3.4.5). Hence, the value of 0.86ϕ interface shear angle (according to Table 3-11 or Koerner, 2005)) was used for this study. Where ϕ is the angle of internal friction value for granular shell fill material.

- Surface area factor (S_{AF}): Used to account for mobilization pullout resistance at both the top and bottom of the geosynthetic. The number of one (1) is used for only one side resistance, whereas the value of two (2) is used for resistance on both sides of the geosynthetic. As a result, the resistance on both sides of the geosynthetic was considered for this investigation, and a value of 2 was employed in the simulation.

- Hence, the software calculates the pullout resistance PR as per the given equation below (SLOPE/W, 2018):

$$PR = (S_{1A} + \sigma'_v \tan\delta) S_{AF} \text{---------- 4-2}$$

Where, $\sigma' v$ represents the effective overburden stress. The effective overburden stress is computed using the soil height above the junction point with the base of the slice, taking into account surcharge loads.

➢ Irrespective of the chosen technique, the following inputs are required:

Resistance Reduction Factor (RRF): This may be applied as a "scale effect correction factor" to account for nonlinear stress reduction throughout the embedded length of highly extensible reinforcement (SLOPE/W, 2018). The resistance correction factor is mostly determined by the strain softening of the compacted granular backfill material, as well as the extensibility and reinforcing length. RRF is about one for inextensible (metallic) reinforcement, but it can be much lower for extensible (geosynthetic) reinforcements. Pullout tests on reinforcements of various lengths can provide these results. In the absence of test data, the values listed in the table below should be utilized for geogrids and geotextiles (Berg, 2009). As a result of the usage of geotextile reinforcement in this study, the RRF value employed in the model is 0.6, as shown in Table 4-4.

Table 4-4: Typical α values (Berg et al. - Vol. I, 2009)

Reinforcement type	Resistance Reduction Factor (RRF)
All metallic reinforcements	1.0
Geogrids	0.8
Geotextiles	0.6

Tensile Capacity (TC): - This refers to the reinforcement's tensile strength. The tensile strength of the geotextile reinforcement is presented in table 3-12 below, and a value of 400kN was employed in this investigation.

Reduction Factor: - Accounts for reductions in the reinforcement's ultimate tensile capacity caused by physical factors such as installation damage, creep, and durability. In the absence of test data, geotechnical literature advises using a value of 1 for design. As a result, the value '1' is taken into account in this study during the modeling process.

Load orientation: - A variable between 0 and 1 that controls the direction of the pullout force on the free body. A value of zero (0) applies the load parallel to the geosynthetics orientation; a value of one (1) applies the force parallel to the slice base. As a result, in this research, a value of zero (0) was employed, which takes into account load application parallel to the geosynthetic orientation.

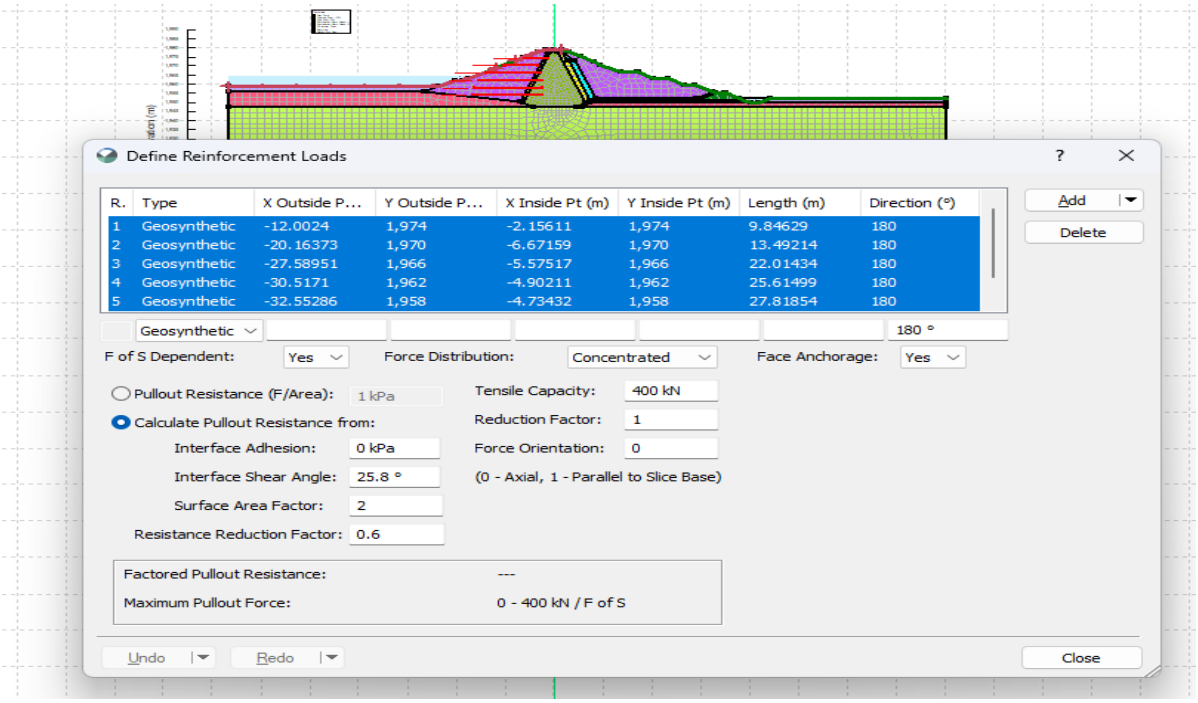

Figure 4-45: The Sample figure from Slope/W Model Showing the Parameters in Limit equilibrium modeling techniques.

SLOPE/W typically has numerous geosynthetic reinforcements from different manufacturers. The reinforcing parameters are determined automatically depending on installation and site conditions, which impact the total reduction factor for tensile capacity. The inputs for each manufacturer's reinforcement vary according on the product type selected. Each of the reducing elements is modified by site and environmental circumstances. Individual reduction factors can be determined by soil type or particle size, fill material, temperature, design life, and/or soil pH levels (GEOSLOPE, 2018).

4.5.1.5.1.1. Stability study of reinforced D/s slope under steady-state seepage conditions

The slope without geosynthetic reinforcement was first analyzed, and then horizontal layers of geotextile were applied to the dam slopes with varied reinforcement spacing. To ensure safety and economics, the distance between reinforcing layers was changed from 1 to 4 m in each example. During each case's analysis, the length of the reinforcing layer and the offset from the dam's downstream face were varied, but the reinforcing layers remained activated, i.e. intersected the potential slip surface, and the governing failure criteria for the reinforcing layer remained tensile. This ensures that the reinforcing layers are used to

their full capacity and saves money. The analysis results for each example are reported in the sections that follow.

Case 1: The downstream dam slope without geosynthetic reinforcement

Figure 4-46 depicts a stability study of a downstream slope assuming long-term steady state seepage conditions prior to reinforcement.

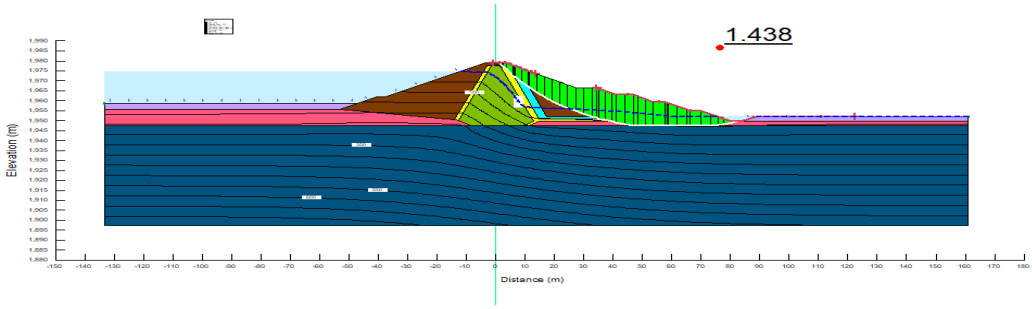

Figure 4-46: Stability study of the downstream slope under steady state conditions (without GS reinforcement)

Case 2: The downstream dam slope with 1m spacing of geosynthetic reinforcement

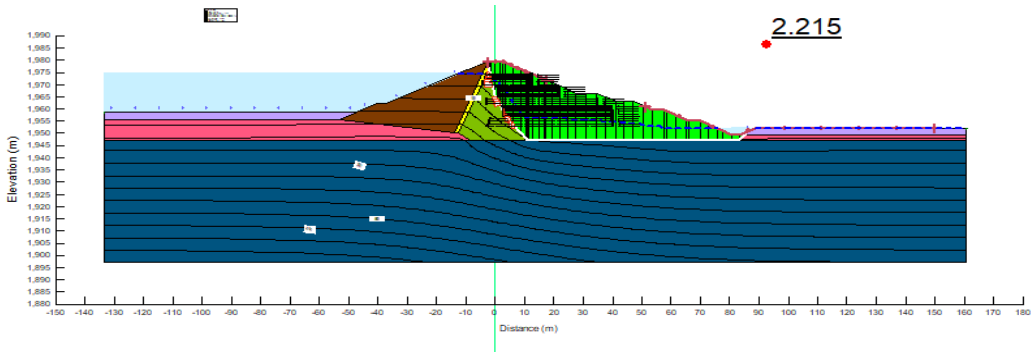

Figure 4-47: Stability investigation of the downstream slope under steady state conditions (with 1m spacing of GS reinforcement).

Case 3: The downstream dam slope with 2m spacing of geosynthetic reinforcement

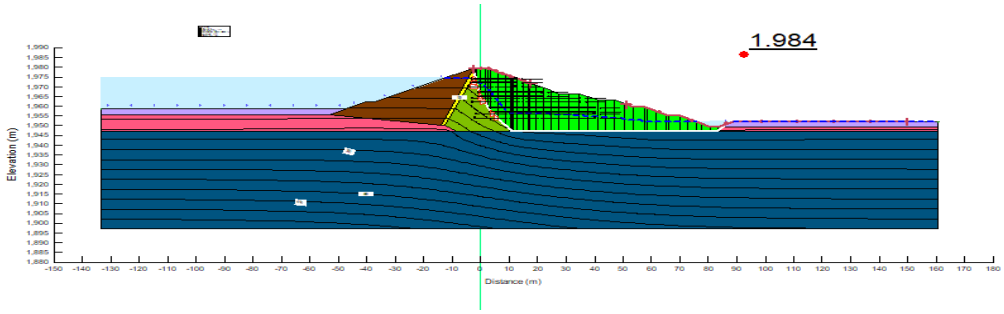

Figure 4-48**:** The downstream slope's stability in steady-state circumstances with GS reinforcement spaced at 2m intervals.

Case 4: The downstream dam slope with 3m spacing of geosynthetic reinforcement

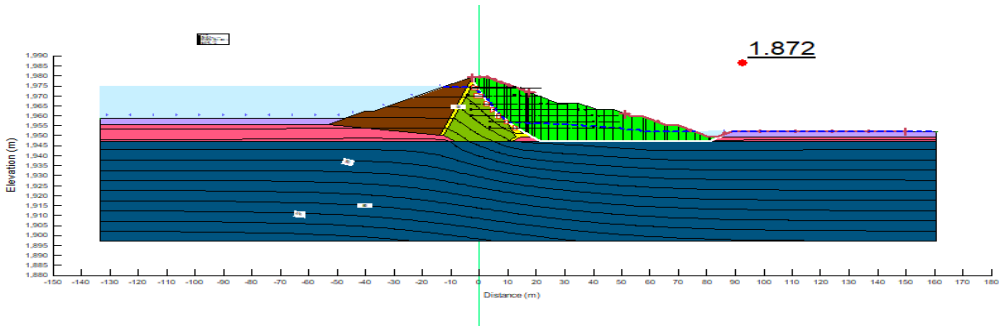

Figure 4-49**:** The downstream slope's stability in steady-state circumstances with GS reinforcement spaced at 3m intervals

Case 5: The downstream dam slope with 4m spacing of geosynthetic reinforcement

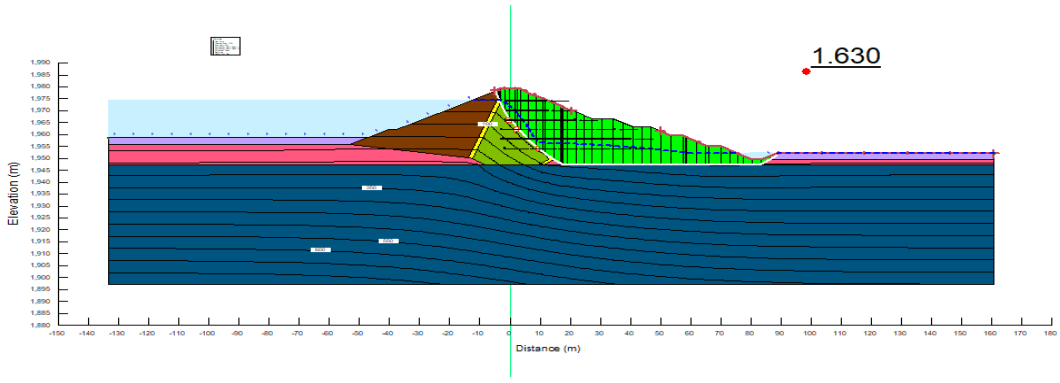

Figure 4-50: The downstream slope's stability in steady-state circumstances with GS reinforcement spaced at 4m intervals

Summary of the downstream-reinforced slope analysis results

Table 4-5 and Figure 4-51 show the findings of the downstream-reinforced dam study under steady-state seepage conditions with varying geosynthetic layer spacing.

Table 4-5: Geosynthetic reinforcement spacing versus D/S Slope Factor of safety

Geosynthetic Spacing (m)	D/S Slope Factor of safety	(%) Decrease in FOS with increasing GS Spacing
1.0	2.215	
2.0	1.984	10.42
3.0	1.872	11.20
4.0	1.630	24.10
Without Reinforcement	1.438	Less than Min. FOS (i.e., 1.5).

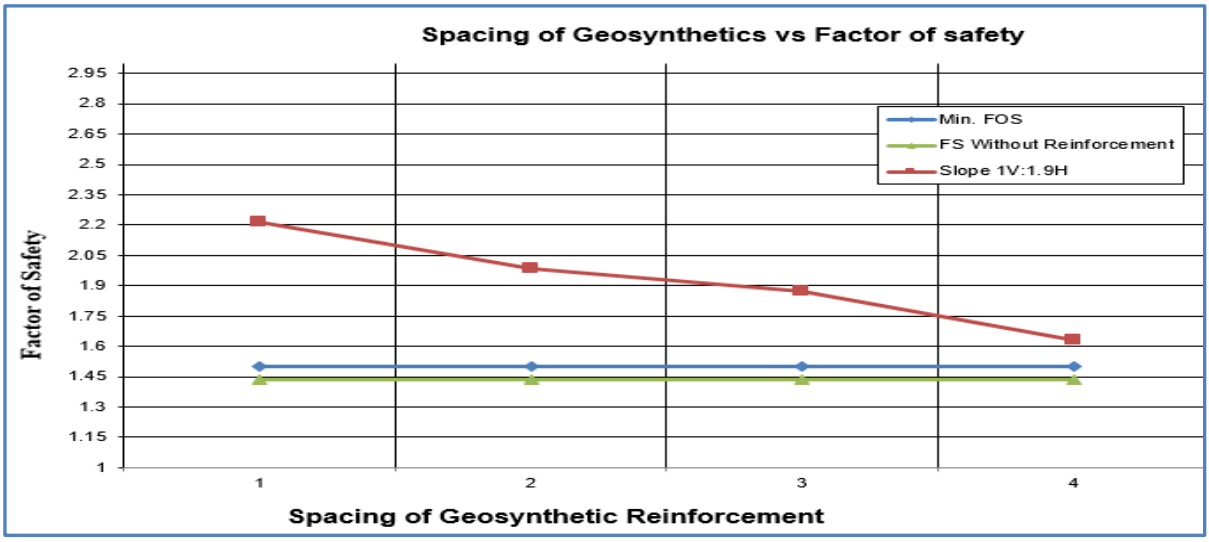

Figure 4-51: Variation of factor of safety with respect to spacing between geosynthetic layers for steady state condition.

- The downstream slope of a dam must be safe for the stated slope of 1. 9H: 1V without a rock fill zone if geosynthetic layers are spaced 4m apart. To accommodate higher slopes, the vertical distance between geosynthetic layers must be lowered.

- The length of the geosynthetic layers necessary to reinforce the downstream slope is determined to be between 13m and 42m.

- The offset from the downstream slope ranges from 1m to 32m, depending on where the geosynthetic layers are located.

- Further increases in geosynthetic layer spacing make the dam's downstream slope dangerous, as shown by the percent drop in factor of safety with subsequent geosynthetic spacing increases in Table 4-5.

4.5.1.5.1.2. Analysis of the Upstream Slope under the worst loading scenario (Sudden Drawdown)

When the pore water pressure and exposure conditions in the system change over time, a time dependent seepage study is needed. This is known as transitory analysis. It denotes anything that is always changing. It is changing because it takes into account the time it takes for the soil to respond to the user-defined boundary conditions. One example is when a reservoir upstream of a dam is abruptly drained.

The upstream slope of the Kalid-Dijo earth fill dam was evaluated to be reinforced with horizontal geotextile layers and tested for the possibility of abrupt drawdown. The addition of geotextile reinforcing layers would raise the factor of safety, bringing the upstream slope to safety after replacing the rock fill

The u/s slope was initially examined without geosynthetic reinforcement, and then horizontal layers of geotextile were applied to the dam slopes with variable reinforcement spacing. To assure safety and economy, the distance between reinforcing layers was adjusted from 1m to 4m in each example. During each case's study, the length of the reinforcing layer and its offset from the dam's upstream face were altered, but the reinforcing layers remained activated, crossing the possible slip surface, and the governing failure requirements for the reinforcing layer remained tensile. This guarantees that the reinforcing layers are completely used, resulting in cost savings. The analytical findings for each example are reported in the following section:

Case 1: The Upstream dam slope stability without geosynthetic reinforcement

Figure 4-52 depicts the stability analysis of an upstream slope under transient seepage conditions before reinforcing.

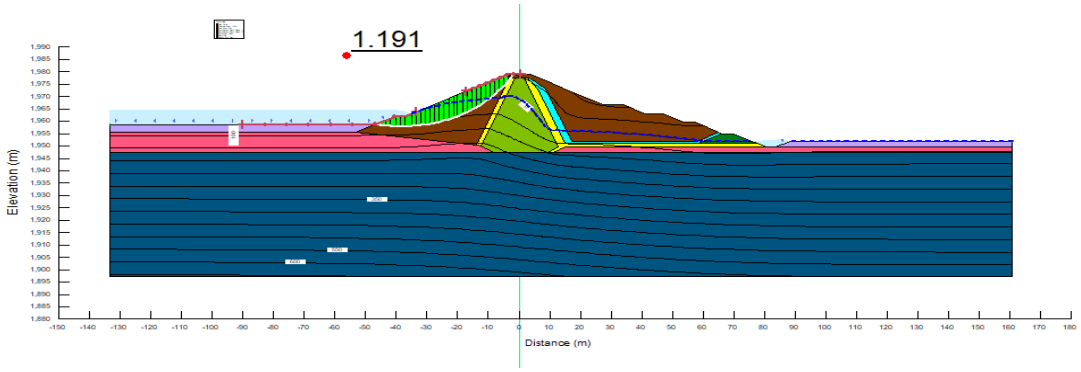

Figure 4-52: Stability analysis of upstream slope under transient condition (without GS reinforcement)

Case 2: The Upstream dam slope stability with 1m spacing of geosynthetic reinforcement

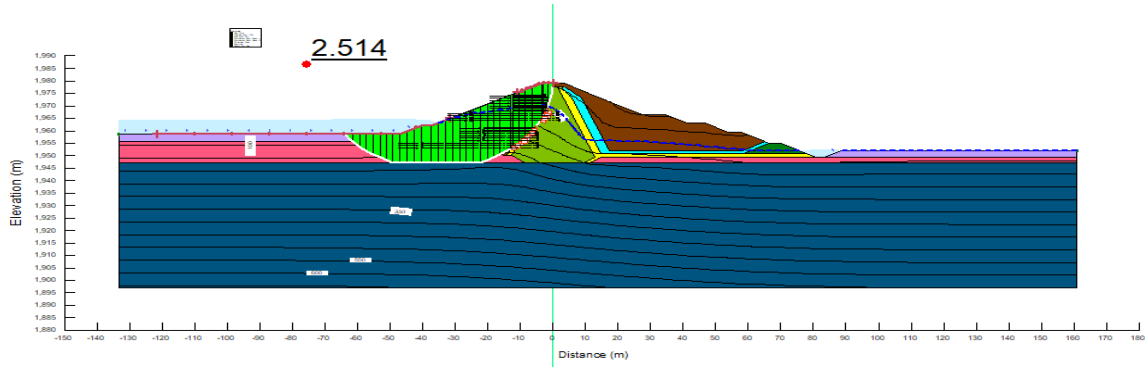

Figure 4-53: Stability investigation of the upstream slope under fast drawdown conditions (with 1m spacing of GS reinforcement).

Case 3: The upstream dam slope stability with 2m spacing of geosynthetic reinforcement

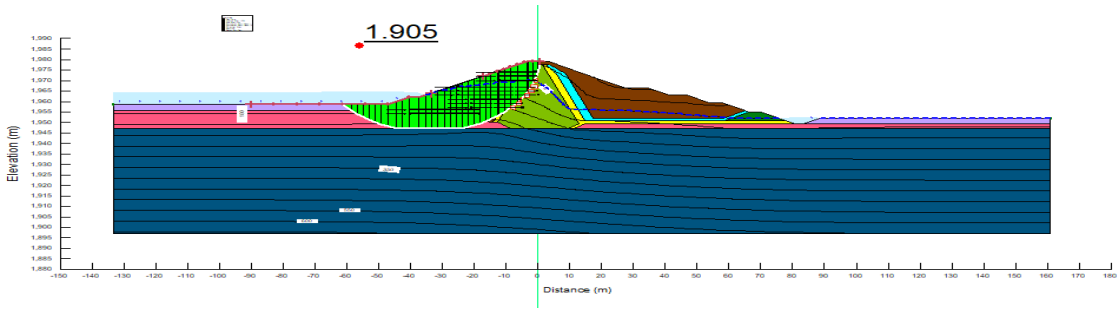

Figure 4-54: Stability investigation of the upstream slope under transient conditions (with 2m spacing of the GS reinforcement).

Case 4: The upstream dam slope stability with 3m spacing of geosynthetic reinforcement

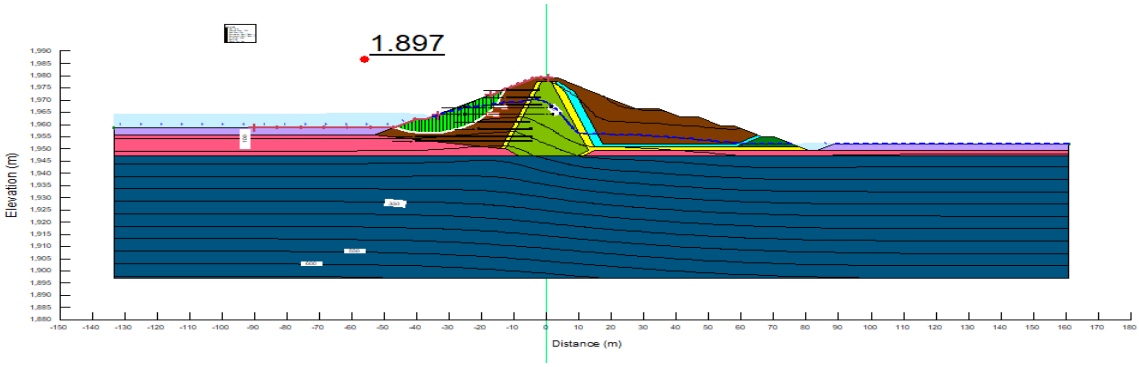

Figure 4-55: Stability investigation of an upstream slope under transient conditions (with 3m spacing of GS reinforcement).

Case 5: The upstream dam slope with 4m spacing of geosynthetic reinforcement

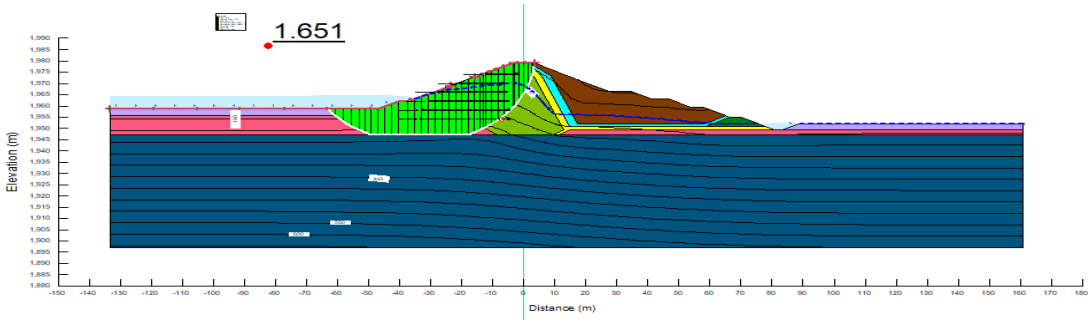

Figure 4-56: Stability investigation of the upstream slope under transient conditions (with 4m spacing of GS reinforcement).

Results and comments for the upstream-reinforced slope analysis

The results of the upstream-reinforced dam analysis under transient seepage condition for different geosynthetic layer spacing have been summarized as shown in Table 4-6 and Figure 4-57.

Table 4-6: Geosynthetic reinforcement spacing versus U/S Slope Factor of safety

Geosynthetic Spacing (m)	U/S Slope Factor of safety	(%) Decrease in FOS with increasing GS Spacing
1	2.514	
2	1.905	24.2
3	1.897	4.2
4	1.651	12.97

Without Reinforcement	1.191	Less than Minimum. Requirement (i.e., 1.3)

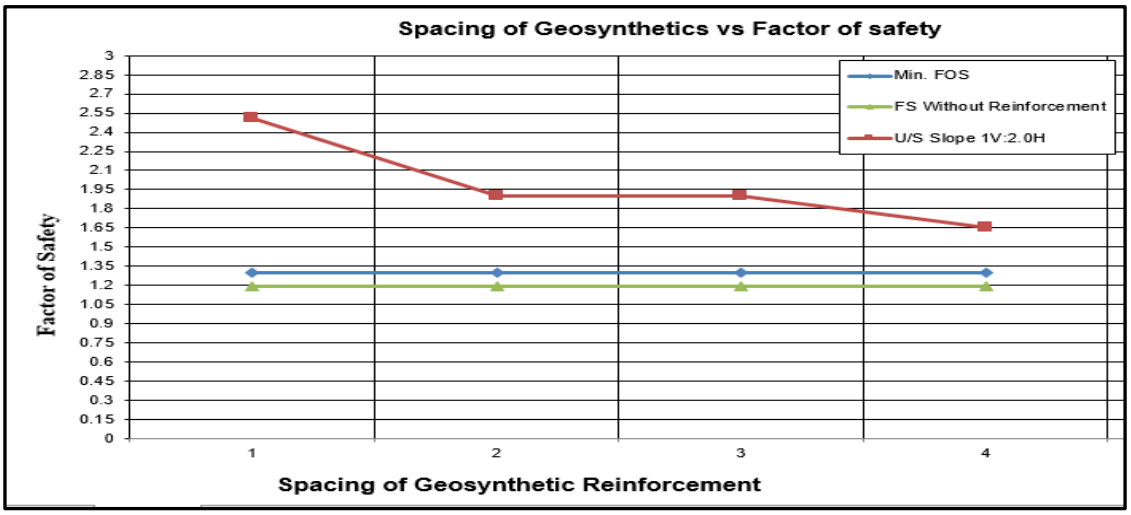

Figure 4-57: Variation of u/s slope factor of safety with respect to spacing between geosynthetic layers for transient condition

- By providing the geosynthetic layers at spacing of 4m, the upstream slope of a dam shall be safe for the given slope of 2.0H: 1V without rock fill zone. For steeper slope, the vertical spacing between geosynthetic layers is required to be reduced.
- The length of the geosynthetic layers necessary to reinforce the upstream slope is determined to be between 10 and 28 meters.
- The offset from the downstream slope ranges from 1m to 20m depending on where the geosynthetic layers are located.
- Further increase in spacing of geosynthetic layer brings the upstream slope of the dam to be unsafe as seen the percent decrease in factor of safety with consecutive geosynthetic spacing increase from Table 4-6.

4.5.1.5.2. Finite element Method of Stability analysis

For this study, the optimized geosynthetic reinforcement spacing, length and offset distance from upstream and downstream slopes in limit equilibrium method were taken for static and dynamic finite element methods of analyses.

For Finite element method of stability analysis, the geosynthetic reinforcement modeled in SIGMA/W, the result was read by SIGMA/W Stress analysis type in SLOPE/W, Geo-Slope International Ltd package, and the analysis results were presented as follow.

4.5.2. Structural Elements in GeoStudio Finite Element Packages

The use of structural support (e.g., beams, cables, geosynthetics) to stabilize a soil mass is an important aspect of geotechnical analysis.

SIGMA/W and QUAKE/W will be used to simulate buildings with variable shape and attributes, as well as their interactions with soil or rock. Bathe (2006) goes into great depth about the formulation of structural elements. Even if certain structural components (such as cables and geosynthetics) do not resist bending, the fundamental ideas of structural elements are best studied by examining an element with flexural stiffness. An axisymmetric analysis may be performed using plate and geosynthetic structural components.

4.5.2.5. Bar elements

In SIGMA/W, a structural element with zero flexural rigidity (EI) is referred to as a bar element. A bar element can resist only axial forces. As a result, the nodes of a bar element do not require a rotational degree of freedom. A bar element is also drawn along a line object, but it does not have to be concurrent with a soil element edge. It can cross over elements but only connects at region points (SIGMA/W, 2018).

4.5.2.6. Beam elements

The beam element is developed using Timoshenko beam theory, which takes into account shear deformations and rotational bending effects. A beam is employed in a plane strain (2D) analysis to simulate structures with axial stiffness, shear resistance, and bending. A beam is applied to a line, resulting in a one-dimensional element within a two-dimensional space.

The finite element modeling of geosynthetic reinforcement can be done using in SIGMA/W and QUAKE/W GeoStudio packages. The geo-fabric (geosynthetic) is modeled as a beam element with zero flexural stiffness. Interface elements are included on either side of the geosynthetic with different frictional properties on the top and bottom of the geosynthetic. Compression forces are not allowed to develop in the fabric (geosynthetic); only tensile forces are allowed during analysis (SIGMA/W, GEOSLOPE International Ltd, 2018).

For, this study, the geosynthetic reinforcement was modeled using beam element with no bending stiffness, but only with axial stiffness in GEOSLOPE International Ltd, 2018, finite element packages SIGMA/W and QUAKE/W. When Plate and geosynthetic structural elements are used in an axisymmetric analysis, the compression forces are not allowed to develop; only tensile forces are allowed. Figure 4-58 below which was taken from SIGMA/W sample model which illustrates the procedures followed during finite element method of geosynthetic reinforcement modeling.

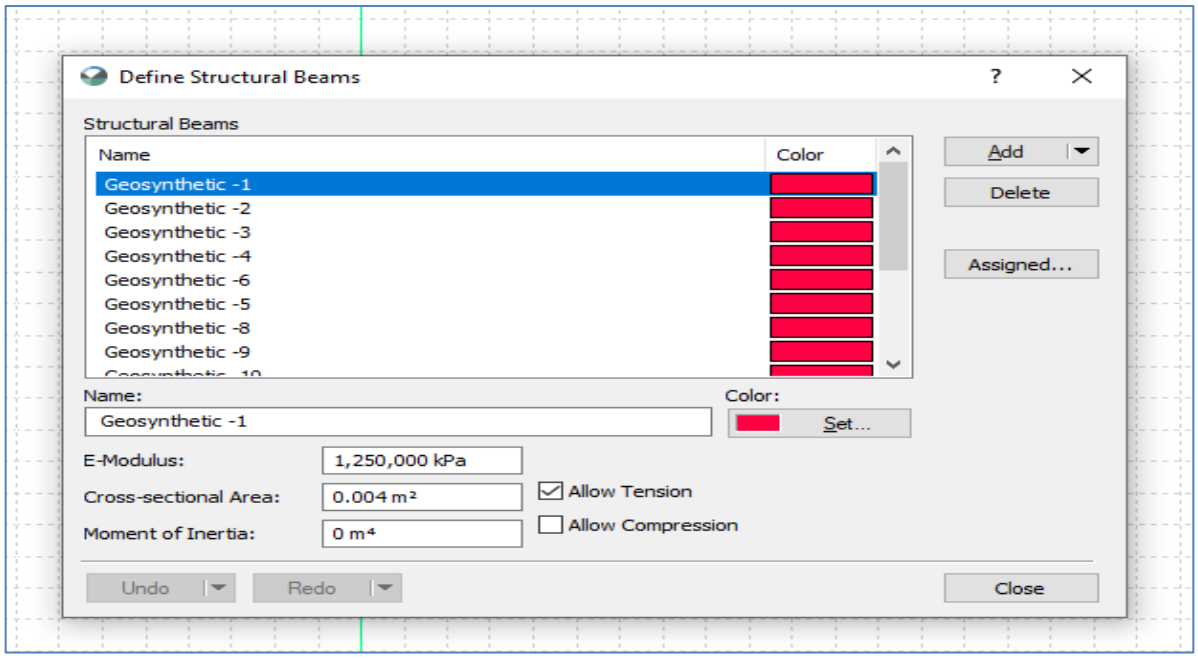

Figure 4-58 : Material properties used for Geosynthetic reinforcement modeling

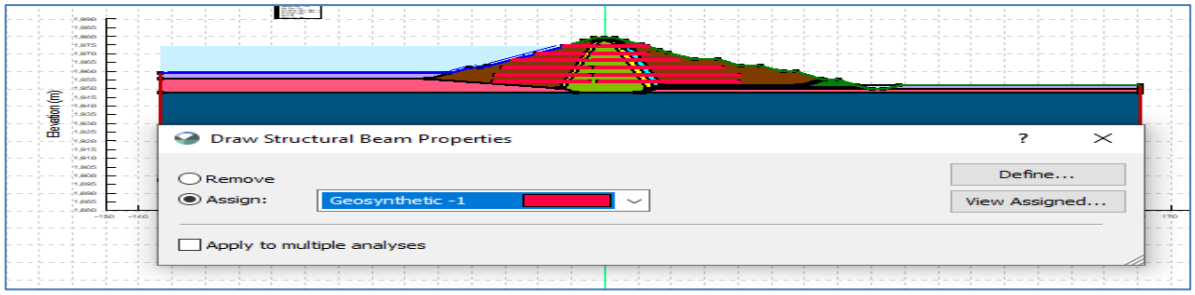

Figure 4-59: Assigning geosynthetic reinforcement material properties to the dam model.

4.5.2.6.1.1. Upstream and Downstream Slopes

For the upstream slope, the finite element calculated factor of safety before earthquake shaking for geosynthetic reinforced dam with slope of 1V : 2.0H, is 1.661 against slope, instability and for the downstream slope of 1V : 1.9H, is 1.719 against slope instability as shown in Figure 4-60 and Figure 4-61,respectively.

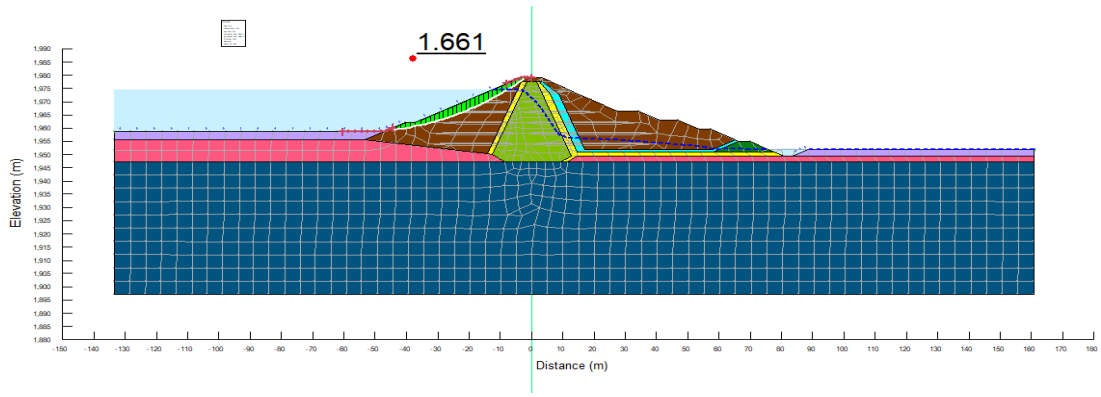

Figure 4-60**:** 1V to 2.0H Upstream slope Finite element reinforced dam static stability (Steady state case)

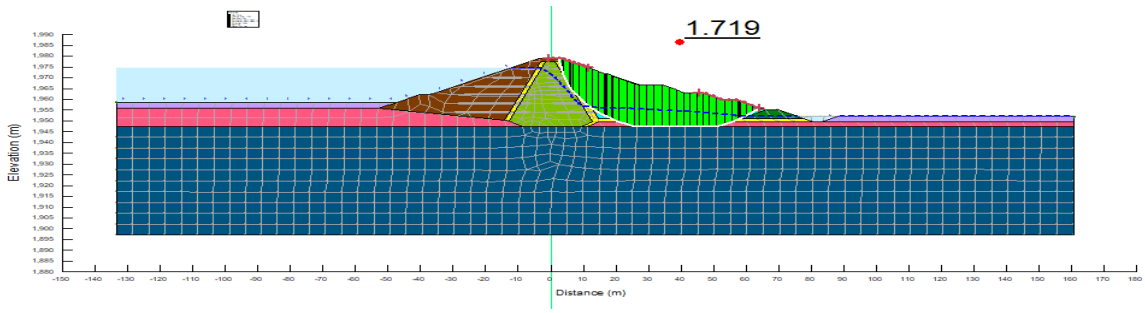

Figure 4-61**:** 1V: 1.9H downstream slope reinforced dam finite element calculated static stability ((steady state case)

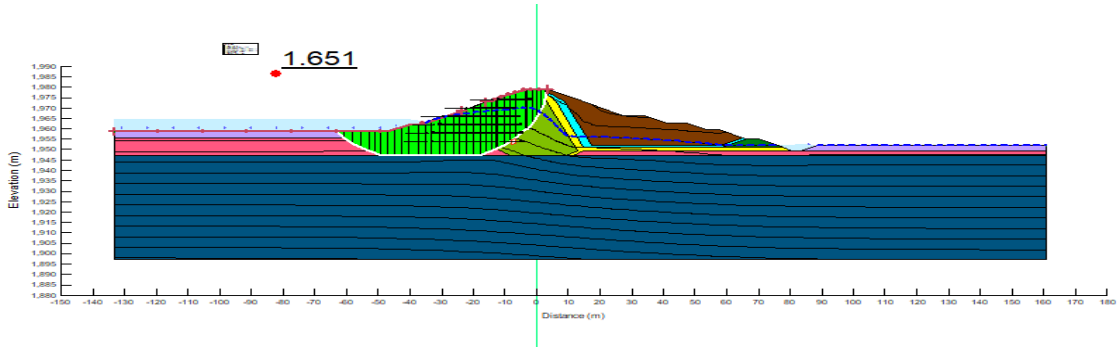

Figure 4-62: 1V: 2.0H Upstream slope Finite Element method reinforced dam static stability (Rapid drawdown case)

As shown above, the entire reinforced dam slopes have a factor of safety larger than 1.5 (the minimum needed factor of safety for a static situation) according to US. Corps of Engineers, 2003 and as depicted in tables (Table 4-2 and Table 4-3).

4.6. Dynamic Stability Analysis for Geosynthetic Reinforced Dam

4.6.1. The Finite Element Model for reinforced dam

The finite element model is done with both structured and unstructured mesh, depending on the geometry. Figure 4-63 shows the finite element model of reinforced dam which is used for the dynamic analysis of Kalid-Dijo earth fill dam. The model is prepared using the QUAKE/W program for the maximum cross-section of the dam. This model consists of 2588 nodes in which equations are checked and 2529 elements, where material properties are extracted, using approximate global element size of 3m. The quadrilateral and triangular element geometry is selected for their compatibility in an unstructured mesh and the interface elements are generated for the geosynthetic reinforcements in Geo-Studio, Sigma/W and Quake/W during modeling.

To minimize the disturbance due to the boundary, wave reflection in the dynamic analyses, the side boundaries were extended by 80m (more than 3 times the dam height) in both left and right directions. The bottom boundary of the model has been located in the foundation rock class II (welded tuff) at a depth of 50m from the bottom of the dam cut-off level.

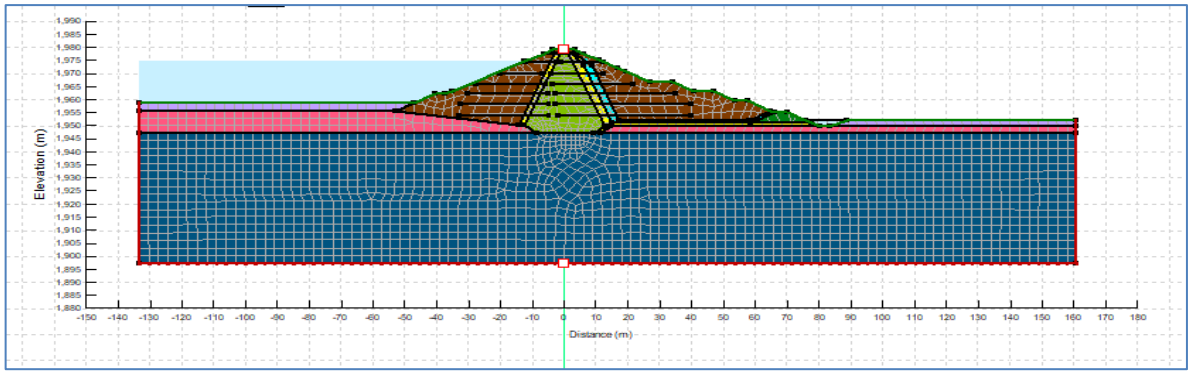

Figure 4-63: QUAKE/W Finite element model to show mesh elements and nodes

4.6.2. Dynamic analysis results and discussions

Figure 4-64 illustrates a sample output for horizontal maximum acceleration. The dam is 25.5 meters high above river bed level and is built on weathered pyroclastic deposit (welded tuff) or Rock class II foundation that is subjected to El Centro ground motion with an amplitude of 0.45g. The dam's side slope is 2H: 1V and 1.9H: 1V upstream and downstream respectively, with a core side slopes of 0.4H: 1V. This section presents the maximum acceleration at the top of the foundation and within the dam.

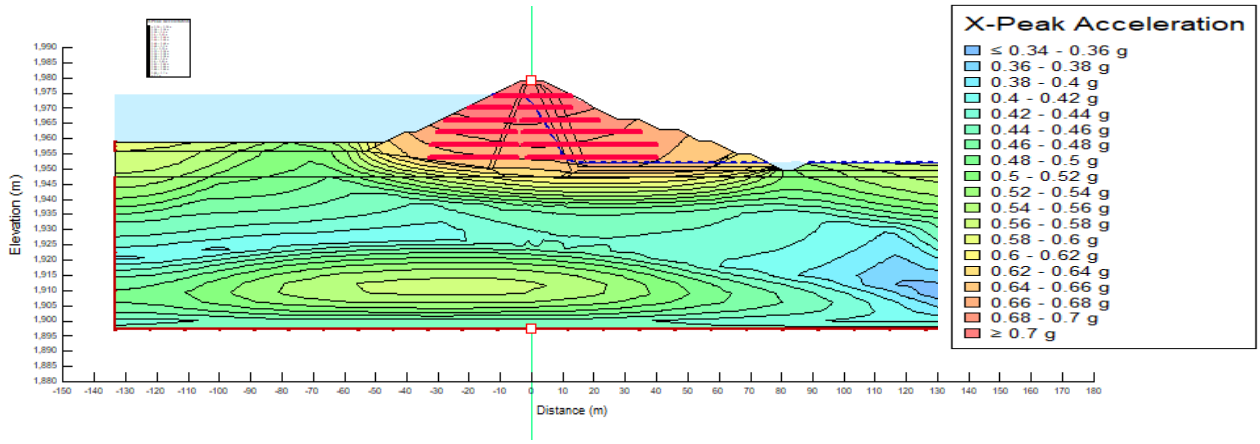

Figure 4-64: Sample FE software output for horizontal maximum acceleration.

4.6.2.5. Acceleration Response at the dam Crest

Figure 4-65 and Figure 4-66 depict the acceleration response at the dam crest during the Hachinohe earthquake, corresponding to the site-specific SEE and OBE horizontal PGA, respectively, in relation to input ground motion. The estimated ground accelerations at the dam crest for horizontal SEE and OBE Hachinohe accelerations are 0.72g and 0.48g, respectively, as illustrated in Figures 4-65 and 4-66. Peak ground accelerations are

expected to be enhanced from 0.45g at the model's base to about 0.72g at the crest for the Kalid-Dijo reinforced dam for the Safety Evaluation Earthquake of Hachinohe. This corresponds to an amplification value of about 0.27g for reinforced dam. Results for other earthquakes shall be given in Appendices at the end of the reports.

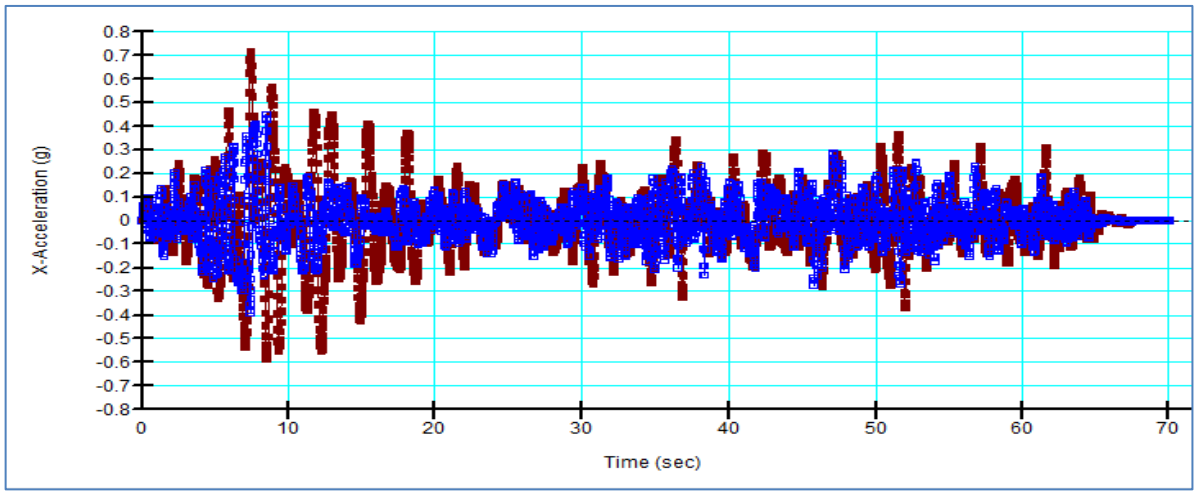

Figure 4-65: X-acceleration response at dam crest and input motion at the base for Hachinohe Safety Evaluation Earthquake (SEE).

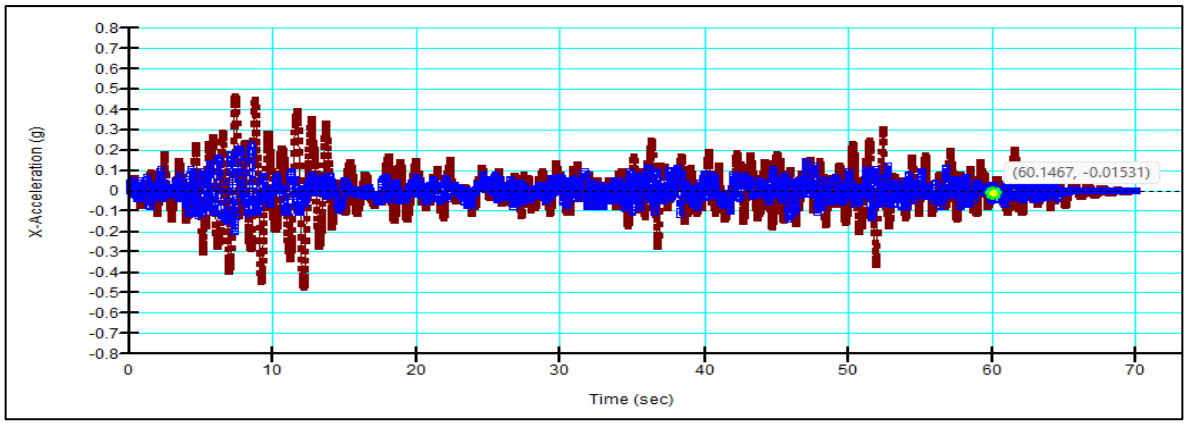

Figure 4-66: X-acceleration response at dam crest and input motion at the base for Hachinohe, Operating Basis Earthquake (OBE).

4.6.2.6. Spectral response at dam crest

Figure 4-67 shows that the dam's highest spectral response to an El Centro, Safety Evaluation Earthquake (SEE) occurs at a period of 1.01 seconds (frequency of 0.99 cycles per second) and is within the normal frequency range of embankment dams (0.5 Hz to 10Hz). Similarly, in the event of an Hachinohe (SEE) Earthquake, as shown in Figure 4-68, the greatest spectrum acceleration response occurs at 0.75sec (1.33 cycles per

second), which is also within the range of natural period or frequency for embankment dams.

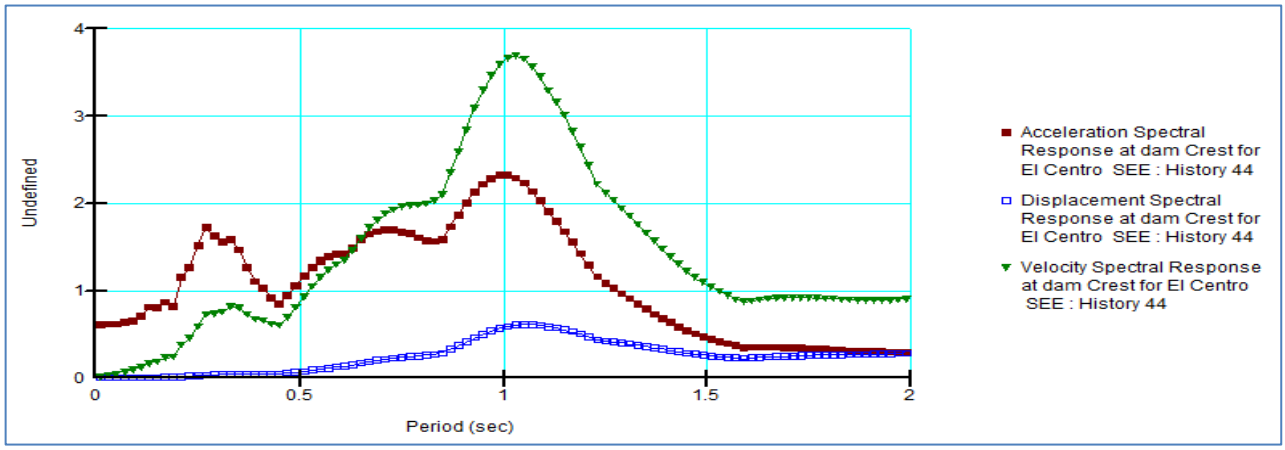

Figure 4-67: Horizontal Spectral response at dam crest corresponding to SEE (El Centro)

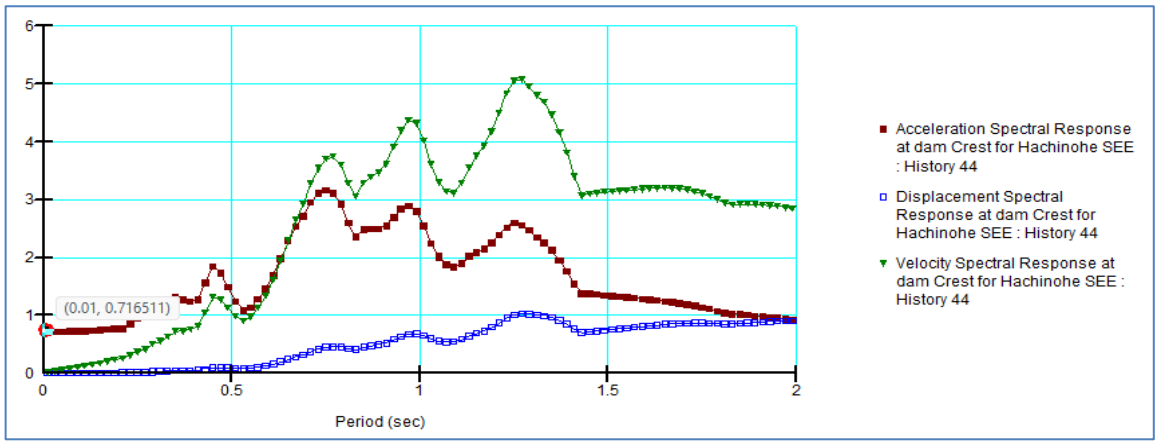

Figure 4-68: Horizontal Spectral response at dam crest corresponding to SEE (Hachinohe)

4.6.2.7. Stability after earthquake shaking

A post-seismic stability investigation was conducted to determine the dam's stability following the earthquake shaking. The Finite element method analysis component of the SLOPE/W Geo-Studio program, QUAKE/W Stress analysis type, was used in the analysis. This is accomplished by calculating post-earthquake pore pressure using QUAKE/W dynamic analysis findings. As illustrated in Figures 4 -69 and 4 -70, the factor of safety is more than the minimum requirements.

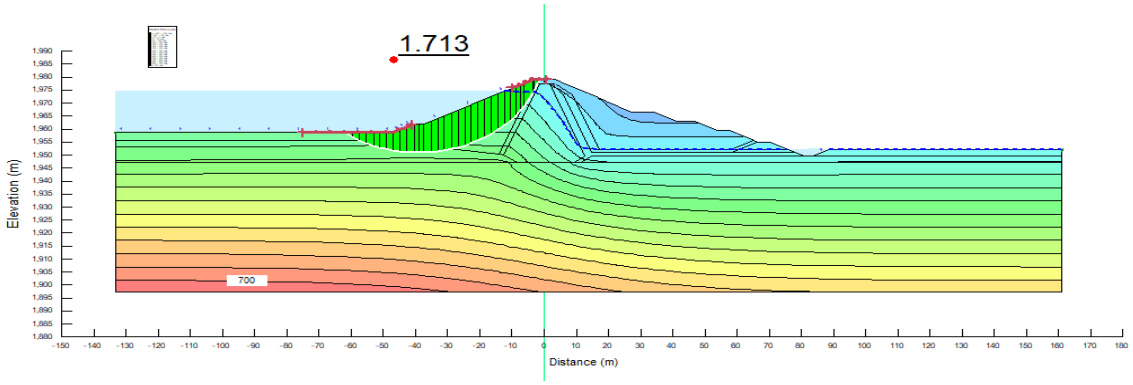

Figure 4-69: Post earthquake reinforced dam stability (upstream slope)

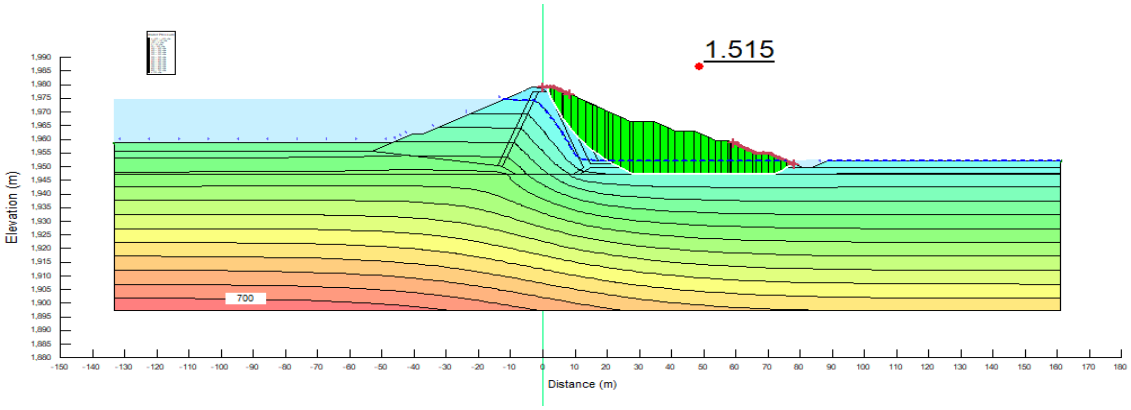

Figure 4-70: Post earthquake reinforced dam stability (downstream slope).

4.6.2.8. Deformation analysis results after earthquake shaking

One of the most significant aspects of dynamic analysis is to do deformation analysis after an earthquake has ended. This refers to the ability to link SIGMA/W with QUAKE/W dynamic analysis output.

Following the QUAKE/W dynamic analysis, the output outcomes will contain the updated soil total stresses and pore-water pressures at each stored time step. SIGMA/W may read the QUAKE/W output at each time step, subtract it from the previous time step, and apply an incremental force to each node. This force will cause a deformation. The peak vertical displacement of 1.30m was recorded. Figure 4-71 depicts the dam's distorted configuration following the earthquake.

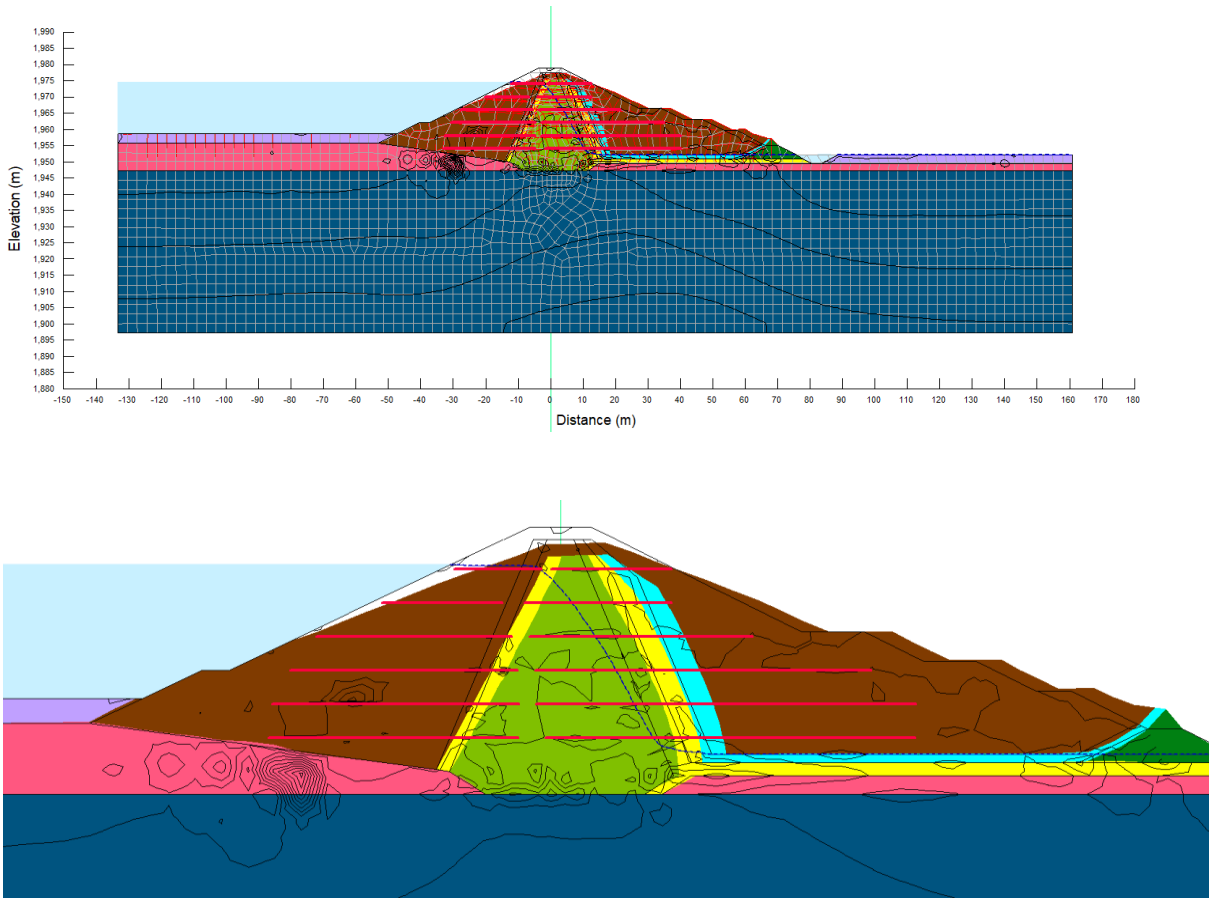

Figure 4-71: Post Earthquake deformation/Deformed mesh

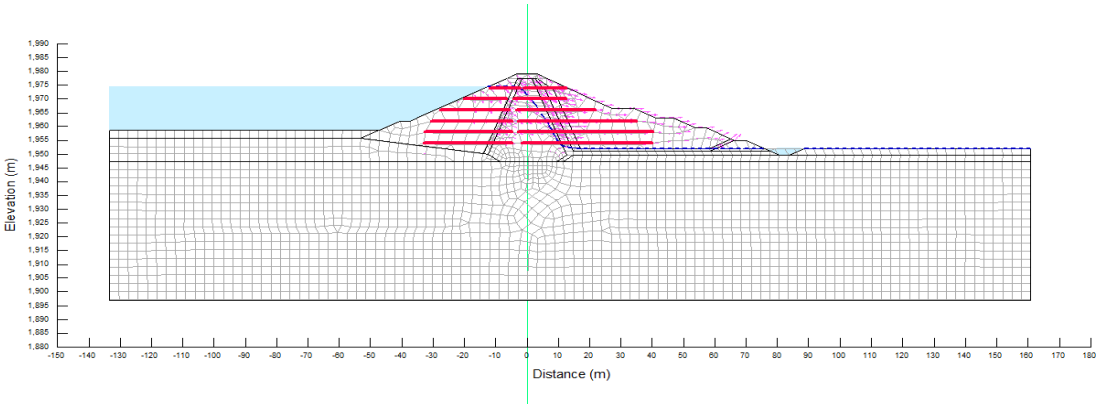

Figure 4-72: Displacement field vectors

4.6.2.9. Liquefaction analysis results for the dam with reinforcements

The computed liquefied zones of the dam at the end of earthquake shaking were shown in Figure 4-73; as can be seen from the yellow shaded zones, the Sandy Silty Clay soil is liquefied during earthquake shaking.

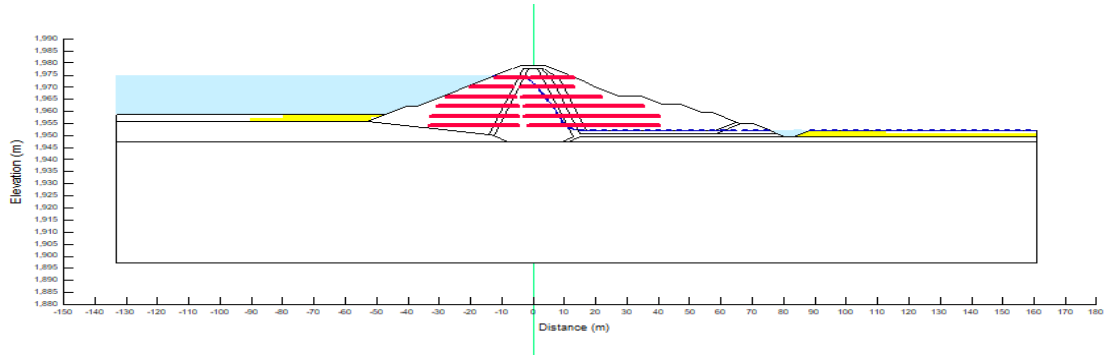

Figure 4-73: Liquefied zone of Kalid Dijo dam with reinforcement, corresponding to SEE (Based on El Centro Records)

4.6.2.10. Newmark deformation Analysis

The shaking caused by earthquakes generates inertial forces. These inertial forces cause the tensions in the earth to change throughout time. Inertial forces cause the mobilized shear strength to rise and fall along a possible slip surface. During shaking, the mobilized shear strength may outweigh the available shear resistance, causing a brief loss of stability. When the safety factor is less than one, the earth may shift somewhat. These displacements accumulate and cause irreversible deformation (QUAKE/W, 2018).

The examination of the permanent deformations caused by dynamic inertial forces is an essential part of dam dynamic analysis. SLOPE/W in GeoStudio employs the QUAKE/W calculated results in conjunction with the Newmark sliding block concept to execute earthquake-induced permanent deformations in dams. The Newmark approach is based on the concept that a prospective sliding mass behaves like a rigid body, moving down a slope when the total driving force (static and dynamic) exceeds the available resisting force. The yield acceleration is the critical value of the resultant acceleration caused by the sliding mass. It corresponds to the resulting (average) acceleration for which the sliding safety factor is equal to 1.0.

4.6.2.10.1. Numerical Procedures to estimate permanent deformation

The stresses from QUAKE/W are the total of the static and dynamic stresses. The static stresses are calculated using the supplied starting or in-situ stresses. By subtracting the initial static stresses from the QUAKE/W stresses, we can calculate the dynamic stresses. It may be calculated using equation 4.1 above. The dynamic stress may be estimated at the base of each slice. The total dynamic mobilized shear is calculated by integrating throughout the whole slip surface. This is the increased shear produced by the earthquake

shaking. The average acceleration is calculated by dividing the total mobilized dynamic shear by the potential sliding mass. This value is generated for each time integration step during the shaking and displayed against the safety factor, as shown in Figure 4 -74.

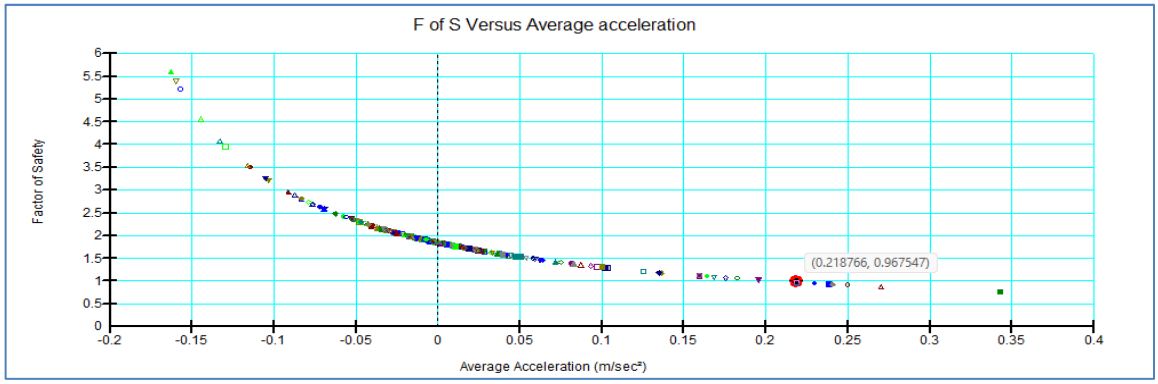

Figure 4-74: Average acceleration vs. Factor of Safety

The average acceleration that corresponds to a factor of safety of 1.0 is known as the yield acceleration, or ay. It is the overall average acceleration that causes the sliding mass to fail or move. In this case, a_y is around 0.22. Figure 4-75 depicts the average acceleration produced at each integration step displayed over time.

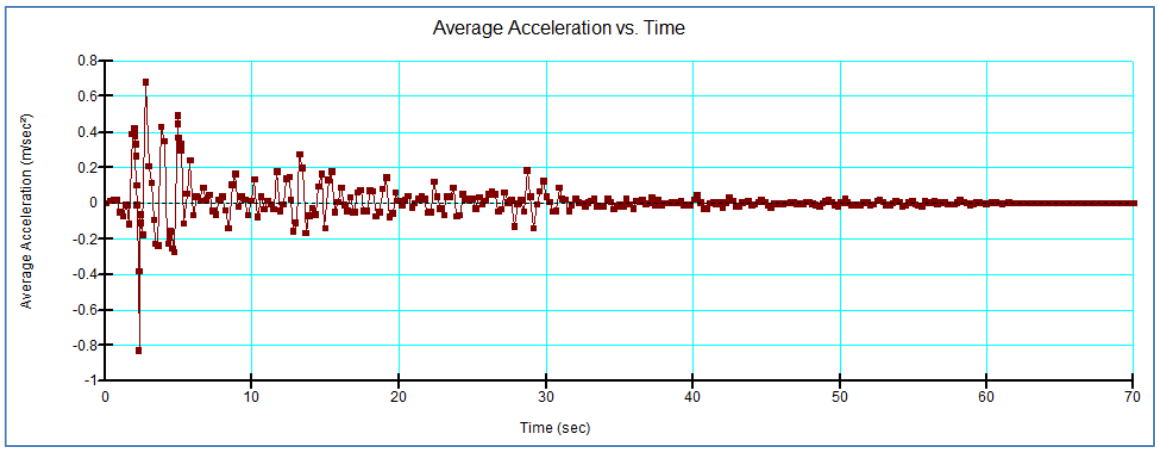

Figure 4-75: Average acceleration versus time during the shaking

Where the average acceleration exceeds a_y, the slope will move. The average acceleration is representative of the resultant of both horizontal and vertical applied accelerations in the QUAKE/W analysis.

Integrating the area under the average acceleration versus time curve where the acceleration exceeds a_y, gives the velocity of the sliding mass during the movement as shown in Figure 4-76.

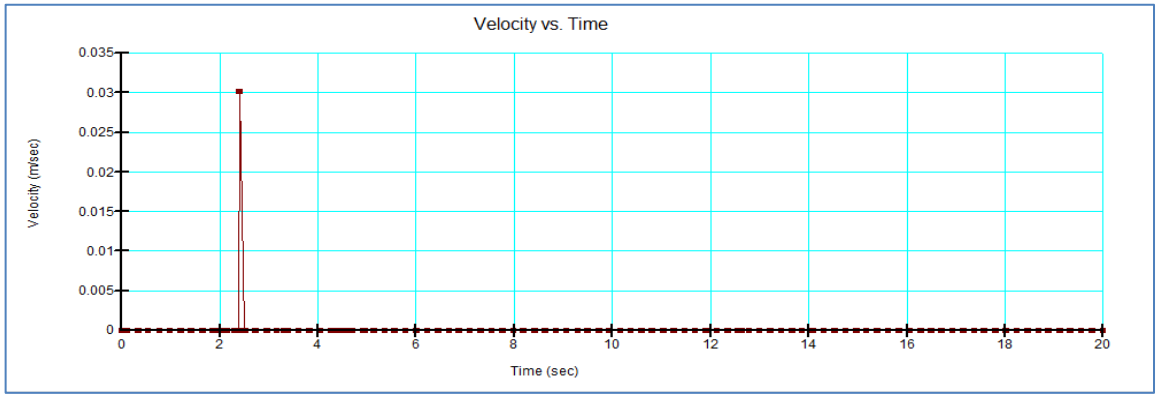

Figure 4-76: Velocity versus time

Integrating the area under the velocity versus time curve gives the cumulative movement during the shaking as seen in Figure 4-77. Based on this figure, the maximum earthquake induced Newmark's permanent deformation is about 0.06m (6cm).

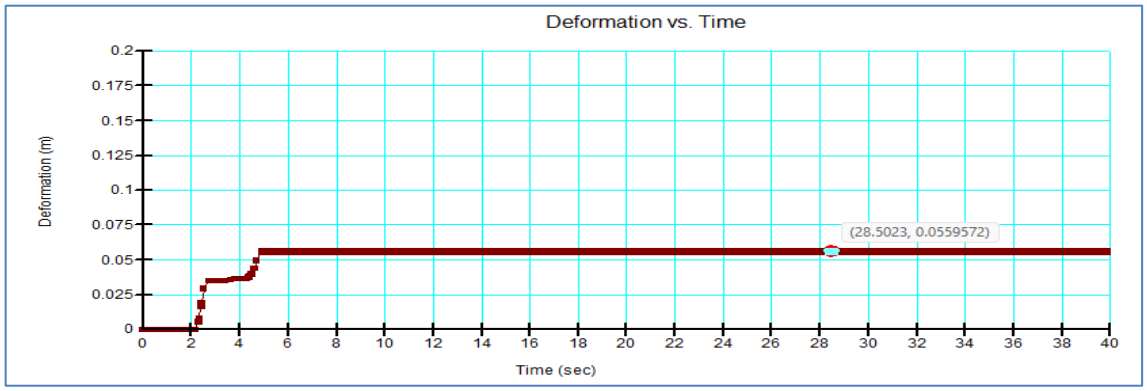

Figure 4-77: Cumulative movement during the shaking

4.7. Safety Comparisons for the Dam with and without Geosynthetic Reinforcements

4.7.1. Static Analysis

Table 4-7: Factor of safety for the dam with and without GSR for Static Stability

I. No.	Dam conditions	Factor of safety		Remark
		Upstream Slope	Downstream Slope (Steady state case)	

1	The dam without GSR, but with Rock fill zone	1.658 (For Rapid drawdown Case)	1.910	Fulfil Min. requirement at margin
		1.739 (For Steady State Case)		
2	The dam without GSR and without rock fill zone	1.313	1.325	Not Fulfil Minimum Requirement
3	The dam with GSR, but without Rock fill zone	1.651	1.630	4m GSR Spacing
		1.897	1.872	3m GSR Spacing
		1.905	1.984	2m GSR Spacing
		2.514	2.215	1m GSR Spacing

4.7.2. Dynamic Analysis

Table 4-8: Dynamic analysis results for the dam with and without GSR

I. No.	Description	Dam Conditions		Remark
		The dam without GSR, but with rock fill zone	The dam with GSR, but without rock fill zone	
1	Post-earthquake Stability for D/S Slope	1.868	1.515	SLOPE/W
2	Post-earthquake stability for U/S Slope	1.783	1.713	SLOPE/W
3	Post-earthquake deformation			
3.1	Peak/maximum crest vertical displacement (m)	1.70	1.30	SIGMA/W
4	Newmark's Permanent deformation(m)	0.45m (45cm)	0.06m (6cm)	SLOPE/W
5	Transmitted Ground Acceleration to dam crest (g)	1.74g	0.72g	QUAKE/W

4.8. Cost Comparison

The optimized reinforced dam section's earthwork is economically analyzed and compared to the unreinforced dam section. The Unit rate of the geosynthetics was taken at the same year (time) when Kalid Dijo dam's Bill of Quantity was estimated (in 2019 GC).

Table 4-9: Economic Analysis of the dam with and without GSR

I. No.	Description	Quantity (m3)	Unit Rate (ETB)	Amount (ETB)	Remark
A	The dam without Geosynthetic Reinforcement, but with rock fill zone				

1	Earth fill for Clay Core	250,088.65	170.38	42,610,104.19	
2	Earth fill for clay blanket	67,253.90	102.71	6,907,648.07	
3	Granular shell fill for toe of the dam	80,372.00	171.01	13,744,415.72	
4	Granular shell fill for shoulder (Zone 3)	231,176.40	196.59	45,446,968.48	
5	Rock fill for shoulder (Zone 4)	361,143.78	397.96	143,720,778.69	
	Total Amount (ETB)			252,429,915.15	
I. No.	Description	Quantity (m3 or m2)	Unit Rate (ETB)	Amount (ETB)	Remark
B	The dam with Geosynthetic Reinforcement, but without rock fill zone				
1	Earth fill for Clay Core	250,088.65	170.38	42,610,104.19	
2	Earth fill for clay blanket	67,253.90	102.71	6,907,648.07	
3	Granular shell fill for toe of the dam	80,372.00	171.01	13,744,415.72	
4	Granular shell fill for shoulders (Zone 3 and Prev. Zone 4)	592,320.18	196.59	116,444,224.2	
5	GSR for U/S Slope (m2)	81,957.64	80	6,556,611.2	
	GSR for D/S Slope(m2)	110,933.24	80	8,874,659.2	
	Total Amount (ETB)			195,137,662.58	
	Difference in Cash for (A) and (B); only for embankment fill work			57,292,252.57	23%

CHAPTER 5 CONCLUSIONS AND RECOMMENDATIONS

5.1. Conclusions

5.1.1. From static stability analysis results

Static stability analysis was performed on a dam under consideration, first without geosynthetic reinforcement and then with horizontal layers of geosynthetic reinforcement introduced into the dam slopes by varying spacing for economic and safety reasons. Based on the results of these analyses, the following conclusions were reached:

- The safety of the dam slope designed previously by ECDSWCo without geosynthetic reinforcement was found to be safe, but not economically optimized for both slopes. The u/s and d/s slopes have safety factors of 1.658 and 1.912, respectively.

- The dam factor of safety without geosynthetic reinforcement and without rock fill zone was seen to be insufficient for both slopes. The factor safety values for the upstream and downstream slopes were 1.313 and 1.325, respectively, which is unsafe.

- The dam were found to be safe without a rock fill zone when geosynthetic reinforcement layers were installed at a 4-meter spacing. The upstream and downstream slopes have factor of safety values of 1.651 and 1.897, respectively; indicating they are in good condition or safe. The safety factors were improved by about 26% and 43% for upstream and downstream slopes, respectively, when compared to the dam without GSR and without rock fill zone.

- As the geosynthetic reinforcement spacing decreases, the safety factor increases. For instance, when a geosynthetic reinforcement spacing decreased to 1m c/c, the upstream and downstream slopes safety factors were increased from 1.651 and 1.897 to 2.514 and 2.215, respectively.

5.1.2. From dynamic analysis results

A detailed dynamic stability analysis was performed on the dam under consideration, first without geosynthetic reinforcements, and then again for the reinforced dam section, which was statistically optimized for safety and economy. Based on the findings of this analysis, the following conclusions were reached:

- According to Newmark's deformation analysis results, the dam crest permanent deformation were observed as 45cm and 6cm without and with geosynthetic reinforcements, respectively.
- According to Post-earthquake dynamic deformation analysis results, the maximum vertical crest displacements were seen as 1.70m and 1.30m for the dam without and with geosynthetic reinforcements, respectively.
- For dams without geosynthetic reinforcements, the input ground motion (0.45g) was amplified to 1.74g at the dam crest, but with geosynthetic reinforcements spaced at 4m c/c, the amplification value was reduced to 0.72g.
- The stability study results after earthquake shaking show a factor of safety values of 1.515 for the downstream slope and 1.713 for the upstream slope for the dam with reinforcement, which is significantly greater than unity (indicating that the reinforced dam is safe after earthquake shaking).

5.1.3. From Cost Comparison

- The economic analysis results show that the dam with geosynthetic reinforcement was approximately 25% more economical than the dam without geosynthetic reinforcements, taking into account only the earth fill work of the main dam body.

5.2. Recommendation

- In this study, geosynthetic reinforcements were only introduced to the dam slopes; however, additional research can be conducted in this area by introducing geosynthetic reinforcements into the soft or weak dam foundations to determine the benefits of these reinforcements in improving dam safety when compared to the dam without geosynthetic reinforcement.

- Furthermore, whereas geosynthetic reinforcement was predicted to have a good impact on liquefaction mitigation, its advantage was not explicitly investigated in this study. As a result, a separate research will be conducted to investigate the impact of geosynthetic reinforcement on dam material and foundation liquefactions.

REFERENCES

Albaisa (1974), „Earthquake Induced Settlements in Saturated Sands, " Journal of the soil mechanics and foundation division. Vol.100. pp. 387-403.

Ambraseys, N. (1960). On the seismic behaviour of earth dams. World conference on Earthquake Engineering, (pp. 331-358).

Ashenafi Yilekal Bogale (2015) ANALYSIS OF GIDABO EARTH FILL DAM BY INTRODUCING GEOTEXTILE REINFORCEMENT A Thesis Submitted to School of Graduate Studies in Partial Fulfillment of the Requirements for Degree of Master of Science in Civil Engineering, Addis Ababa Institute of Technology

ASTM American Society of Testing Materials [Report]. - D4439.

Beadenkopf, E. (2013). Federal Guidelines for Inundation Mapping of Flood Risks Associated with Dam Incidents and Failures.

Briaud, J. L. (2013). Geotechnical Engineering: unsaturated and saturated soils. New Jersey: John Wiley & Sons.

Burland J. B. Closing Session Discussions, Proceedings of the First International Conference on unsaturated Soil Conference [Conference] // Proceedings of the First International Conference on unsaturated Soil Conference. - Paris: A.A.Balkema, 1996. - Vol. 3. - p. 1562.

Burland J. B. Nash Lecture: The Teaching of Soil Mechanics – a Personal view [Conference] // 9th ECSMFE. - Dublin: [s.n.], 1987. - Vol. 3. - pp. 1427 - 1447.

Christopher B. R. and Holtz R. D. Geotextiles Engineering Manual [Conference]. - Washington, DC: National Highway Institute, FHWA, 1985. - Vols. Contract DTFH61-80-C00094.

Das B. M. Principles of soil dynamics [Book]. - [s.l.]: Brooks/Cole, 1993.

DeAlba P., Chan C. K. and Seed H. B. Determination of soil liquefaction characteristics by large scale laboratory tests [Report] = Report EERC 75 - 25 / Earthquake engineering center; University of California. - Berkeley: [s.n.], 1975. - EERC 75 - 25.

DeAlba P., Seed H. B. and Chan C. K. Sand liquefaction in large scale simple shear tests [Journal] // Geotechnical engineering. - [s.l.]: ASCE, 1976. - GT9: Vol. 102. - pp. 909 - 927.

Duncan J. B. State of the art - static stability and deformation analysis in Stability andPerformance of slope and embankment [Journal] // ASCE Geotechnical Special Publication. - [s.l.] : ASCE, 1992. - 31. - pp. 222 - 266.

Duncan J. Michael and Wright Stephen G. Soil Strength and Slope Stability [Book]. - USA: JOHN WILEY & SONS, INC., 2005.

Duncan J. M. State of the art: limit equilibrium and finite element analysis of slopes [Journal] // Journal of Geotechnical Engineering. - [s.l.]: ASCE, 1996a. - 7: Vol. 122. - pp. 577 - 597.

Duncan J. M. State of the Art: Limit Equilibrium and Finite Element Analysis of Slopes [Journal] // Journal of Geotechnical Engineering. - 2005. - pp. 577 - 596.

ECDSWCo. Final Detail Design Report of Kalid-Dijo Dam and Irrigation Project, Kalid-Dijo Dam and Appurtenant Structures Final Detail Report [Report]. - Addis Ababa: WEDSWS, 2019.

ECDSWCo. Final Detail Design Report of Kalid-Dijo Dam and Irrigation Project, Geological and Geotechnical Investigation Final Feasibility Report [Report]. - Addis Ababa: GIGEUDSWS, 2019.

Fell Robin [et al.] Geotechnical engineering of dams [Book Section]. - London: Taylor and Francis group plc, 2005.

Fellenius W. Calculation of the Stability of Earth Dams [Journal] // proceeding of the second of Congress of Large Dams. - 1936. - 4. - pp. 445 - 463.

(FEMA, 2008): Geotextiles in Embankment Dams Status Report on the Use of Geotextiles in Embankment Dam Construction and Rehabilitation

FHWA Mechanically Stabilized Earth Walls and Reinforced Soil Slopes [Report] / Department of Transportation; Federal highways Administration. - Washington DC: FHWA, 2000. - Report FHWA-NHI-00-043,

Fowler J. Theoretical design considerations for fabric - reinforced embankments [Conference] // Second International Conference on Geotextiles. - Las Vegas: [s.n.], 1982. - Vol. 3. - pp. 665 - 670.

Fredlund D. G. and Krahn J. Comparison of slope stability methods of analysis. Canadian [Journal] // Canadian Geotechnical Journal. - 1977. - 3: Vol. 14. - pp. 429 - 439.

Getu Debebe (2022) NUMERICAL MODELING OF EMBANKMENT DAMS IN LIQUEFIABLE SOILS DURING EARTHQUAKES A Project Submitted to the School of Graduate Studies in Partial Fulfillment of the Requirements for the Degree of Masters in Geotechnical Engineering

Idriss I. M. Response of soft soil sites during earthquakes, [Conference] // Proceedings, Memorial symposium to honor professor Harry Bolton Seed. - Berkeley, California: [s.n.], 1990. - Vol. II.

IFAI [Article] // Geosynthetics magazine. - [s.l.]: Industrial Fabrics Association International, 2012.

Ishibashi I. and Zhang X. Unified Dynamic shear moduli and damping ratios of sand and clay [Journal] // Soils and foundations. - 1993. - 1: Vol. 33. - pp. 182 - 191.

Ishihara K. Post-earthquake failure of a tailings dam due to liquefaction of the pond deposit [Conference] // International conference on case histories in geotechnical engineering. - [s.l.]: University of Missouri, 1984. - Vol. 3. - pp. 1129 - 1143.

Koerner Robert M. Designing with Geosynthetics [Book]. - New Jersy : Prentice Hall, 2005.

Kramer Steven L. Geotechnical Earthquake Engineering [Book]. - New Jersey: Prentice-Hall, Upper Saddle River, 1996.

Krhan J. Seepage modeling with Seep/W: An engineering methodology [Book]. - [s.l.] : GEO-SLOPE International Ltd, 2007.

Lee K. L. and Albaisa A. Earthquake induced settlements in saturated sands [Journal] // Journal of the soil mechanics and foundation division. - [s.l.]: ASCE, 1974. - Vol. 100. - pp. 387 - 403. - GT4.

Malla S. [et al.] Seismic analysis and safety assessment of earth fill dam founded on alluvium soil [Report] / Commission Internationale. - Barcelona: Des grands barrages, **Messele H. Haile** Critical Assessment of Site Effect Parameters for Strong Ground Motion Prediction [Report]: Doctoral thesis / Tokyo Institute of technology. - Tokyo: [s.n.], 1996. 2005.

Messele Haile and Hadush Seged Earthquake induced liquefaction analysis of tendaho earth fill dam [Journal]. - Addis Ababa: Ethiopian civil engineers and architect's association, 2006. - Vol. 29.

Morgenstern N. R. and Price V. E. The Analysis of the Stability of General Slip Surfaces [Journal] // Journal of Geotechnical Engineering. - 1965. - 1. - pp. 79 - 93.

Mulat, Y. (2015), "Dynamic Analysis of Middle Awash Multi-Purpose Dam, " Addis Ababa University, Civil Environmental Engineering in partial fulfillment of the Degree of Masters of Science in Civil Engineering (Major in Hydraulic Engineering).

Newmark N. M. Effects of earthquakes on dams and embankments, Rankine Lecture [Journal] // Geotechnique. - 1965. - 2: Vol. 15.

QUAKE/W Dynamic modeling with QUAKE/W 2018: an engineering methodology [Book]. - [s.l.]: Geo - Slope International ltd, 2018.

Robert B. Jansen (1988): Advanced dam engineering for design, construction and rehabilitation.

Seed H. B. [et al.] Representation of irregular stress time histories by equivalent uniform stress series in liquefaction analyses [Book]. - Berkeley: Earthquake Engineering Research Center, University of California, 1975. - Vols. EERC75-29.

Seed H. B. and Idriss I. M. Simplified Procedure for evaluating soil liquefaction potential [Journal] // Journal of the soil mechanics and foundation Division, - ASCE: [s.n.], 1971. - SM9: Vol. 107. - pp. 1249 - 1274.

Seed H. B., Tokimatsu K. and Harder L. The influence of SPT procedures in evaluating soil liquefaction resistance evaluations [Journal] // Journal of geotechnical engineering. - Berkley: [s.n.], 1975. - 12: Vol. 111. - pp. 701-712.

Seed H. B. [et al.] Moduli and damping factors for dynamic analysis of cohesion less soils [Journal] // Journal of geotechnical engineering, ASCE. - [s.l.]: ASCE, 1986. - Vol. 112. - pp. 1016 - 1032. - GT11.

Seed H. B. and Harder Variation of correction factor Ka with initial /normal stress ratio [Conference]. - [s.l.]: BiTech Publishers Ltd, 1990. - Vol. 2. - p. 364.

Seed H. B. and Idriss I. M. Soil moduli and damping factors for dynamic response anayses [Report] / Earthquake engineering research center; University of California. - Berkeley: [s.n.], 1970a. - Report no. EERC/70-10.

Seed H. B. Considerations in the earthquake - resistant design of earth and rockfill dams [Journal] // Geotechnique. - 1979. - 3: Vol. 29. - pp. 215 - 263.

SEE/W Seepage modeling with Seep/W 2018: An engineering methodology [Book]. - [s.l.]: Geo-Slope international ltd, 2018.

SIGMA/W Stress- deformation modelling with SIGMA/W 2007: An engineering methodology [Book]. - Canada: Geo- slope international ltd, 2018.

SLOPE/W Stability Modeling with Slope/W: An egineering methodology [Book]. - [s.l.]: Geo-Slope International ltd, 2018.

Tensay G. Berhe (2010) Effect of Canyon Geometry and Ground Conditions on the Seismic Performance of Tendaho Earth fill Dam in Ethiopia. 2010-Fifth International

Conference on Recent Advances in Geotechnical Earthquake Engineering and Soil Dynamics

USCOLD Observed performance of dams during earthquakes [Report] / Committee of earthquakes. - Denver, USA: [s.n.], 2000.

Vanapalli S. K. [et al.] Model for the prediction of shear strength with respect to soil suction [Journal] // Canadian Geotechnical journal. - 1996. - Vol. 33. - pp. 379 - 392.

Wang W. Some findings in soil liquefaction. - Beijing: Water Conservancy and Hydroelectric Power Scientific Research Institute, 1979.

Yeabsra Tesfaye (2020): THE EFFECT OF VARYING GEOMETRY ON THE AMPLIFIFCATION OF GROUND MOTION IN ZONED EARTHEN DAMS A Thesis Submitted to School of Graduate Studies in Partial Fulfillment of the Requirements for Degree of Master of Science in Civil Engineering, Addis Ababa Institute of Technology

APPENDIX: A

- **Kalid-Dijo dam site photos during site visit and sampling**

APPENDIX B:

- **Input Ground Motion for both the dam with and without reinforcement.**

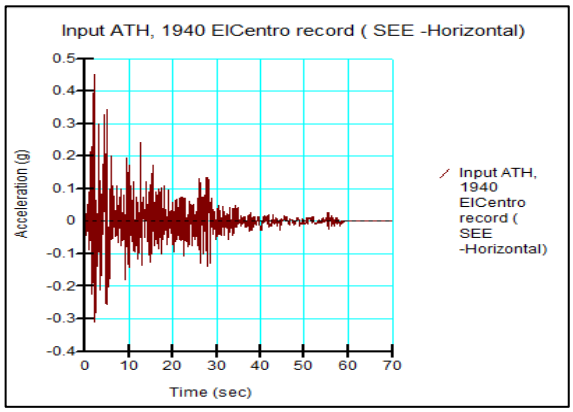

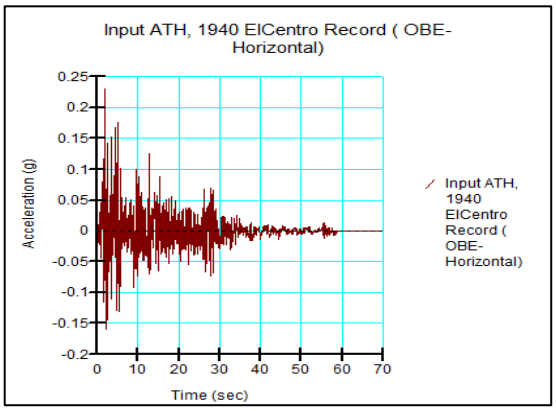

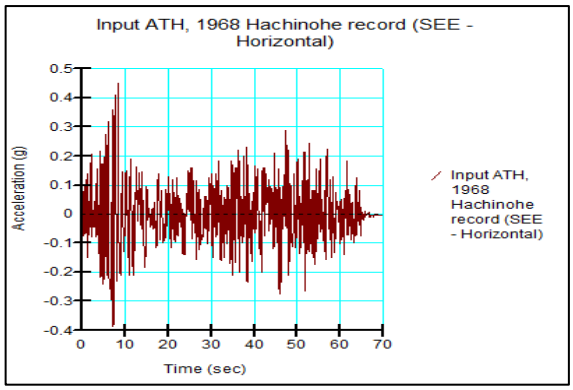

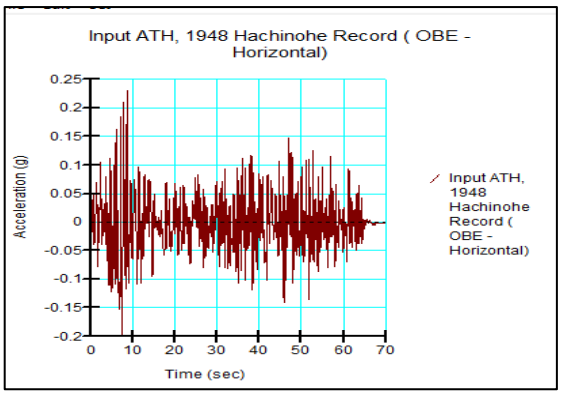

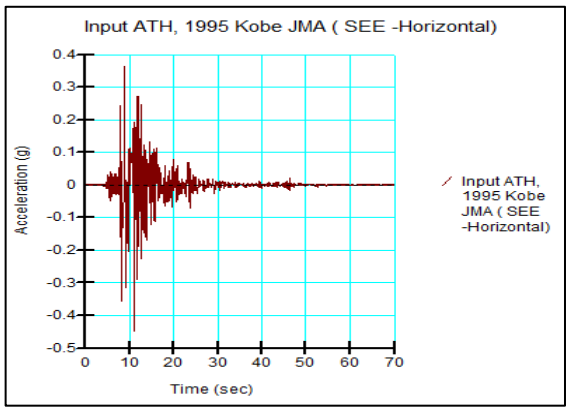

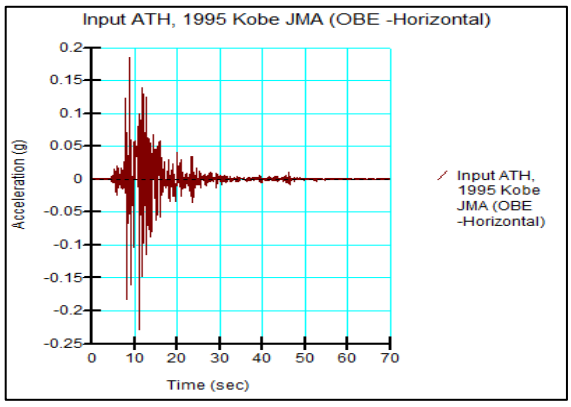

APPENDIX C:

C-I: Dynamic Analysis Results

Case 1: For the Dam without Geosynthetic Reinforcement

Acceleration response at dam crest

El Centro 1940 _ ATH (SEE and OBE– Horizontal)

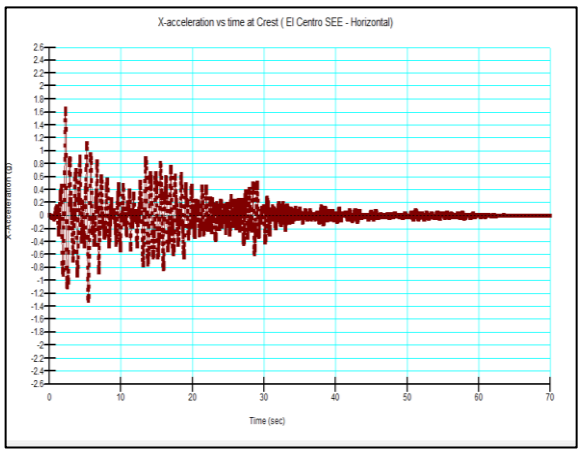

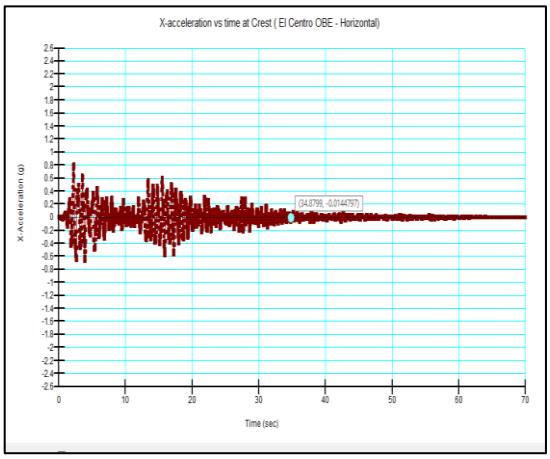

Hachinohe 1968_ATH (SEE and OBE- Horizontal)

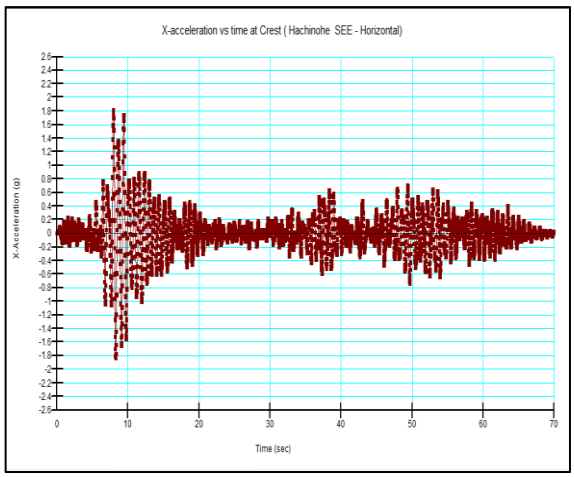

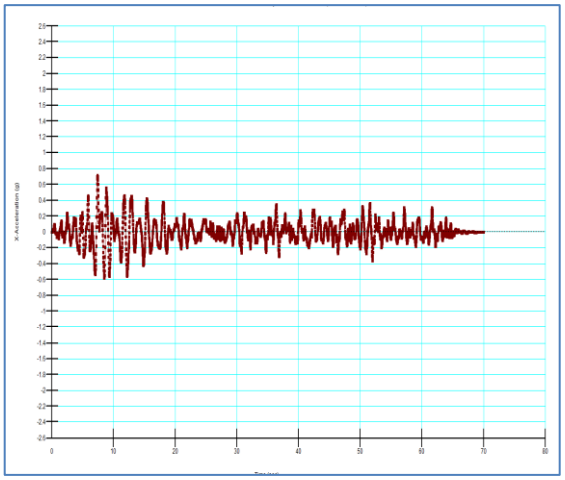

Kobe 1995_ATH (SEE and OBE - Horizontal)

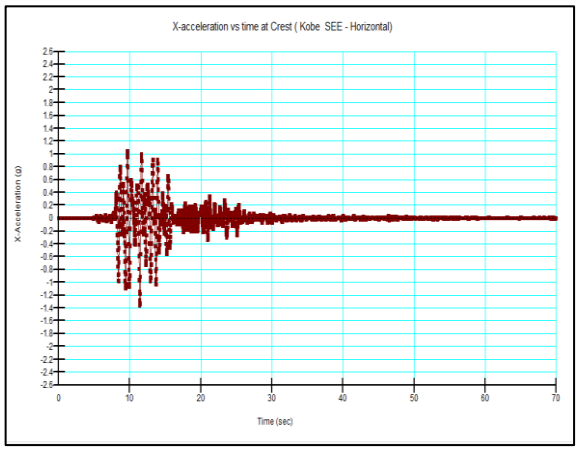

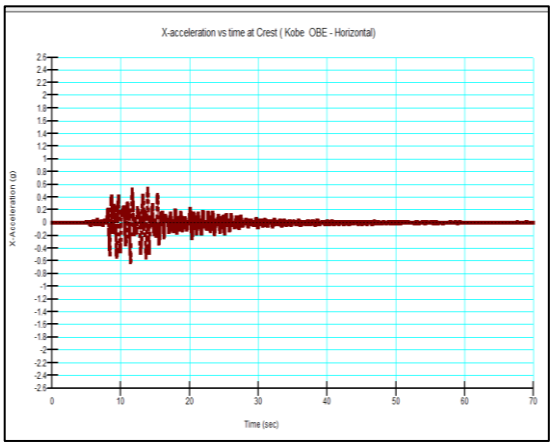

Spectral response at dam crest

El Centro- SEE

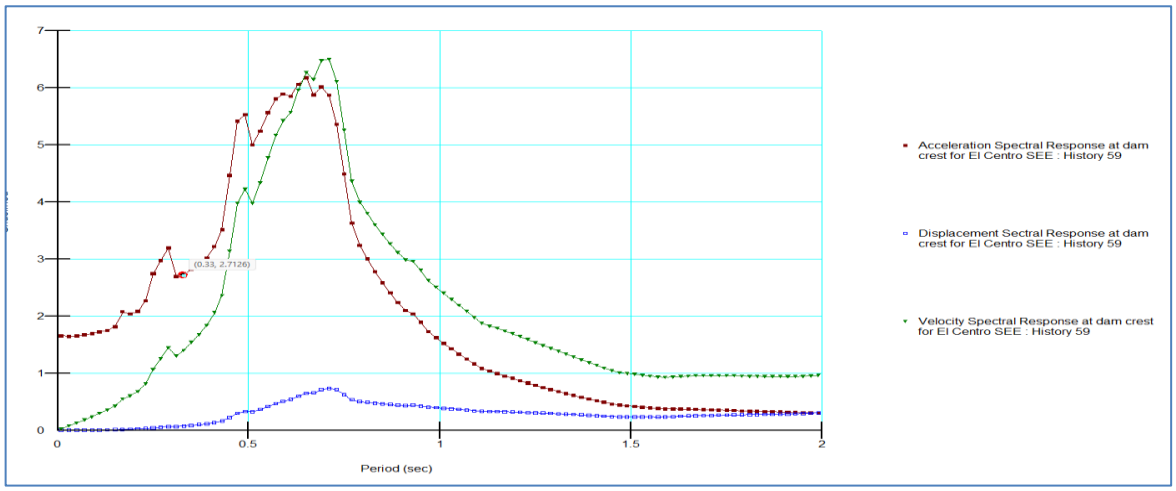

Kobe - SEE

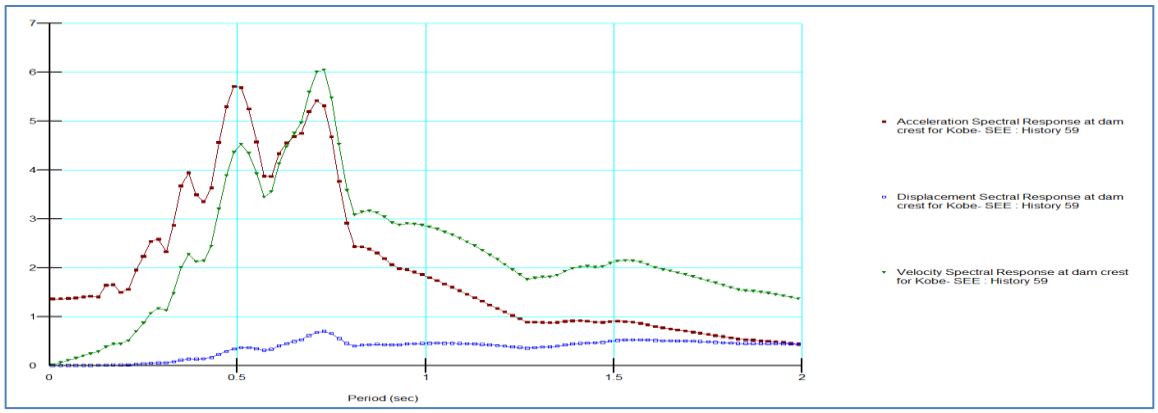

Case 2: For the Dam with Geosynthetic Reinforcement

Acceleration response at dam crest

El Centro 1940 _ ATH (SEE and OBE – Horizontal)

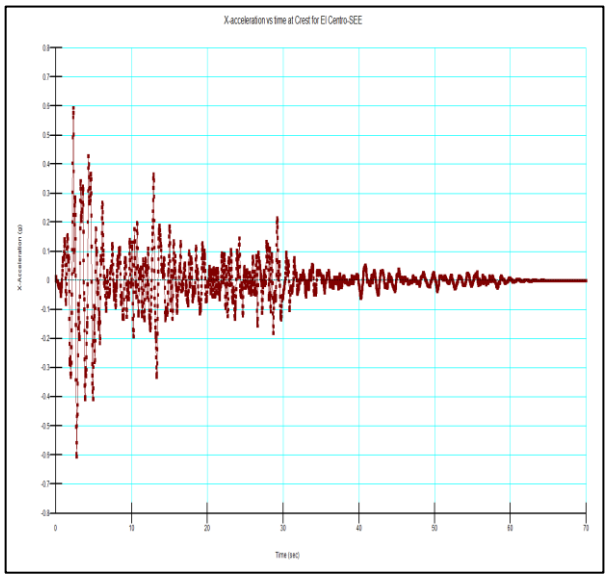

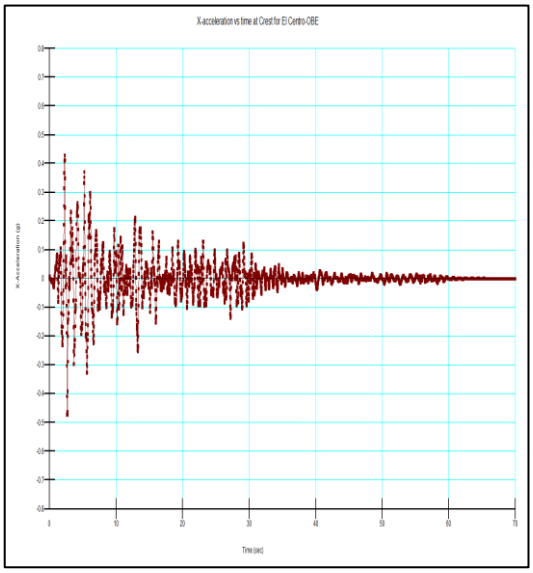

Hachinohe 1968_ATH (SEE and OBE - Horizontal)

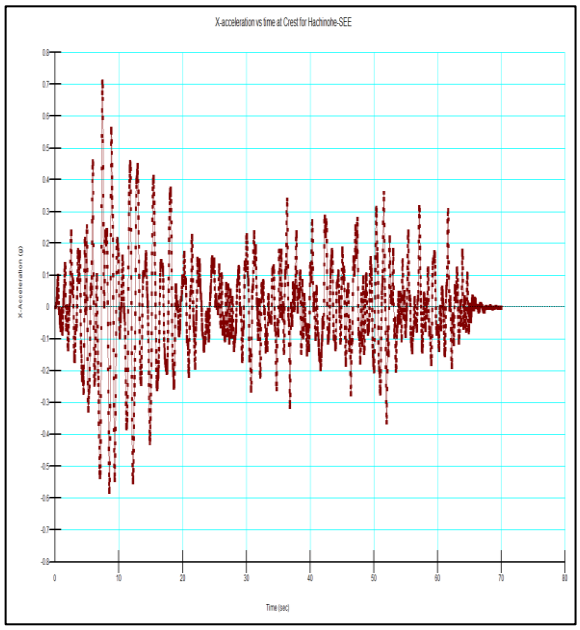

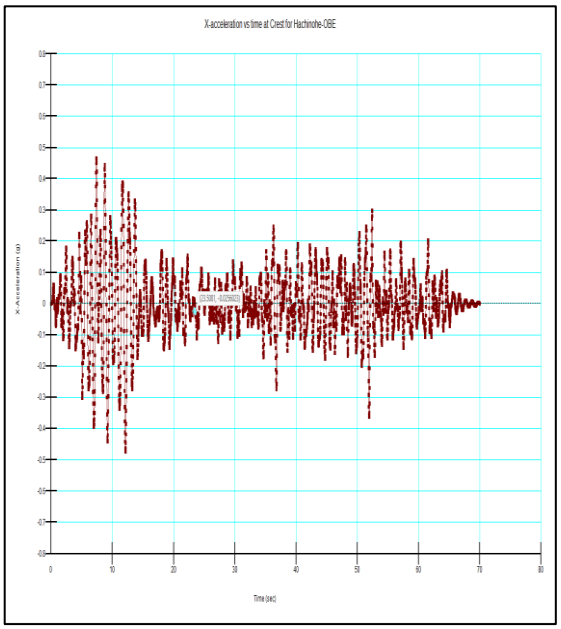

Kobe 1995_ATH (SEE and OBE - Horizontal)

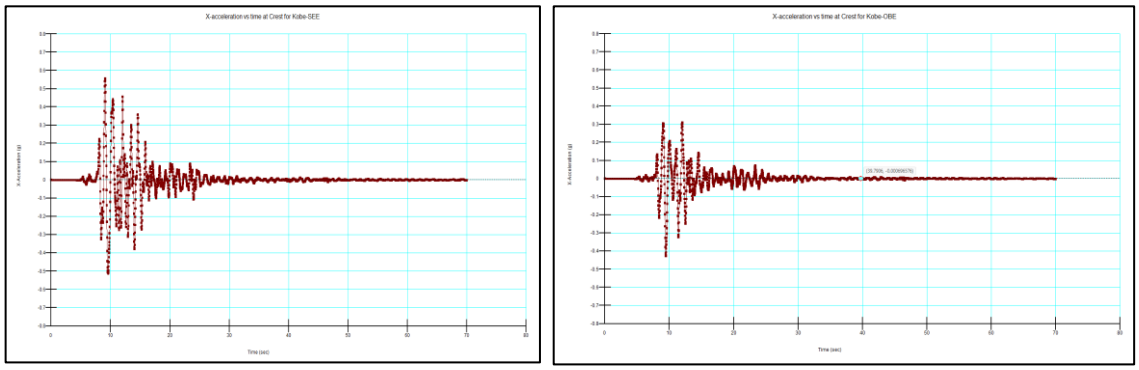

Spectral response at dam crest

For El Centro, SEE

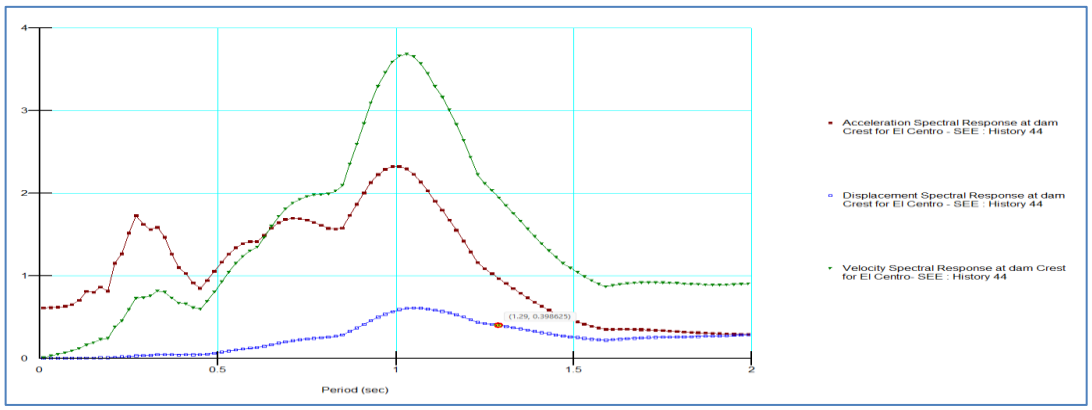

For Hachinohe, SEE